الجمهورية الجزائرية الديمقراطية الشعبية
وزارة التعليم العالي والبحث العلمي

BADJI MOKHTAR-ANNABA UNIVERSITY
UNIVERSITE BADJI MOKHTAR-ANNABA

جامعة باجي مختار- عنابة

Faculty of Engineering Sciences
Department of Electronics

Year: 2020

A THESIS

Submitted for Graduation Degree of

Es-Science Doctorate

Theme

SYNTHESIS OF TECHNIQUES USED FOR DIAGNOSING FAULTS IN ELECTRIC MACHINES

Option :

Automatic

By
LEKSIR Abdeslem

Tutor: **BENSAKER Bachir Professor at University of Badji Mokhtar-Annaba**

THE JURY

President:	**SAAD Salah**	**Professor**	**University of Annaba**
EXAMINERS:			
	KHEZAR	**Professor**	**University of Constantine1**
	LACHOURI	**Professor**	**University of Skikda**
	MEHNNAOUI	**MCA**	**University of Skikda**

الجمهورية الجزائرية الديمقراطية الشعبية
وزارة التعليم العالي والبحث العلمي

BADJI MOKHTAR-ANNABA UNIVERSITY
UNIVERSITE BADJI MOKHTAR-ANNABA

جامعة باجي مختار- عنابة

Faculté des sciences de l'ingéniorat
Département d'Électronique

Année : 2020

THÉSE

Présentée en Vue de l'obtention du Diplôme

de Doctorat Es-Science

Thème

SYNTHESE DES TECHNIQUES DE DIAGNOSTIC DES DEFAUTS DES MACHINES ELECTRIQUES

Option :

Automatique

Par
LEKSIR Abdeslem

Directeur de thèse : **BENSAKER Bachir Professeur Université Badji Mokhtar-Annaba**

DEVANT LE JURY

Président :	**SAAD Salah**	**Professeur**	**Université d'Annaba**
EXAMINATEURS:			
	KHEZAR Abderezak	**Professeur**	**Université Constantine1**
	LACHOURI	**Professeur**	**Université de Skikda**
	MEHNNAOUI	**MCA**	**Université de Skikda**

Acknowledgement

Special thanks for my advisor Pr. Bachir Bensaker for his support and encouragement during the development of this research.

Great salutations to president and all members of jury for their help and advices:

Special thanks to President of jury **SAAD Salah**	University Annaba
Special thanks to Professor **KHEZAR ABDEREZAK,**	University Constantine
Special thanks to Professor **LACHOURI**	University Skikda
Special thanks to MCA **MEHNNAOUI**	University Skikda

Finally, I would like to thanks all my family for their support and motivation during this long time, and particularly my parents for their sustenance.

ملخص: يتناول هذا البحث محاكاة لطرق الاستطاعة المختلفة لاكتشاف وتشخيص أخطاء مولد الحث. يتم إعادة النظر في الاستطاعة الجزئية والكلية, الاستطاعة النشيطة المتفاعلة والتفاعلية, الاستطاعة الظاهرية المعقدة و الاستطاعة المحوَّلة من الطبيعة الميكانيكية إلى الكهربائية. ويتم محاكاتها ومناقشتها في هذا البحث من أجل كشف أخطاء المولد الحثي وتشخيصه. أهم أخطاء مولد الحث الرئيسية هي قضبان الدوار المكسورة، قصر الدارة في الثابت وانعدام التوازن المحوري في الدوار.
يتم استخدام خوارزمية فوريه السريع (FFT) و PQ كأدوات مقارنة. تظهر نتائج المحاكاة أنه، من ناحية، لا يمكن استخدام الاستطاعة النشطة التفاعلية والمتفاعلة إلا للكشف عن تطور أخطاء الدوار. من ناحية أخرى الاستطاعة الجزئية، الكلية، و الاستطاعة المنقولة من الطبيعة الميكانيكية إلى الكهربائية قادرة على كشف تطور أخطاء مولد الحث مع الاستفادة من القضاء على التشوهات الكهربائية والتأثير على الجودة المنخفضة للجهد. علاوة على ذلك، يوفر تطبيق تحويل PQ إمكانية عزل تأثير الحمل من أخطاء الدوار و الجزء الثابت.
كلمات البحث:
مولد الحث. نمذجة الاستطاعة ، الاستطاعة الجزئية والكاملة، الاستطاعة التفاعلية و المتفاعلة، تشخيص أخطاء الدوار والجزء الثابت؛ المحاكاة.

Abstract: This thesis deals with an overall overview of power based techniques, used for induction generator faults detection and diagnosis. Instantaneous partial and total power, active and reactive power, complex apparent power and transformed power from mechanic to electric nature are all revisited, in faulty and healthy conditions, simulated and discussed in this thesis. The main major induction generator faults are the rotor broken bars, the stator shorted turns and the air-gap eccentricities.

Fast Fourier transforms (FFT) and PQ transform algorithms are used as comparison tools. Simulation results show that, on one hand, active, reactive and complex apparent power can only be used to detect evolution of rotor faults. On the other hand, partial, total and power transferred from mechanical to electrical nature are able to detect induction generator faults evolution, with the advantage of eliminating electrical distortions and influences of low supplying voltage quality. Furthermore, the implementation of the PQ transformation offers the possibility to isolate load influences from rotor faults and stator ones.

Keywords: Induction Generator; Power Modeling; Partial and Total Power; Active-Reactive Power; Rotor & Stator Fault Diagnosis; Simulation.

Résumé: Ce travail présente une vue d'ensemble des techniques de détection et de diagnostic des défauts dans les machines électriques, en insistant plus particulièrement sur les méthodes basées sur les différentes puissances. La puissance instantanée partielle et totale, la puissance active et réactive, la puissance apparente complexe et la puissance transformée de l'état mécanique à l'état électrique sont tous réexaminées, simulées et discutées dans ce travail pour la détection et le diagnostic des pannes de rotor/stator de générateur à induction. Les principales défaillances du générateur asynchrone sont les barres cassées du rotor, les courts circuits du stator et les excentricités de l'entrefer.

Les algorithmes de transformation rapide de Fourier (FFT) et de transformation PQ sont utilisés comme outils de comparaison. Les résultats de la simulation montrent que, d'une part, la puissance active, réactive et complexe ne peut être utilisée que pour détecter l'évolution des défauts du rotor. D'autre part, les puissances partiels, total et la puissance transféré de nature mécanique à électrique sont capables de détecter l'évolution des défauts d'un générateur d'induction avec l'avantage d'éliminer les distorsions électriques et l'influence de la qualité de la tension d'alimentation. En outre, la mise en œuvre de la transformation PQ offre la possibilité d'isoler l'influence de la charge des défauts de rotor et de stator.

Mots-clés: Générateur à induction; Modélisation de puissance; Puissance partielle et totale; Puissance réactive active; Diagnostic des défauts de rotor et de stator; Simulation.

Contents

List of Figures, Tables and abbreviations

1- List of Figures ……

2- List of tables……

3-List of abbreviations……

3-List of abbreviations

f_b: Rotor broken bar frequency.

f_s: supply frequency

s: slip

f_{sc}: Short cut frequency.

p= number of pole pairs.

v_{sd} : Direct Park component of stator voltage.

v_{sq} : Quadrature Park component of stator voltage.

v_{rd} : Direct Park component of rotor voltage.

v_{rq}: Quadrature Park component of rotor voltage.

$\mathbf{v_a}, \mathbf{v_b}, \mathbf{v_c}$: Three phases (a, b, c) components of stator voltages.

i_{sd} : Direct component of stator current.

i_{sq} : Quadrature component of stator current.

i_{rd} : Direct component of rotor current.

i_{rq} : Quadrature component of rotor current.

$\mathbf{i_a}, \mathbf{i_b}, \mathbf{i_c}$: Three phases (a, b, c) components of stator currents.

φ_{sd}: Direct component of stator flux.

φ_{sq}: Quadrature component of stator flux.

φ_{rd}: Direct component of rotor flux.

φ_{rq}: Quadrature component of rotor flux.

$\mathbf{R_s}$: Stator resistance.

$\mathbf{R_r}$: Rotor resistance.

$\mathbf{L_s}$: Stator self-inductance.

$\mathbf{L_r}$: Rotor self-inductance.

M: Mutual inductance between stator and rotor.

P(**θ**): Park matrix transformation.

θ : Park transformation angle between three phase conventional system.

$\boldsymbol{\omega_a}$: Angular velocity of the arbitrary reference frame.

$\boldsymbol{\omega_r}$: Angular velocity of the rotor reference frame.

ω : Angular velocity of the rotor reference frame.

α : Electrical angle between voltage and current components.

δ, T_r : leakage inductance, and rotor time constant.

Ω_{as} : Synchronous speed of the magnetic field.

Ω_m : Rotor rotating speed.

P : Healthy active power.

Q : Healthy reactive power Q.

$\boldsymbol{T_e}$: Electromagnetic torque.

R : Distance between no-load ellipse center and the faulty one.

R_f: Major axis of faulted power ellipse.

rf: Faulted power ellipse min axis.

$\boldsymbol{\nabla_r}$: Rotor fault severity factor.

∇ : Represents a new fault severity factor.

$\mathbf{P_0}, \mathbf{Q_0}$: Active and reactive power for no-load case.

SF : New severity factor proposed

$\mathbf{P_f}, \mathbf{Q_f}$: Active and reactive power for faulty generator.

P', Q': Active and reactive represents the real case of the system.

H : HILBERT transformation.

$\mathbf{r_{max}}$, $\mathbf{r_{min}}$: Major and min axis of the combination between active and reactive powers related to real and healthy conditions.

$\boldsymbol{i_f}$: Faulted stator current.

$\boldsymbol{I_l}$, $\boldsymbol{I_r}$: The magnitudes of the left and right sideband current components respectively.

$\boldsymbol{\alpha_l}$, $\boldsymbol{\alpha_r}$: The phases of the left and right sideband current components respectively.

$\boldsymbol{P_a}$: Instantaneous power of one phase.

$\boldsymbol{P_t}$: Total instantaneous power for three phase's induction generator.

$\mathbf{P_{ab}}$: Instantaneous partial power between phases *a* and *b.*

$\mathbf{v_{ab}}$: Line to line voltage between the phase *a* and *b.*

$\boldsymbol{S}$: Instantaneous complex apparent power.

$\boldsymbol{P_{ac}}$: Mechanic to electric transformed power.

INTRODUCTION

Electric machines are the main equipment used in industrial environments, to transform energy from electrical nature to mechanical or inversely. The majority of this machines manufactured currently are induction machines.

Induction machines are widely used in industrial applications as electrical entrainment, for their reliability and simplicity of construction. Even though, due to complicated operating conditions together with construction limitations, sudden failures could be occurring and may leads to cutoff of the whole working chain.

Literature review point out that the most common failures reported for induction generators are rotor broken bars, stator short cuts and bearing balls defect. Induction generator squirrel cage rotor is mainly constructed from metallic bars fixed and interconnected by end rings, total or partial break of one or many bars represents the most common failure. Induction generator stator is formed by

three winding connected to power supply and shifted by 120° each one from other. Stators are constructed from preformed insulated copper coils, the insulation material are selected to handle the operating voltages. The insulation material plays an essential role to prevent stator failure. The most common failures occurred in stator are turn to turn short circuits, open circuits and turn to stator body short circuits. The rotor (rotating part) is fixed to the stator (fixed part) by bearing system; any misalignment due to faults will appear as additional drags on the bearings, which will reduce their life. In order to overcome the above difficulties, on-line condition monitoring is highly recommended.

In order to overcome the above limitations, a series of methods for faults detection has been implemented. Well-known invasive methods are monitoring of vibration, noise and temperature, those methods are efficiently used for large and medium induction machines. Conversely, introducing those methods in low-voltage induction machine, diagnosis faces great barriers, concerning sensors size, cost and possibility to realize a continuous monitoring. However, non-invasive techniques are more suitable for low-voltage machines, almost all amounts used are already measured for several reasons as control and security. The most recent researches carried out are founded on electrical measurements, where currents and voltages represent the most popular signals used in non-invasive techniques. Moreover, via state modeling and observer methods the whole induction machine behavior will be reconstructed and accordingly more electrical measures could be used as diagnosis features, as stator and rotor fluxes and powers, torque, velocity, rotor currents, …ect.

Invasive techniques are used in diagnosing process as noise, temperature, vibration, speed, torque and flux, even that they suffer from the necessity of implementation of additional sensors and complexity to differentiate fault from other machine features.

Noninvasive techniques are in fact the most popular methods in terms of on-line condition monitoring and faults detectable features. Motor current signature analysis (MCSA) is widely used in induction machine diagnosis process; it is based on detection of variations induced by faults in sidebands nearby the main frequency of stator current signal. There are several researches presented in literatures that develop wide range of diagnosis methods based on MCSA, as zero crossing time (ZCT) and transient state motor current signature analysis (TMCSA). However, it has to be mentioned that the interaction of other faults together with electrical distortion, influences of load and supply frequency all can appear in almost the same frequency interval. This leads to doubt situation, and consequently fault's detection becoming a hard task.

Induction machines are widely used in industrial applications as energy generators mainly in wind energy conversion systems (WECS) (Amirat et all., 2009). However, their control, condition monitoring and faults diagnosis is still a challenge task for academic and industrial researches (Gidwani and Tiwari., 2012; Dybowski et all., 2008; Samaga and Vittal, 2012).Consequently, real time induction generator diagnosis is highly demanded(Lebaroud and Medoued, 2013).

To achieve this goal divers diagnosis techniques are proposed in the literature (Singh and Saad Ahmed, 2003; Chilengue et all., 2011; Liang et all., 2013). The earliest and the most used method is the well-known vibration analysis technique (Patel et al., 2014). Even that this method presents numerous advantages such as the elimination of electrical distortions and influence of supplying voltage low quality it contains some disadvantages given by the influence of voltage non-sinusoidality, incipient fault detection under varying supply/frequency and load conditions (Mehla and Dahiya, 2007; Mehrjou et all., 2011; Singhal and Khandekar, 2013). To overcome these disadvantages some are consecrated on the use of MSCA as a medium for modeling and detection of induction machine faults (Shehata et all., 2013; Prakasam, K., Ramesh, S.,

2016). The mean advantage of the MCSA technique is the availability of the stator current measurements in the major industrial applications. But it has to be mentioned that electrical distortions, load variations and influence of supplying voltage low quality could lead to appearance of harmonics in current signal at the same frequency as a fault harmonics, which may leads to wrong diagnosis (Trzynadlowski, 1999; Zagirnyak et all.,2013). Further details of the theory and application of MCSA can be found in (Singhal and Khandekar, 2013).Other methods use partial discharge monitoring (Elayaraja and Natarajan, 2015) and supply voltage unbalance analysis techniques(Pablo et all., 2016; Mohamed et all., 2017), these methods require costly sensor equipment and have a limited capability to diagnosis induction machine faults.

Also there is a series of methods for fault detection under transient conditions (Mustafa et all., 2013). But these methods provide best results for analysis of starting, braking modes, and modes under transient load, when there are significant signal changes both in time and frequency domains. Thus, these methods are less convenient for steady state modes analysis.

In order to overcome the above barriers a new domain was opened, using diverse presentation of induction generator power with the minimum influences of noise compared to MCSA (Trzynadlowski, A. M., 1999). Instantaneous total and partial powers (Samaga and Vittal, 2012; Maouche et all., 2014 ; Kucuker and Bayrak, 2013), active and reactive power (Akagi et all., 1984; Olivier et all., 2009; Drif and Cardoso, 2009 ; Intesar et all., 2010 ; Drif and Cardoso, 2012), complex apparent power (Bitoleanu et all., 2007; Fiorucci, 2015), PQ transformation method (Jin et al. 2007, Liu et all. 2007), and power transferred from rotor to stator (Boudebbouz et all., 2014), are all employed.

Thus, the use of power analysis methods allows one to make estimation of the energy of fault and the correlation of this energy to further damage of IG parts

under influence of additional vibrations caused by proper harmonic (Dmytro M., October 2011). Thus, all previous methods allow detecting most common damages of induction generator IG. In order to design the best technique for achievement IG diagnostic, it is necessary to compare all powers based methods.

The first method is an induction generator fault diagnostic method, based on active and reactive power; different active and reactive models are proposes to be used as diagnosis tools. PQ transformation is detailed too, finally a severity factor is proposed as faults indicator. This method will be referred as the PQ diagnosis method throughout this thesis.
The second method is an induction generator fault monitoring technique which classifies the operating condition of induction generator as faulty or healthy.
In this context several IG power presentations are detailed in healthy, faulty and under load conditions.

Thus, in this thesis we oriented toward different power analysis, based on FFT and PQ transformation, a study will be performed. Different powers analysis permit, first to select the suitable type of power that will be used to detect faults, in the second stage it can give the possibility to discriminate one fault either from other faults or from load influence, and finally it can offer a severity factor of selected fault.

In the first chapter of this thesis we present induction generator faults diagnosis methodology. Rotor and stator faults are all detailed in order to fault detection and isolation from load influences.

In the second chapter of this thesis we present induction generator model. Stator voltages are selected as inputs, stator currents and rotor fluxes are used as state variables. Via observer technique, all generators' functioning information will be obtained.

In the third chapter we focus on developing different power models presentations. Active and reactive power, total and partial power, complex and power transferred from stator to rotor are all modeled for both healthy and faulty state.

In the fourth chapter we concentrates on powers simulation; all theoretical results detailed in the previous sections are proved by figures.

Chapter1: Induction Generator Faults Diagnosis Methodology.

1.1 Generality, Diagnostic Method Strategy

The most common faults in induction generator are rotor broken bars (Mehrjou et all., 2011, Shehata et all., 2013), turn-to-turn stator failure (Shehata et all., 2013) and air gap eccentricity (Ahmed et all., 2010). These faults can be modeled as a step increase in energy of power (Kucuker, A. and Bayrak, M. 2013). It is well known that mechanical power developed by induction machine generates electromechanical power that is function of current, flux and other generator's parameters. Then any variation in electromechanical power appears as variation of theses parameters.

In this thesis two different types of faults in induction generators are detailed: broken rotor bars and inter-turn short circuits in stator windings. First, faults evolution detection technique gives a classification of power signal by induction generator fault. Second, this method identifies the fault severity for both faults,

and builds proportionality to the number of broken bars or the number of short circuit turns and selects the faulted induction generator element stator or rotor.

The signal processing is becoming an essential tool for condition monitoring and fault diagnosis. Induction generator presents many signals for condition monitoring and fault diagnosis, such as electrical signal and vibration. However, two important factors of generator condition monitoring and fault diagnosis, are how to extract the features and which signal is the suitable for such fault. Using appropriate signal analysis algorithms, it is feasible to detect changes in extracted signals caused by faulty components; the easiest signal processing is that the magnitude of the input signals, generally stator currents, is examined on a regular basis in the time or frequency domain.

A conventional diagnostic technique consists of comparing the actual current signal with the healthy one. Analyzing the changes introduced, by faults, into current signal will leads to diagnosis

The signal processing can be classified into three main classes: time domain, frequency domain, and time-frequency domain (A. Prudhom, et All. 2017). Time domain averaging (TDA) is a typical method to detect fault signals in rotating machines. It extracts the interest periodic component from a noisy complex signal. Time-domain analysis is a powerful tool for a three – phase squirrel cage induction generator. In this thesis an averaged pattern will be extracted by eliminating transitional signal, to serve as the electrical unbalance indicator, such DC signals my leads to wrong diagnosis. Time-domain technique can follows the fundamental frequency of the machine, to estimate a diagnostic index without any spectrum analysis. Different aspects are available for time domain analysis such as; time period of the signal, the peak value reached by the signal, the average value of the signal, RMS value of the signal etc. The choice

of such approaches depends on the signal type, quality and the required information.

In this thesis the process of obtaining diagnosis usable indicator from TSA (Time signature analysis) is summarized as follows: (1) Extract periodic signals from the original raw inputs of induction generator by eliminating transient section. (2) Through a state reconstruction process output powers are obtained. (3) Finally, power elliptic shape is attained and by consequence a fault type selection severity factor is offered.

In the frequency domain, spectral analysis is a very useful technique of signal processing used in fault diagnosis. Related to the nature of signals, stationary or non-stationary, spectral analysis is classed as FT (Fourier Transform) or STFT (Short time Fourier Transform) respectively. In this thesis a stationary signal will be studied, as a consequence an FFT analysis will be used. There is multiple other frequency analysis as cepstrum; periodogram…ect. Frequency analysis has the possibility to extract useful information and highlights many important hidden features.

In the present thesis, frequency of error is used to analyze the different induction generator power expression in frequency domain. Instead of study induction generator behavior healthy and faulty separately, and because healthy system is the reference, this proposition based on the fusion of the two specters into that one contains all information. More details will be exposed in section three.

1.2 Induction Generator Faults

Even though induction generators are reliable electric machines, they are subject to many electrical and mechanical faults (Benbouzid, 2000). Electrical faults include inter-turn short circuits or open-circuits in stator windings, broken rotor bars, and broken end rings; whereas mechanical faults contain bearing failures

and rotor eccentricities. The effects of such faults in induction generators can lead to unbalanced currents and stator voltages, torque oscillations, overheating, efficiency reduction, excessive vibration, and torque reduction (Shehata et all., 2013).

In this thesis we focus on two types of induction generator faults, inter-turn short circuits in stator windings and broken rotor bars. These faults are detailed in the next section.

1.2.1 Broken Rotor Bars

Squirrel cage rotor of an induction generator involves rotor bars and end rings. A broken bar can be partially or completely. Generator's bars can break, during live working cycle, and the reason may be thermal stresses, mechanical stress or a metal fatigue (Shehata et all., 2013). A well-known effect of a broken bar is the appearance of the sideband components, on the left and right sides of the fundamental frequency component in current and power spectrum (Shehata et all., 2013; Intesar et all., 2010; Liang et all., 2013; Maouche et all., 2014). Fig.1 presents the propagation of rotor broken bars frequency throughout rotor, stator and generator's mechanical speed. Sideband frequencies are given by:

$$f_b = (1 \pm 2s) f_s \quad (1)$$

Where $f_b$is the rotor broken bar frequency. s is the slip and $f_s$is supply frequency.

In the case of healthy system, the fundamental frequency components for stator f and rotor f_s appear only. In the case of stator faults, new components take place in the stator spectrum at frequencies $((1 \pm 2ks) f_s)$. $(k = 0,1,2..)$

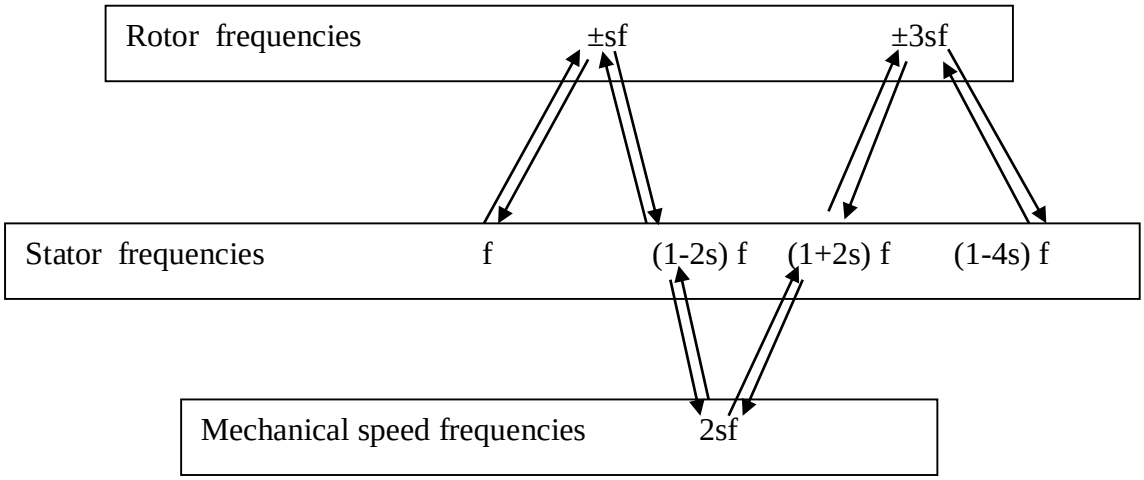

Fig.1 Frequency propagation for rotor fault (Gritli, et all., 2013)

The sideband components are widely used to induction generator fault classification purposes (Zagirnyak et all., 2013*;* Ahmed et All., 2010). In addition, in this thesis different instantaneous stator powers spectrum are used to differentiate faulted from healthy system, in order to evaluate faults evolution (Maouche et all., 2014; Zagirnyak et all., 2013). Other electric properties of broken bars are used for generator faults classification purposes, including speed oscillations (Filippetti et all., 1998), torque ripples (Pablo et all., 2016), and stator current envelopes (Da Silva et all., 2008).

1.2.2 Stator Short Circuits

Generally, stator short circuit is caused by electrical voltage transients and mechanical friction, leading to insulation damage of stator winding (Elayaraja and Natarajan, 2015). Stator windings damage constitutes a category of faults that is most common in induction generators. Normally, short circuit in stator winding occurs between conductors of the same phase, conductors of different phase or conductor and stator core. Excessive heating of stator winding or totally burned are usually resulted of rotor over loads or blocked, frequent starts and rotation reversals originate of starting mechanism can also leads to stator damaged (Shehata et all.2013).

Hence, in presence of a fault the three phases symmetry of induction generator system is lost, then an asymmetry appears in the stator that leads to electrical and mechanical no equilibrium (Mohamed et all., 2017). Generator fault diagnostic methods presented in this thesis are developed for one phase stator windings inter-turn short circuits. This type of fault is referred as inter-turn short circuit of stator throughout the thesis. Several induction generator power features will be used for inter-turn short circuit classification, and will be discussed.

Below is the frequency component due to stator fault:

$$f_{sc} = f_s \left[k \pm \frac{n}{p}(1 - s) \right] \quad (2)$$

Where $f_{sc}$is the Short cut frequency, k=1, 3, 5.., n=1, 2, 3…andp is the number of pole pairs.

In the same way, as rotor broken bars, the reflected in the stator short cut leads to unbalanced stator circuit and consequently stator currents, which produce an inverse magnetic field, related to an inverse current sequence component. This inverse sequence, reflected on the rotor side producing a new components at frequency (s-2)f on rotor quantities. These frequency components appear as an interaction in terms of electromagnetic and mechanical between stator and rotor at frequency 2f by means of frequencies propagation as represented in Fig.2.

If the stator faults occur, the symmetry of the machine will be lost; consequently an inverse magnetic field will be generated. This later creates speed oscillation and induces torque pulsation at stator frequency 2f.

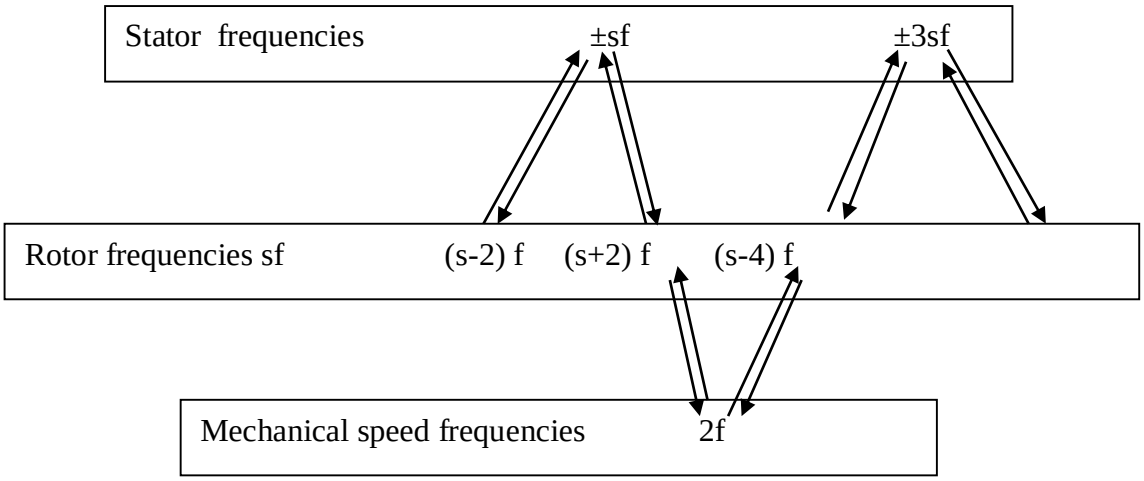

Fig.2 Frequency propagation for stator fault (Gritli, et all., 2013)

1.3 Diagnosis Methodology

In this section, both Induction generator FFT diagnosis method and PQ based diagnosis method are detailed. Rather than the conventional assumption based on fault detection, in which a faulty condition represents any number of rotor broken bars or stator inter-turn short circuits, this method is oriented to study the fault evolution and severity, tested with a simulation experiment to confirm their capability to detect variation in induction generator faults.

Based on the active and reactive power theory introduced by (Akagi et all., 1984), different power expressions are presented and discussed in the following using Park's transformation for induction machine faults diagnosis. Supply voltage and current measurements are assumed to be the only on-line available measurements.

1.3.1 On-Line Induction Generator Condition Monitoring

On-line induction generator condition monitoring, observes and detects any variation of generator's behavior during working conditions. On-line monitoring,

Fig.3 aims focus on preventing major problems, via the examination of the generator's behavior in running conditions in order to detect any undesirable events in early stage.

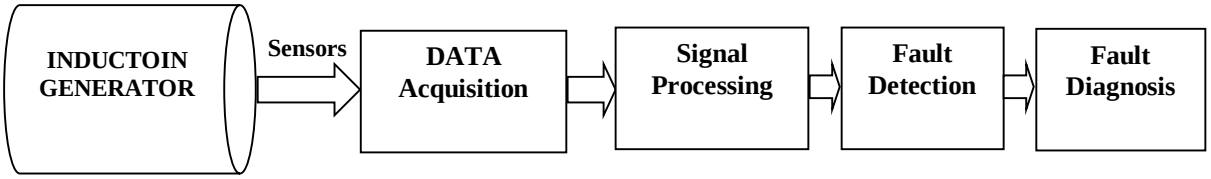

Fig.3 Induction Generator condition monitoring process

Monitoring system is mainly divided into five parts, sensors and observers, data acquisition, fault detection and analysis (diagnosis).Sensors and observers include direct measured quantities as stator current and tension, and observed quantities as flux and rotor parameters.

Data acquisition part encloses row signals acquired from sensors and observer signals obtained to reconstruct induction generator state. Finally, different types of power presentations for induction generator are acquired, at the end of acquisition process.

Fault's detection and analysis part represents the heart of monitoring system, their objective is to find out the earliest fault characteristics observed in acquired data. The fault detection process uses healthy reference model, this method is based on mathematical simulation model for healthy system and compare the real measurements results, to the healthy ones to confirm the presence or not of the fault. The second step is detection of fault evolution; a spectral analysis is used to evaluate the capability of method to detect fault gravity.

1.3.2 Observed-Based State Estimation

Development of estimation techniques and availability of new low cost DSP-based (Digital Signal Processing) microcontrollers, have reinforced the industrial applications of this idea for sensor less control and monitoring purposes.

Any model of the induction generator system can be written in the following unified state space model:

$$\frac{dX(t)}{dt} = AX(t) + BU(t) \quad (3)$$

$$Y(t) = CX(t) \quad (4)$$

Where $X(t)$is the selected as state variable vector and$U(t)$ is the input vector, $Y(t)$is the measured output vector. A, B and C are the evolution, the control and the observation matrices respectively. The general form of the observer is (I.Bakhti et all., 2019; A. Zaafouri et all., 2015):

$$\frac{d\hat{X}(t)}{dt} = A\hat{X}(t) + BU(t) + G\left[Y(t) - \hat{Y}(t)\right] \quad (5)$$

$$\hat{Y} = C\hat{X}(t) \quad (6)$$

Where $\hat{X}(t)$ is the estimated state variable vector of the unknown state variable vector. $\hat{Y}(t)$ is the estimated output of the measured output signal $Y(t)$. G is the observer gain matrix. The gain is constant if the observed system is linear and varying if the observed system is nonlinear. Relations Eq.5 and Eq.6 can be written as:

$$\frac{d\hat{X}(t)}{dt} = \left[A\text{-}GC\right]\hat{X}(t) + BU(t) + GY(t) \quad (7)$$

$$\hat{Y} = C\hat{X}(t) \quad (8)$$

This relation shows that the observer is a system in which the inputs are the input and the output of the system, to be observed and the output is the estimated state variable vector of the observed system. The dynamics of the observer are determined by the eighen values of the evolution matrix$[A - GC]$.A practical choice of the gain matrix is based on the fact that, the observer must be dynamically faster than the induction motor system. Pole placement technique is generally used in this case (A. Zaafouri et all., 2015).

In order to take into account the noise of the measured signals, and the model parameter deviations. Nonlinear Kalman filtering technique must be used to estimate the state variables, as well as the system parameters, the rotor angular velocity and the rotor (stator) resistance. Nonlinear techniques are generally avoided due to the high computational load required (I. Bakhti et all., Jan 2019; A. Zaafouri et all., 2015).

1.3.3 Stator Fault Detection

The algorithm used for stator faults detection and power selection is presented inFig.4. Initially, voltages and currents are directly measured and generator's state reconstruction is acquired. Through the analysis of fault evolution the suitable power for stator fault's detection will be defined. Finally, discovering stator faults via severity factor and spectral analysis are achieved.

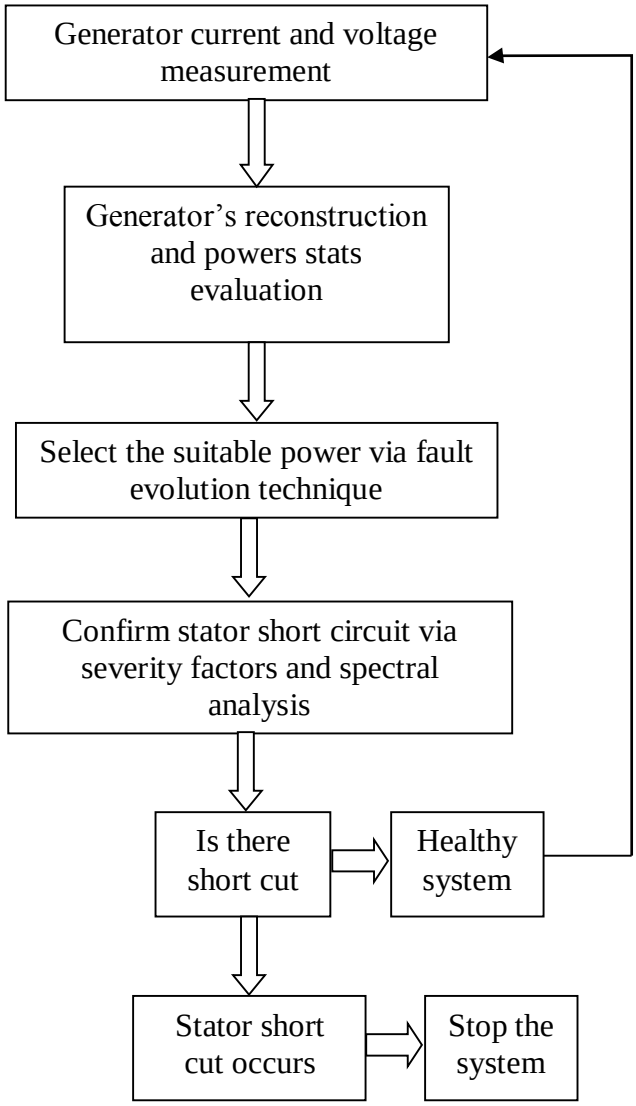

Fig.4 Decision tree of stator faults detection via power analysis.

1.3.4 Rotor Fault Detection

Following the same steps as stator faults, the rotor broken bars could be detected using the algorithm illustrated in the **Fig 5.**

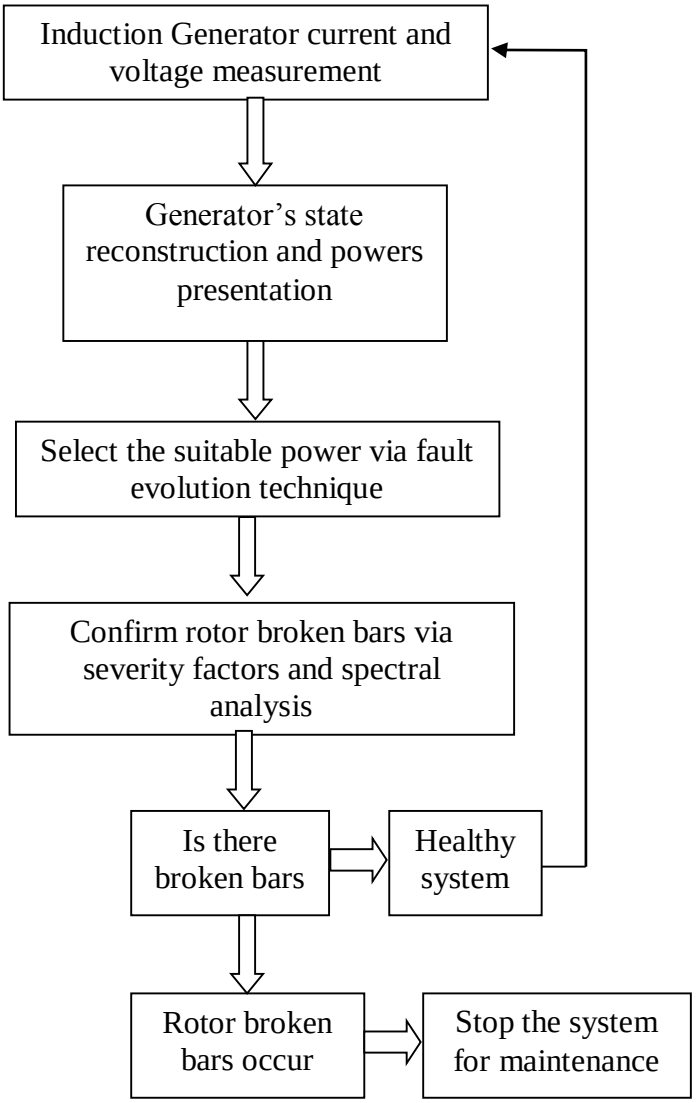

Fig.5 Decision tree of rotor faults detection via power analysis.

1.3.5 Faults-Load Interferences

Faults detection is the way of recognizing and discriminating the desired fault from the generator's features. Generally, induction generator's diagnosis method is composed of three levels. First, abnormalities are detected by FFT analysis or features recognition system. Second, detect the concerned fault from the induction generator features. Finally, distinguish fault from generator's load variations. **Fig**.4 and **Fig**.5 present an overall view of different frequency levels and the way of interaction.

One of the most critical decisions in the diagnostic process is the discrimination capability between different faults. The interaction between faults apparition in spectral analysis, faults frequencies are close one to other, makes diagnosis hard task. In **Fig**.6 An algorithm has been presented to recognize the exact fault occurred, using severity factor and spectral analysis the apparition of each fault will be then clearly defined.

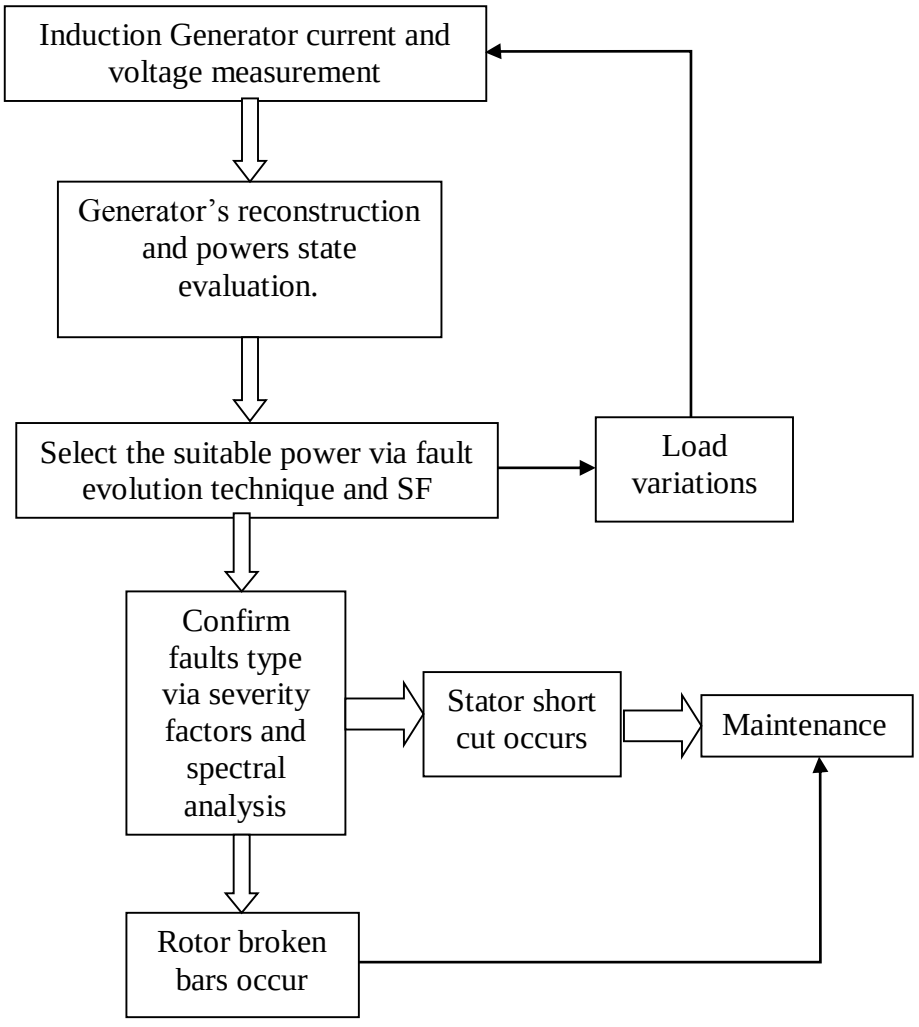

Fig.6 Decision tree of faults discrimination via power analysis.

The load influences is inevitable in industrial environment. Consequently, diagnostic process should be protected from the interaction of load variations.

Fig6. Present the flowchart that clarifies the manner of eliminating the influence of the load on diagnosis process.

Compared to the conventional diagnosis method, this method presents benefits of using minimum number of sensors. The introduction of the severity factor and the selected power in the diagnostic process, ensure the reliability of the decision in the fault detection and identification.

Chapter2: Induction Generator PQ based Diagnostic Methods

2.1 The Considered Induction Generator Model

Different induction generator models are available in the machinery literature (Bensaker et all., 2003;Arkan et all., 2005; Leksir and Bensaker, 2011). In this thesis, a combination of stator current and rotor flux is selected as state variables for the considered induction generator model. In an arbitrary rotating reference frame, the induction model can be expressed in Park's coordinate as the follows (Leksir and Bensaker. 2011; Dmytro October 2011):

$$\boldsymbol{v_{sd} = r_s i_{sd} + \frac{d}{dt}\varphi_{sd} - \omega_a \varphi_{sq}} \quad (9)$$

$$\boldsymbol{v_{sq} = r_s i_{sq} + \frac{d}{dt}\varphi_{sq} + \omega_a \varphi_{sd}} \quad (10)$$

$$\boldsymbol{v_{rd} = r_r i_{rd} + \frac{d}{dt}\varphi_{rd} - (\omega_a - \omega_r)\,\varphi_{rq}} \quad (11)$$

$$\boldsymbol{v_{rq} = r_r i_{rq} + \frac{d}{dt}\varphi_{rq} + (\omega_a - \omega_r)\varphi_{rd}} \quad (12)$$

Electromagnetic relations between stator and rotor components are the following:

$$\boldsymbol{\varphi_{sd} = l_s i_{sd} + m i_{rd}} \quad (13)$$

$$\boldsymbol{\varphi_{sq} = l_s i_{sq} + m i_{rq}} \quad (14)$$

$$\boldsymbol{\varphi_{rd} = l_r i_{rd} + m i_{sd}} \quad (15)$$

$$\boldsymbol{\varphi_{rq} = l_r i_{rq} + m i_{sq}} \quad (16)$$

Where the index s and r refers to stator and rotor components respectively and the index d and q refers to the direct and the quadrature components of the Park reference frame respectively. vis the voltage, i is the current and φis the flux. r is the resistance, l is he self-inductance and m is the mutual inductance between stator and rotor phase. ω_a and ω_r are the angular velocity of the arbitrary reference frame and the rotor reference frame respectively.

To return to three phases reference frame system (a, b, c) one has to use the following inverse Park transformation:

$$\begin{bmatrix} \boldsymbol{x_a} \\ \boldsymbol{x_b} \\ \boldsymbol{x_c} \end{bmatrix} = \boldsymbol{P(\theta)^{-1}} \begin{bmatrix} \boldsymbol{x_d} \\ \boldsymbol{x_q} \\ \boldsymbol{x_o} \end{bmatrix} \quad (17)$$

Where x stands for the induction generator variable in the three phase reference frame (a, b, c) and in the arbitrary reference frame (d, q, o) and $P(\theta)$is the Park matrix transformation defined by:

$$\boldsymbol{P(\theta)} = \sqrt{\frac{2}{3}}\begin{bmatrix} \boldsymbol{cos(\theta)} & \boldsymbol{cos\left(\theta - \frac{2\pi}{3}\right)} & \boldsymbol{cos\left(\theta + \frac{2\pi}{3}\right)} \\ \boldsymbol{-sin(\theta)} & \boldsymbol{-sin\left(\theta - \frac{2\pi}{3}\right)} & \boldsymbol{-sin\left(\theta + \frac{2\pi}{3}\right)} \\ \boldsymbol{\frac{1}{\sqrt{2}}} & \boldsymbol{\frac{1}{\sqrt{2}}} & \boldsymbol{\frac{1}{\sqrt{2}}} \end{bmatrix} \quad (18)$$

$\boldsymbol{\theta}$is the Park transformation angle between three phase conventional system and two axis Park system, where $\theta = \omega t$.

The measured stator voltages and currents in the (a, b, c) reference frame are defined as:

$$\mathbf{x_a} = \sqrt{2}\mathbf{X}\cos(\boldsymbol{\omega t} - \boldsymbol{\alpha}) \quad (19)$$

$$\mathbf{x_b} = \sqrt{2}\mathbf{X}\cos\left(\boldsymbol{\omega t} - \boldsymbol{\alpha} - \frac{2\pi}{3}\right) \quad (20)$$

$$\mathbf{x_c} = \sqrt{2}\mathbf{X}\cos\left(\boldsymbol{\omega t} - \boldsymbol{\alpha} + \frac{2\pi}{3}\right) \quad (21)$$

Where $\omega = 2\pi f$, with f as the supply frequency. Xis the maximum value of the voltage (current). $\boldsymbol{\alpha}$is the electrical angle between the voltage and current components.

Using the previous relations equations Eq(9-12), Eq(13-16), Eq(17-18) and Eq(19-21) wide range of models could be found(Bensaker et all. 2003). In this thesis the model selected is the one relates the stator currents, rotor flux and the stator voltages, while the rotor voltages are nulls. The projection of the equation was realized based on axis related to stator. This will leads to eliminate numerous parameters and maximum simplification of the model, without determining the performance of the induction generator system.

The model selected was defined by the matrixes: Rs, Rr, Ls, Lr, Msr, Mrs given bellow:

$$R_S = \begin{bmatrix} r_S & 0 \\ 0 & r_S \end{bmatrix}; R_r = \begin{bmatrix} r_r & 0 \\ 0 & r_r \end{bmatrix}; \mathrm{L}_s = \begin{bmatrix} \mathrm{l}_s & 0 \\ 0 & \mathrm{l}_s \end{bmatrix}; L_r = \begin{bmatrix} l_r & 0 \\ 0 & l_r \end{bmatrix}; M_{sr} = M_{sr}^T = \begin{bmatrix} m_{sr} & 0 \\ 0 & m_{sr} \end{bmatrix}$$

Finally the model can be written as follow:

$$\frac{d}{dt}\begin{pmatrix} \boldsymbol{i_{sd}} \\ \boldsymbol{i_{sq}} \\ \boldsymbol{\varphi_{rd}} \\ \boldsymbol{\varphi_{rq}} \end{pmatrix} = \begin{bmatrix} \frac{\left(-ml_r^{-1}r_r l_r^{-1}m - r_s\right)}{\left(l_s - ml_r^{-1}m\right)} & \mathbf{0} & \frac{ml_r^{-1}r_r l_r^{-1}}{\left(l_s - ml_r^{-1}m\right)} & \frac{\left(-ml_r^{-1}\Omega_m\right)}{\left(l_s - ml_r^{-1}m\right)} \\ \mathbf{0} & \frac{\left(-ml_r^{-1}r_r l_r^{-1}m - r_s\right)}{\left(l_s^{-1}ml_r^{-1}m\right)} & \left(\frac{-ml_r^{-1}\Omega_m}{\left(l_s - ml_r^{-1}m\right)}\right) & \frac{ml_r^{-1}r_r l_r^{-1}}{\left(l_s - ml_r^{-1}m\right)} \\ \boldsymbol{r_r l_r^{-1} m} & \mathbf{0} & \boldsymbol{-r_r l_r^{-1}} & \boldsymbol{\Omega_m} \\ \mathbf{0} & \boldsymbol{r_r l_r^{-1} m} & \boldsymbol{\Omega_m} & \boldsymbol{-r_r l_r^{-1}} \end{bmatrix} \begin{pmatrix} \boldsymbol{i_{sd}} \\ \boldsymbol{i_{sq}} \\ \boldsymbol{\varphi_{rd}} \\ \boldsymbol{\varphi_{rq}} \end{pmatrix} + \begin{bmatrix} \frac{1}{l_s - \frac{m^2}{l_r}} & \mathbf{0} & \mathbf{0} & \mathbf{0} \\ \mathbf{0} & \frac{1}{l_s - \frac{m^2}{l_r}} & \mathbf{0} & \mathbf{0} \\ \mathbf{0} & \mathbf{0} & \mathbf{0} & \mathbf{0} \\ \mathbf{0} & \mathbf{0} & \mathbf{0} & \mathbf{0} \end{bmatrix} \begin{bmatrix} \boldsymbol{V_{sd}} \\ \boldsymbol{V_{sq}} \\ \mathbf{0} \\ \mathbf{0} \end{bmatrix} \quad (22)$$

Knowing that δ and Tr are given by:

$$\delta = \boldsymbol{l_s} - \frac{\boldsymbol{m^2}}{\boldsymbol{l_r}}, T_r = \frac{\boldsymbol{l_r}}{\boldsymbol{r_r}}$$

The introduction of the parameters, δandT_r, will guide to the following simplified model:

$$\frac{d}{dt}\begin{pmatrix} i_{sd} \\ i_{sq} \\ \varphi_{rd} \\ \varphi_{rq} \end{pmatrix} =$$

$$\begin{bmatrix} \frac{(\delta-1-r_s)}{\delta} & 0 & \frac{(1-\delta){T_r}^{-1}}{m\delta} & \frac{((\delta-1)\Omega_m)}{m\delta} \\ 0 & \frac{(\delta-1-r_s)}{\delta} & \left(\frac{(\delta-1)\Omega_m}{m\delta}\right) & \frac{(1-\delta){T_r}^{-1}}{m\delta} \\ {T_r}^{-1}m & 0 & -{T_r}^{-1} & \Omega_m \\ 0 & {T_r}^{-1}m & \Omega_m & -{T_r}^{-1} \end{bmatrix} \begin{pmatrix} i_{sd} \\ i_{sq} \\ \varphi_{rd} \\ \varphi_{rq} \end{pmatrix} +$$

$$\begin{bmatrix} \frac{1}{l_s\delta} & 0 & 0 & 0 \\ 0 & \frac{1}{l_s\delta} & 0 & 0 \\ 0 & 0 & 0 & 0 \\ 0 & 0 & 0 & 0 \end{bmatrix} \begin{bmatrix} V_{sd} \\ V_{sq} \\ 0 \\ 0 \end{bmatrix} \quad (23)$$

2.2. Modeling of Active and Reactive Power of Induction Generator

Stator and rotor state variable are used to generate different models of induction generator. Each model uses as selected state variables a combination of stator and rotor variable such as current and flux. In the following we derive different active and reactive power models by selecting different combination of state variable of the considered induction generator (Leksir and Bensaker, 2011).

2.2.1. Active and Reactive Power Model using Stator Current and Flux as Selected State Variables

In the first model stator current and flux, are used as state variables to express active and reactive power of an induction generator of energy conversion systems.

Introducing electric voltage values granted Eq.9 and Eq.10, in power equations.

$$[\boldsymbol{P}] = \left(\boldsymbol{r_s i_{sd}} + \frac{\boldsymbol{d}}{\boldsymbol{dt}}\boldsymbol{\varphi_{sd}}\right).\boldsymbol{i_{sd}} + \left(\boldsymbol{r_s i_{sq}} + \frac{\boldsymbol{d}}{\boldsymbol{dt}}\boldsymbol{\varphi_{sq}}\right).\boldsymbol{i_{sq}} \quad (24)$$

$$[\boldsymbol{Q}] = \left(\boldsymbol{r_s i_{sd}} + \frac{\boldsymbol{d}}{\boldsymbol{dt}}\boldsymbol{\varphi_{sd}}\right).\boldsymbol{i_{sq}} - \left(\boldsymbol{r_s i_{sq}} + \frac{\boldsymbol{d}}{\boldsymbol{dt}}\boldsymbol{\varphi_{sq}}\right).\boldsymbol{i_{sd}} \quad (25)$$

Active P and reactive power Q can be expressed in the stator related reference as:

$$[\boldsymbol{P}] = \boldsymbol{r_s i_{sd}^2} + \boldsymbol{r_s i_{sq}^2} + \boldsymbol{i_{sd}} \frac{\boldsymbol{d}}{\boldsymbol{dt}} \boldsymbol{\varphi_{sd}} + \boldsymbol{i_{sq}} \frac{\boldsymbol{d}}{\boldsymbol{dt}} \boldsymbol{\varphi_{sq}} \quad (26)$$

$$[\boldsymbol{Q}] = \boldsymbol{i_{sq}} \frac{\boldsymbol{d}}{\boldsymbol{dt}} \boldsymbol{\varphi_{sd}} - \boldsymbol{i_{sd}} \frac{\boldsymbol{d}}{\boldsymbol{dt}} \boldsymbol{\varphi_{sq}} \quad (27)$$

Finally, PQ matrix form

$$\begin{bmatrix} \boldsymbol{P} \\ \boldsymbol{Q} \end{bmatrix} = \begin{bmatrix} \boldsymbol{r_s} & \boldsymbol{r_s} \\ \boldsymbol{0} & \boldsymbol{0} \end{bmatrix} \begin{bmatrix} \boldsymbol{i_{sd}}^2 \\ \boldsymbol{i_{sq}}^2 \end{bmatrix} + \begin{bmatrix} \boldsymbol{i_{sd}} & \boldsymbol{i_{sq}} \\ \boldsymbol{i_{sq}} & -\boldsymbol{i_{sd}} \end{bmatrix} \begin{bmatrix} \frac{\boldsymbol{d}}{\boldsymbol{dt}} (\boldsymbol{\varphi_{sd}}) \\ \frac{\boldsymbol{d}}{\boldsymbol{dt}} (\boldsymbol{\varphi_{sq}}) \end{bmatrix} \quad (28)$$

The first right component expresses the effect Joule losses while the second right component corresponds to the electromagnetic power stored in the magnetic circuit.

Relation (Eq.28) can be used in modeling and defects detection in stator induction generator by representing only variations in stator resistance.

In order to reduce significantly the model one can use, in addition to the stator reference frame, the stator field orientation technique also known as vector control. Via this technique the direct component of the stator flux must be aligned with the real axis, that leads to φs=φsd and φsq=0.

Electromagnetic torque model in the space of state variable is given by the product of the current and the Hilbert transformation of the flux as:

$$-\boldsymbol{T_e} = \boldsymbol{p}[-\boldsymbol{H\varphi_a} \quad -\boldsymbol{H\varphi_b} \quad -\boldsymbol{H\varphi_c}] \begin{bmatrix} \boldsymbol{i_a} \\ \boldsymbol{i_b} \\ \boldsymbol{i_c} \end{bmatrix} \quad (29)$$

The standard expression is:

$$\boldsymbol{T_e} = \boldsymbol{p}(\boldsymbol{\varphi_{sd} i_{sq}} - \boldsymbol{\varphi_{sq} i_{sd}}) \quad (30)$$

One can use the oriented stator field technique to reduce torque relation as:

$$\boldsymbol{T_e} = \boldsymbol{p\varphi_s i_{sq}} \quad (31)$$

The motion relation is:

$$J\frac{d\Omega}{dt} = T_e - T_l \quad (32)$$

The no load case can be obtained by setting $T_l = 0$. The oriented stator field technique leads to the following reduced relation:

$$\frac{d\Omega}{dt} = \frac{1}{J} p\varphi_s i_{sq} \quad (33)$$

Double PQ transformation based diagnostic method uses no load PQ curve characteristics as reference.

2.2.2. Active and Reactive Power Model using Stator and Rotor Currents as Selected State Variables

In this case stator and rotor currents are used to estimate both reactive and active powers. Substitute the stator flux as function of stator and rotor currents (Eq.13 and Eq.14), in the active and reactive power expressions (Eq.26 and Eq.27), leads to the following active and reactive relations.

$$[P] = r_s {i_{sd}}^2 + \frac{d}{dt}(l_s i_{sd} + m i_{rd}).\, i_{sd} + r_s {i_{sq}}^2 + \frac{d}{dt}\left(l_s i_{sq} + m i_{rq}\right).\, i_{sq} \quad (34)$$

$$[P] = r_s {i_{sd}}^2 + r_s {i_{sq}}^2 + l_s \frac{d}{dt}(i_{sd}).\, i_{sd} + m\frac{d}{dt}(i_{rd}).\, i_{sd} + \\ + l_s \frac{d}{dt}\left(i_{sq}\right).\, i_{sq} + m\frac{d}{dt}\left(i_{rq}\right).\, i_{sq} \quad (35)$$

$$[Q] = \frac{d}{dt}(l_s i_{sd} + m i_{rd}).\, i_{sq} - \frac{d}{dt}\left(l_s i_{sq} + m i_{rq}\right).\, i_{sd} \quad (36)$$

$$[Q] = l_s \frac{d}{dt}(i_{sd}).\, i_{sq} + m\frac{d}{dt}(i_{rd}).\, i_{sq} - l_s \frac{d}{dt}\left(i_{sq}\right).\, i_{sd} - m\frac{d}{dt}\left(i_{rq}\right).\, i_{sd} \quad (37)$$

In matrix form presentation the PQ model is then:

$$\begin{bmatrix} \mathbf{P} \\ \mathbf{Q} \end{bmatrix} = \begin{bmatrix} \mathbf{r_s} & \mathbf{r_s} \\ \mathbf{0} & \mathbf{0} \end{bmatrix} \begin{bmatrix} \mathbf{i_{sd}}^2 \\ \mathbf{i_{sq}}^2 \end{bmatrix} + \mathbf{l_s} \begin{bmatrix} \mathbf{i_{sd}} & \mathbf{i_{sq}} \\ \mathbf{i_{sq}} & -\mathbf{i_{sd}} \end{bmatrix} \begin{bmatrix} \frac{\mathbf{d}}{\mathbf{dt}}(\mathbf{i_{sd}}) \\ \frac{\mathbf{d}}{\mathbf{dt}}(\mathbf{i_{sq}}) \end{bmatrix} + \mathbf{m} \begin{bmatrix} \mathbf{i_{sd}} & \mathbf{i_{sq}} \\ \mathbf{i_{sq}} & -\mathbf{i_{sd}} \end{bmatrix} \begin{bmatrix} \frac{\mathbf{d}}{\mathbf{dt}}(\mathbf{i_{rd}}) \\ \frac{\mathbf{d}}{\mathbf{dt}}(\mathbf{i_{rq}}) \end{bmatrix} \quad (38)$$

or

$$\begin{bmatrix} \mathbf{P} \\ \mathbf{Q} \end{bmatrix} = \begin{bmatrix} \mathbf{r_s} & \mathbf{r_s} \\ \mathbf{0} & \mathbf{0} \end{bmatrix} \begin{bmatrix} \mathbf{i_{sd}}^2 \\ \mathbf{i_{sq}}^2 \end{bmatrix} + \begin{bmatrix} \mathbf{i_{sd}} & \mathbf{i_{sq}} \\ \mathbf{i_{sq}} & -\mathbf{i_{sd}} \end{bmatrix} \begin{bmatrix} \mathbf{l_s}\frac{\mathbf{d}}{\mathbf{dt}}(\mathbf{i_{sd}}) + \mathbf{m}\frac{\mathbf{d}}{\mathbf{dt}}(\mathbf{i_{rd}}) \\ \mathbf{l_s}\frac{\mathbf{d}}{\mathbf{dt}}(\mathbf{i_{sq}}) + \mathbf{m}\frac{\mathbf{d}}{\mathbf{dt}}(\mathbf{i_{rq}}) \end{bmatrix} \quad (39)$$

Stator resistance (rs) can be used to model stator defects. Eccentrics and bearing defects can be modeled using the mutual inductance and the self-inductance. In the case of reactive power there is only self-inductance of stator and mutual inductance (Schaeffer et all., 1998).

In this case of stator and rotor currents as selected state variable the torque generated by the wind in the generator is given by:

$$\boldsymbol{T_e = p\, m\, (i_{rd} i_{sq} - i_{rq} i_{sd})} \quad (40)$$

The dynamic relation for no load conditions is:

$$\frac{\mathbf{d\Omega}}{\mathbf{dt}} = \frac{\mathbf{Pm}}{\mathbf{J}}(\mathbf{i_{rd}} \mathbf{i_{sq}} - \mathbf{i_{rq}} \mathbf{i_{sd}}) \quad (41)$$

2.2.3. Active and Reactive Power Model using Stator Current and Rotor Flux as Selected State Variables

In this type of model, active and reactive powers are expressed as functions of stator current and rotor flux components. Via Eq.15 and Eq.16 the rotor current components are:

$$\boldsymbol{i_{rd}} = \frac{\mathbf{1}}{\boldsymbol{l_r}}\boldsymbol{\varphi_{rd}} - \frac{\boldsymbol{m}}{\boldsymbol{l_r}}\boldsymbol{i_{sd}} \quad (42)$$

$$\boldsymbol{i_{rq}} = \frac{\mathbf{1}}{\boldsymbol{l_r}}\boldsymbol{\varphi_{rq}} + \frac{\boldsymbol{m}}{\boldsymbol{l_r}}\boldsymbol{i_{sq}} \quad (43)$$

Thus allows expressing active and reactive power as:

$$[\boldsymbol{P}] = \boldsymbol{r_s i_{sd}}^{\mathbf{2}} + \boldsymbol{r_s i_{sq}}^{\mathbf{2}} + \boldsymbol{l_s}\frac{\boldsymbol{d}}{\boldsymbol{dt}}(\boldsymbol{i_{sd}}) \times \boldsymbol{i_{sd}} + \boldsymbol{m}\frac{\boldsymbol{d}}{\boldsymbol{dt}}\left(\frac{\mathbf{1}}{\boldsymbol{l_r}}\boldsymbol{\varphi_{rd}} - \frac{\boldsymbol{m}}{\boldsymbol{l_r}}\boldsymbol{i_{sd}}\right) \times \boldsymbol{i_{sd}} + \boldsymbol{l_s}\frac{\boldsymbol{d}}{\boldsymbol{dt}}\left(\boldsymbol{i_{sq}}\right) \times \boldsymbol{i_{sq}} + \boldsymbol{m}\frac{\boldsymbol{d}}{\boldsymbol{dt}}\left(\frac{\mathbf{1}}{\boldsymbol{l_r}}\boldsymbol{\varphi_{rq}} + \frac{\boldsymbol{m}}{\boldsymbol{l_r}}\boldsymbol{i_{sq}}\right) \times \boldsymbol{i_{sq}} \quad (44)$$

$$[\boldsymbol{Q}] = \boldsymbol{l_s}\frac{\boldsymbol{d}}{\boldsymbol{dt}}(\boldsymbol{i_{sd}}) \times \boldsymbol{i_{sq}} + \boldsymbol{m}\frac{\boldsymbol{d}}{\boldsymbol{dt}}\left(\frac{\mathbf{1}}{\boldsymbol{l_r}}\boldsymbol{\varphi_{rd}} - \frac{\boldsymbol{m}}{\boldsymbol{l_r}}\boldsymbol{i_{sd}}\right) \times \boldsymbol{i_{sq}} - \boldsymbol{l_s}\frac{\boldsymbol{d}}{\boldsymbol{dt}}\left(\boldsymbol{i_{sq}}\right) \times \boldsymbol{i_{sd}} - \boldsymbol{m}\frac{\boldsymbol{d}}{\boldsymbol{dt}}\left(\frac{\mathbf{1}}{\boldsymbol{l_r}}\boldsymbol{\varphi_{rq}} + \frac{\boldsymbol{m}}{\boldsymbol{l_r}}\boldsymbol{i_{sq}}\right) \times \boldsymbol{i_{sd}} \quad (45)$$

After simplification active and reactive powers will be:

$$[\boldsymbol{P}] = \boldsymbol{r_s i_{sd}}^{\mathbf{2}} + \boldsymbol{r_s i_{sq}}^{\mathbf{2}} + \left(\boldsymbol{l_s} - \frac{\boldsymbol{m}^{\mathbf{2}}}{\boldsymbol{l_r}}\right)\boldsymbol{i_{sd}}\frac{\boldsymbol{d}}{\boldsymbol{dt}}(\boldsymbol{i_{sd}}) + \frac{\boldsymbol{m}}{\boldsymbol{l_r}}\boldsymbol{i_{sd}}\frac{\boldsymbol{d}}{\boldsymbol{dt}}(\boldsymbol{\varphi_{rd}}) + \left(\boldsymbol{l_s} - \frac{\boldsymbol{m}^{\mathbf{2}}}{\boldsymbol{l_r}}\right)\boldsymbol{i_{sq}}\frac{\boldsymbol{d}}{\boldsymbol{dt}}\left(\boldsymbol{i_{sq}}\right) + \frac{\boldsymbol{m}}{\boldsymbol{l_r}}\boldsymbol{i_{sq}}\frac{\boldsymbol{d}}{\boldsymbol{dt}}\left(\boldsymbol{\varphi_{rq}}\right) \quad (46)$$

$$[\boldsymbol{Q}] = \left(\boldsymbol{l_s} - \frac{\boldsymbol{m}^{\mathbf{2}}}{\boldsymbol{l_r}}\right)\boldsymbol{i_{sq}}\frac{\boldsymbol{d}}{\boldsymbol{dt}}(\boldsymbol{i_{sd}}) + \frac{\boldsymbol{m}}{\boldsymbol{l_r}}\boldsymbol{i_{sq}}\frac{\boldsymbol{d}}{\boldsymbol{dt}}(\boldsymbol{\varphi_{rd}}) - \left(\boldsymbol{l_s} - \frac{\boldsymbol{m}^{\mathbf{2}}}{\boldsymbol{l_r}}\right)\boldsymbol{i_{sd}}\frac{\boldsymbol{d}}{\boldsymbol{dt}}\left(\boldsymbol{i_{sq}}\right) - \frac{\boldsymbol{m}}{\boldsymbol{l_r}}\boldsymbol{i_{sd}}\frac{\boldsymbol{d}}{\boldsymbol{dt}}(\boldsymbol{\varphi_{rd}}) \quad (47)$$

By setting$\boldsymbol{\delta} = \mathbf{l_s}\left(\mathbf{1} - \frac{\mathbf{m}^{\mathbf{2}}}{\mathbf{l_s l_r}}\right)$, previous relations will be:

$$[\boldsymbol{P}] = \boldsymbol{r_s i_{sd}}^{\mathbf{2}} + \boldsymbol{r_s i_{sq}}^{\mathbf{2}} + \boldsymbol{l_s}\boldsymbol{\delta}\boldsymbol{i_{sd}}\frac{\boldsymbol{d}}{\boldsymbol{dt}}(\boldsymbol{i_{sd}}) + \frac{\boldsymbol{m}}{\boldsymbol{l_r}}\boldsymbol{i_{sd}}\frac{\boldsymbol{d}}{\boldsymbol{dt}}(\boldsymbol{\varphi_{rd}}) + \boldsymbol{l_s}\boldsymbol{\delta}\boldsymbol{i_{sq}}\frac{\boldsymbol{d}}{\boldsymbol{dt}}\left(\boldsymbol{i_{sq}}\right) + \frac{\boldsymbol{m}}{\boldsymbol{l_r}}\boldsymbol{i_{sq}}\frac{\boldsymbol{d}}{\boldsymbol{dt}}\left(\boldsymbol{\varphi_{rq}}\right) \quad (48)$$

$$[\boldsymbol{Q}] = \boldsymbol{l_s \delta i_{sq}} \frac{\boldsymbol{d}}{\boldsymbol{dt}}(\boldsymbol{i_{sd}}) + \frac{\boldsymbol{m}}{\boldsymbol{l_r}} \boldsymbol{i_{sq}} \frac{\boldsymbol{d}}{\boldsymbol{dt}}(\boldsymbol{\varphi_{rd}}) - \boldsymbol{l_s \delta i_{sd}} \frac{\boldsymbol{d}}{\boldsymbol{dt}}\left(\boldsymbol{i_{sq}}\right) - \frac{\boldsymbol{m}}{\boldsymbol{l_r}} \boldsymbol{i_{sd}} \frac{\boldsymbol{d}}{\boldsymbol{dt}}\left(\boldsymbol{\varphi_{rq}}\right) \quad (49)$$

The matrix presentation of model is then:

$$\begin{bmatrix} \boldsymbol{P} \\ \boldsymbol{Q} \end{bmatrix} = \begin{bmatrix} \boldsymbol{r_s} & \boldsymbol{r_s} \\ \boldsymbol{0} & \boldsymbol{0} \end{bmatrix} \begin{bmatrix} \boldsymbol{i_{sd}}^2 \\ \boldsymbol{i_{sq}}^2 \end{bmatrix} + \boldsymbol{l_s \delta} \begin{bmatrix} \boldsymbol{i_{sd}} & \boldsymbol{i_{sq}} \\ \boldsymbol{i_{sq}} & -\boldsymbol{i_{sd}} \end{bmatrix} \begin{bmatrix} \dfrac{\boldsymbol{d}}{\boldsymbol{dt}}(\boldsymbol{i_{sd}}) \\ \dfrac{\boldsymbol{d}}{\boldsymbol{dt}}\left(\boldsymbol{i_{sq}}\right) \end{bmatrix} + \frac{\boldsymbol{m}}{\boldsymbol{l_r}} \begin{bmatrix} \boldsymbol{i_{sd}} & \boldsymbol{i_{sq}} \\ \boldsymbol{i_{sq}} & -\boldsymbol{i_{sd}} \end{bmatrix} \begin{bmatrix} \frac{\boldsymbol{d}}{\boldsymbol{dt}}(\boldsymbol{\varphi_{rd}}) \\ \frac{\boldsymbol{d}}{\boldsymbol{dt}}\left(\boldsymbol{\varphi_{rq}}\right) \end{bmatrix} \quad (50)$$

Which can be simply written as follow

$$\begin{bmatrix} \mathbf{P} \\ \mathbf{Q} \end{bmatrix} = \begin{bmatrix} \mathbf{R_s} & \mathbf{R_s} \\ \mathbf{0} & \mathbf{0} \end{bmatrix} \begin{bmatrix} \mathbf{I_{sd}}^2 \\ \mathbf{I_{sq}}^2 \end{bmatrix} + \begin{bmatrix} \mathbf{I_{sd}} & \mathbf{I_{sq}} \\ \mathbf{I_{sq}} & -\mathbf{I_{sd}} \end{bmatrix} \begin{bmatrix} \boldsymbol{L_s \delta} \frac{\mathbf{d}}{\mathbf{dt}}(\mathbf{I_{sd}}) + \frac{\boldsymbol{M}}{\boldsymbol{L_r}} \frac{\mathbf{d}}{\mathbf{dt}}(\mathbf{I_{rd}}) \\ \boldsymbol{L_s \delta} \frac{\mathbf{d}}{\mathbf{dt}}\left(\mathbf{I_{sq}}\right) + \frac{\boldsymbol{M}}{\boldsymbol{L_r}} \frac{\mathbf{d}}{\mathbf{dt}}\left(\mathbf{I_{rq}}\right) \end{bmatrix} \quad (51)$$

The product of stator current and the rotor flux results in the following torque:

$$\boldsymbol{T_e} = \boldsymbol{p} \frac{\boldsymbol{m}}{\boldsymbol{l_r}} \left(\boldsymbol{\varphi_{rd} i_{sq}} - \boldsymbol{\varphi_{rq} i_{sd}}\right) \quad (52)$$

Rotor orientation field technique, $\varphi_r = \varphi_{rd}$ and $\varphi_{rq} = 0$, make the torque uncomplicated as:

$$\boldsymbol{T_e} = \boldsymbol{p} \frac{\boldsymbol{m}}{\boldsymbol{l_r}} \boldsymbol{\varphi_r i_{sq}} \quad (53)$$

By the use of statements, no load and oriented field technique, dynamic behavior will be:

$$\frac{\boldsymbol{d\Omega}}{\boldsymbol{dt}} = \frac{\boldsymbol{Pm}}{\boldsymbol{l_r J}} \boldsymbol{\varphi_r i_{sq}} \quad (54)$$

The main objective of this model is to establish a relationship between the types of defects and induction generator variation parameters.

2.2.4. Active and Reactive Power Model using Stator and Rotor Flux as Selected State Variables

Active and reactive powers are represented by equations Eq.24 and Eq.25 define stator current and flux, while stator current will be replaced by stator and rotor flux through the following relations.

By multiplying electromagnetic stator relations Eq.13 and Eq.14 by the rotor self-inductance leads to:

$$\boldsymbol{l_r\varphi_{sd} = l_r l_s i + l_r m i_{rd}} \quad (55)$$

$$\boldsymbol{l_r\varphi_{sq} = l_r l_s i_{sq} + l_r m i_{rq}} \quad (56)$$

And multiplying electromagnetic rotor relations Eq.15and Eq.16 by the mutual inductance leads to:

$$\boldsymbol{m\varphi_{rd} = m l_r i_{rd} + m^2 i_{sd}} \quad (57)$$

$$\boldsymbol{m\varphi_{rq} = m l_r i_{rq} + m^2 i_{sq}} \quad (58)$$

Subtract Eq.57 from Eq.56 leads to:

$$\boldsymbol{l_r\varphi_{sd} - m\varphi_{rd} = l_r l_s i_{sd} - m^2 i_{sd}} \quad (59)$$

$$\boldsymbol{l_r\varphi_{sd} - m\varphi_{rd} = l_r l_s \left(1 - \frac{m^2}{l_r l_s}\right) \mathbf{i_{sd}}} \quad (60)$$

Using$\boldsymbol{\delta = \left(1 - \frac{m^2}{l_s l_r}\right)}and\boldsymbol{K = \frac{m}{\delta l_s l_r}}$, stator current is given by:

$$\boldsymbol{i_{sd} = \frac{1}{\delta l_s}\varphi_{sd} - K\varphi_{rd}} \quad (61)$$

Through the same way the second Park's component of stator current is obtained by subtracting Eq.58 and Eq.60 leads to:

$$\boldsymbol{l_r\varphi_{sq} - m\varphi_{rq} = -l_s l_r\left(\frac{m^2}{l_s l_r} - 1\right) i_{sq}} \quad (62)$$

$$\boldsymbol{i_{sq} = \frac{1}{\delta l_s}\varphi_{rq} - k\varphi_{sq}} \quad (63)$$

Introducing i_{sd}andi_{sq} in PQ equations Eq.24 and Eq.25.

$$\boldsymbol{[P] = r_s\left(k\varphi_{rd} - \frac{1}{\delta l_s}\varphi_{sd}\right)^2 + r_s\left(\frac{1}{\delta l_s}\varphi_{rq} - k\varphi_{sq}\right)^2 + \left(k\varphi_{rd} - \frac{1}{\delta l_s}\varphi_{sd}\right)\frac{d}{dt}\varphi_{sd} + \left(\frac{1}{\delta l_s}\varphi_{rq} - k\varphi_{sq}\right)\frac{d}{dt}\varphi_{sq}} \quad (64)$$

$$\boldsymbol{[P] = r_s k^2{\varphi_{rd}}^2 + r_s\left(\frac{1}{\delta l_s}\right)^2{\varphi_{sd}}^2 - 2r_s\frac{m}{(\delta l_s)^2 l_r}\varphi_{rd}\varphi_{sd} + r_s k^2{\varphi_{rq}}^2 + r_s\left(\frac{1}{\delta l_s}\right)^2{\varphi_{sq}}^2 + 2r_s\frac{k}{\delta l_s}\varphi_{sq}\varphi_{rq} + k\varphi_{rd}\frac{d}{dt}\varphi_{sd} + \frac{1}{\delta l_s}\varphi_{sd}\frac{d}{dt}\varphi_{sd} + \frac{1}{\delta l_s}\varphi_{rq}\frac{d}{dt}\varphi_{sq} - k\varphi_{sq}\frac{d}{dt}\varphi_{sq}} \quad (65)$$

$$\boldsymbol{[Q] = \frac{1}{\delta l_s}\varphi_{rq}\frac{d}{dt}\varphi_{sd} - k\varphi_{sq}\frac{d}{dt}\varphi_{sd} - \frac{1}{\delta l_s}\varphi_{rq}\frac{d}{dt}\varphi_{sq} + k\varphi_{sq}\frac{d}{dt}\varphi_{sq}} \quad (66)$$

$$\boldsymbol{[P] = r_s k^2\left({\varphi_{rd}}^2 + {\varphi_{rq}}^2\right) + r_s\left(\frac{1}{\delta l_s}\right)^2\left({\varphi_{sd}}^2 + {\varphi_{sq}}^2\right) - 2r_s\frac{k}{\delta l_s}\left(\varphi_{rd}\varphi_{sd} + \varphi_{sq}\varphi_{rq}\right) + k\left(\varphi_{rd}\frac{d}{dt}\varphi_{sd} - \varphi_{sq}\frac{d}{dt}\varphi_{sq}\right) + \frac{1}{\delta l_s}\left(\varphi_{sd}\frac{d}{dt}\varphi_{sd} + \varphi_{rq}\frac{d}{dt}\varphi_{sq}\right)} \quad (67)$$

$$\boldsymbol{[Q] = \frac{1}{\delta l_s}\varphi_{rq}\left(\frac{d}{dt}\varphi_{sd} - \frac{d}{dt}\varphi_{sq}\right) + k\varphi_{sq}\left(\frac{d}{dt}\varphi_{sq} - \frac{d}{dt}\varphi_{sd}\right)} \quad (68)$$

Assume that: $\boldsymbol{\varphi_r^2 = {\varphi_{rd}}^2 + {\varphi_{rq}}^2}and\boldsymbol{\varphi_s^2 = {\varphi_{sd}}^2 + {\varphi_{sq}}^2}$ then we have

$$\boldsymbol{\begin{bmatrix}P\\Q\end{bmatrix} = \begin{bmatrix}r_s k^2 & r_s\left(\frac{1}{\delta l_s}\right)^2\\0 & 0\end{bmatrix}\begin{bmatrix}\varphi_s^2\\\varphi_r^2\end{bmatrix} - 2r_s\frac{k}{\delta l_s}\begin{bmatrix}\varphi_{sd} & \varphi_{sq}\\0 & 0\end{bmatrix}\begin{bmatrix}\varphi_{rd}\\\varphi_{rq}\end{bmatrix} +}$$

$$k\begin{bmatrix}\varphi_{rd} & -\varphi_{sq}\\ -\varphi_{sq} & \varphi_{sq}\end{bmatrix}\begin{bmatrix}\frac{d}{dt}\varphi_{sd}\\ \frac{d}{dt}\varphi_{sq}\end{bmatrix}\frac{1}{\delta l_s}\begin{bmatrix}\varphi_{sd} & \varphi_{rq}\\ \varphi_{rq} & -\varphi_{rq}\end{bmatrix} \quad (69)$$

Or

$$\begin{bmatrix}P\\ Q\end{bmatrix}=\begin{bmatrix}r_s k^2 & r_s\left(\frac{1}{\delta l_s}\right)^2\\ 0 & 0\end{bmatrix}\begin{bmatrix}\varphi_s^2\\ \varphi_r^2\end{bmatrix}-2r_s\frac{k}{\delta l_s}\begin{bmatrix}\varphi_{sd} & \varphi_{sq}\\ 0 & 0\end{bmatrix}\begin{bmatrix}\varphi_{rd}\\ \varphi_{rq}\end{bmatrix}+$$

$$+\begin{bmatrix}k\varphi_{rd}-\frac{1}{\delta l_s}\varphi_{sd} & \frac{1}{\delta l_s}\varphi_{rq}-k\varphi_{sq}\\ \frac{1}{\delta l_s}\varphi_{rq}-k\varphi_{sq} & k\varphi_{sq}-\frac{1}{\delta l_s}\varphi_{rq}\end{bmatrix}\begin{bmatrix}\frac{d}{dt}\varphi_{sd}\\ \frac{d}{dt}\varphi_{sq}\end{bmatrix} \quad (70)$$

This model is very abundant of magnetic parameters as ls, lr, and m.
Electromagnetic torque is the product of rotor flux and the stator flux, caused by the transformation from current-voltage model to flux model a new coefficient come out, the final torque equation is given by:

$$T_e=\frac{p}{m}\frac{1-\delta}{\delta}\left(\varphi_{sq}\varphi_{rd}-\varphi_{sd}\varphi_{rq}\right) \quad (71)$$

Stator or rotor field orientation technique can be used for no load situation, the application of the first way offer the following system of torque and dynamics:

$$T_e=\frac{p}{m}\frac{\delta-1}{\delta}\varphi_s\varphi_{rq} \quad (72)$$

$$\frac{d\Omega}{dt}=\frac{p}{mJ}\frac{\delta-1}{\delta}\varphi_s\varphi_{rq} \quad (73)$$

The second way can be expressed in the system as:

$$T_e=\frac{p}{m}\frac{1-\delta}{\delta}\varphi_{sq}\varphi_r \quad (74)$$

$$\frac{d\Omega}{dt}=\frac{p}{mJ}\frac{1-\delta}{\delta}\varphi_{sq}\varphi_r \quad (75)$$

Steady-state and transient the power drawn by an ideal IG has a single component at the supply frequency. In the case of any mechanical or magnetic asymmetry, however, other frequency components according to the specific faults will appear in the stator current spectrum of the machine. When a rotor bar is broken, no current flows through it, and thus no magnetic flux is generated around that bar. This phenomenon generates an asymmetry in the rotor magnetic field by producing a non-zero back ward rotating field that rotates at the slip frequency speed with respect to the rotor. Therefore, it induces harmonic currents in the stator windings, which are super imposed on the stator currents.

2.3PQ Transformation Principle

Plotting the active power *P* as a function of the reactive power *Q* leads to a pattern which is a circle or a dot in the case of ideally healthy generator and to an elliptic shape in the faulty case (Leksir and Bensaker, 2011). In order to reach a total separation between a fault and the load influence different fault severity factors are proposed in the literature based upon the obtained plotting pattern (Jin et all., 2007 ; Leksir and Bensaker. 2011 ; Liu. 2007). In (Jin et all., 2007) and (Liu. 2007) a geometric approach is proposed which considers the major axis $R_f$of the obtained ellipse as a fault detection index. Variations in the elliptic shape appear as changes in the axis length. The following relationship as a rotor fault severity factor is suggested.

$$\boldsymbol{\nabla_r = \frac{R_f}{R}} \tag{76}$$

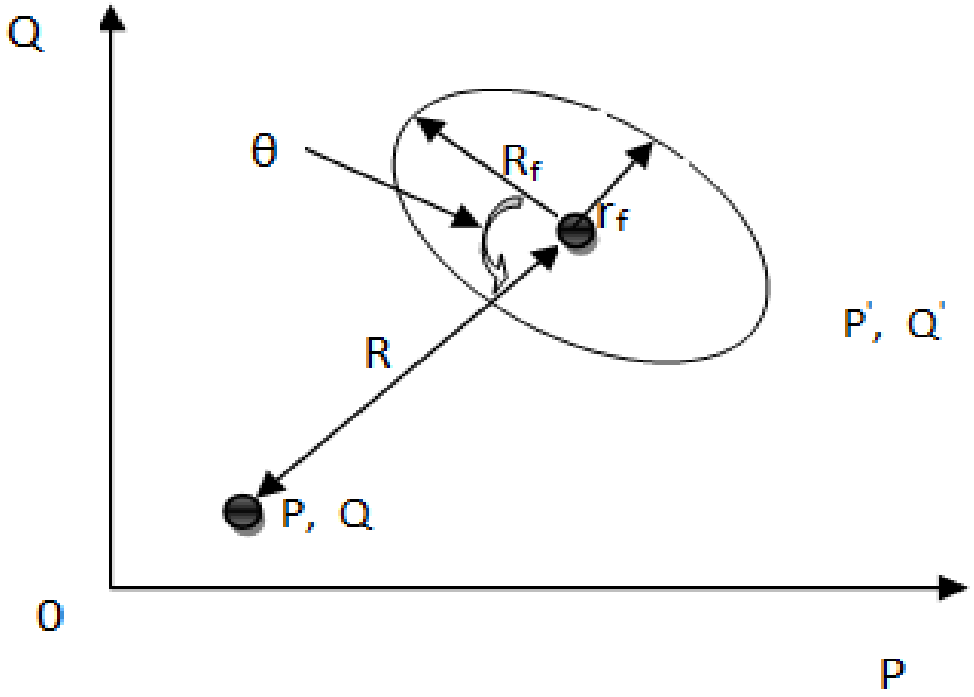

Fig.7 PQ Power ellipse

Here *R* is the distance between no-load ellipse center and the faulty one.

In (Liu. 2007) it is theoretically proved that the previous assumption is not entirely independent from the load influences.

P and Q represents induction motor active and reactive power for healthy conditions, while P' and Q' represents the real case of the system. R is the distance between healthy and broken bar ellipse center. Rf and rf represents ellipse major and min axis respectively.

The above fault factor will increase with the fault and a new severity factor can be defined as (*Leksir, A. and Bensaker, B. 2011*):

$$\boldsymbol{\nabla} = \frac{\boldsymbol{3UI}}{\sqrt{(\boldsymbol{P}-\boldsymbol{P_0})^2-(\boldsymbol{Q}-\boldsymbol{Q_0})^2}} \tag{77}$$

Where $\boldsymbol{\nabla}$ represents the new fault severity factor. P_0 and Q_0 correspond to active and reactive power for no-load case.

It can be clearly seen in the previous relation that the severity factor is oriented to study the load influences rather than faults analysis.

Literature review of the proposed severity factor SF may be presented before newSF, is proposed in this thesis, based on the extraction of fault components from the behavior of the machine, relation Eq.78, as (leksir and bensaker 2019):

$$\boldsymbol{SF = MAX}\sqrt{\frac{(\boldsymbol{P_f - P})^2 - (\boldsymbol{Q_f - Q})^2}{(\boldsymbol{P})^2 - (\boldsymbol{Q})^2}} \quad (78)$$

P_f,Q_f represent active and reactive power for faulty generator and P, Q for healthy generator.

In order to estimate the variations of fault characteristics compared to healthy conditions, the severity factor is calculated for each fault. The differences of powers used in SF simplify the evaluation of faults evolution survey.

2.4. PQ Based Induction Machine Faults Diagnosis Methods

Load and inertia influences represent the main problem encountered while analyzing induction generator behavior for faults diagnostic.

How to differentiate between load and faults influences is a key feature for using PQ transformation as diagnosis based method. In (Jin et all. 2007) a new diagnostic method that presents new diagnosis technique employ the ellipse major axis angle (α), $90° \geq \alpha \geq 0°$ correspond to load influences while $180 ° \geq \alpha \geq 90°$ the failing region. Curve analysis is an insufficient tool for machine behavior judgment, fault degradation gravity must be identified, and furthermore, in practical conditions, a combination of load and fault influences appear, this makes the differentiation between the two behaviors more difficult.

Belling in (Belling, 2001) propose fault detection factor which is proportional to the PQ ellipse major axis Rf. Variations in ellipse shape appear as changes in axis length (Liu. 2007). Influences of further factors on PQ signals other than faults make this method not ready to give a hand. (Cruz et all.,2003)

recommends $\frac{R_f}{R}$as a rotor fault factor. This ratio improves the separation of faults index from load influences. On the other hand, Jin (Jin et all., 2007) proved theoretically that the previous assumption is not entirely independent from the load influences, because, the preceding factor will augment with the increase of the indicator, and he proposes a new severity factor as:

$$\nabla = \frac{K_1}{S} \tag{79}$$

Where:∇represents the new fault severity factor, $K_1 = 3UI_1$and

$S = \sqrt{(P - P_0)^2 - (Q - Q_0)^2}$.

$P_0$and Q_0 correspond to active and reactive power for no-load condition.

One of the main issues faces that the accurate analysis of induction generator state is the capability to distinguish between different faults and load influences. It has been clearly indicated in literature (Jin et all.,2007 ; Leksir and Bensaker. 2011 ; Liu. 2007)that load changes in one hand and stator and rotor faults in the other hand appear in almost the same frequency intervals, therefore the use of conventional specter analysis is impracticable. Using PQ theory, lot of works deal with the induction generator diagnosis to minimize the influence of load, and consequently, numerous severity factors have been discussed to improve faults detection accuracy.

Through PQ ellipse's characteristics, several works have been carried out to break some barriers encountered while diagnosing induction generator. Certain papers found in literature have been dealt with separation of induction faults from other influences as load, noise, harmonics and supply power or any other external phenomena, as in (Jin et all. 2007) where the PQ ellipse angle has been proposed to be used as indicator for induction generator rotor bar faults separation from load influence.

Both active and reactive power models for rotor broken bar are modeled using supplementary components by:

$$\begin{bmatrix} \mathbf{P'} \\ \mathbf{Q'} \end{bmatrix} = \begin{bmatrix} \mathbf{P} \\ \mathbf{Q} \end{bmatrix} + \mathbf{3U} \begin{bmatrix} \mathbf{I_l \cos(2s\omega_I t + \alpha_l) + I_r \cos(2s\omega_I t - \alpha_r)} \\ \mathbf{I_l \sin(2s\omega_I t + \alpha_l) - I_r \sin(2s\omega_I t - \alpha_r)} \end{bmatrix} \quad (80)$$

Where $\mathbf{I_r}$,$\mathbf{I_l}$, $\boldsymbol{\alpha_l}$,$\boldsymbol{\alpha_r}$ are the magnitudes and phases of the left and right side band current components respectively.

The first part of the Eq. (80), $\begin{bmatrix} P \\ Q \end{bmatrix}$, correspond to the healthy behavior, the second part represents the rotor faults which characterize the ellipse parameters.
Major and minor axis can be resorted from the combination between active and reactive powers related to real and healthy conditions as presented in the following relation (Leksir and Bensaker 2009):

$$\boldsymbol{r_{min}} \leq \sqrt{(\boldsymbol{P'} - \boldsymbol{P})^2 + (\boldsymbol{Q'} - \boldsymbol{Q})^2} \leq \boldsymbol{r_{max}} \quad (81)$$

Applying a similar manner as the major, minor axis the angle is deduced from the following relation:

$$\boldsymbol{tan(\theta)} = \frac{\boldsymbol{Y}}{\boldsymbol{X}} = \frac{(\boldsymbol{Q'} - \boldsymbol{Q})}{(\boldsymbol{P'} - \boldsymbol{P})} \quad (82)$$

Introducing fault powers representations in the ellipse major and minor axis will lead to the following relations:

$$\mathbf{r_{ellipse}} = \mathbf{3U}\sqrt{(\mathbf{I_l \cos(2s\omega_I t + \alpha_l) + I_r \cos(2s\omega_I t - \alpha_r)})^2 + (\mathbf{I_l \sin(2s\omega_I t + \alpha_l) - I_r \sin(2s\omega_I t - \alpha_r)})^2} \quad (83)$$

$$\mathbf{r_{ellipse}} = \mathbf{3U}\sqrt{\mathbf{I_l}^2 \mathbf{\cos^2(2s\omega_I t + \alpha_l) + I_r}^2 \mathbf{\cos^2(2s\omega_I t - \alpha_r) +}}$$

$$\overline{\mathbf{I_l}^2\,\mathbf{sin}^2(2\mathbf{s\omega_I t}+\boldsymbol{\alpha}_\mathbf{l})+\mathbf{I_r}^2\,\mathbf{sin}^2(2\mathbf{s\omega_I t}-\boldsymbol{\alpha}_\mathbf{r})+\overline{2\mathbf{I_r I_l}\,\mathbf{cos}(2\mathbf{s\omega_I t}+\boldsymbol{\alpha}_\mathbf{l})\,\mathbf{cos}(2\mathbf{s\omega_I t}-\boldsymbol{\alpha}_\mathbf{r})-\overline{2\mathbf{I_r I_l}\,\mathbf{sin}(2\mathbf{s\omega_I t}+\boldsymbol{\alpha}_\mathbf{l})\,\mathbf{sin}(2\mathbf{s\omega_I t}-\boldsymbol{\alpha}_\mathbf{r})}}} \quad (84)$$

Finally ellipse axis will be:

$$\mathbf{r_{ellipse}}=\mathbf{3U}\sqrt{\mathbf{I_l}^2+\mathbf{I_r}^2+\mathbf{2\,I_r I_l\,cos}(\mathbf{4s\omega_I t}+\boldsymbol{\alpha}_\mathbf{l}-\boldsymbol{\alpha}_\mathbf{r})} \quad (85)$$

The major axis corresponds to $\mathbf{cos}(\mathbf{4s\omega_I t}+\boldsymbol{\alpha}_\mathbf{l}-\boldsymbol{\alpha}_\mathbf{r})=\mathbf{1}$, and short axis corresponds to$\mathbf{cos}(\mathbf{4s\omega_I t}+\boldsymbol{\alpha}_\mathbf{l}-\boldsymbol{\alpha}_\mathbf{r})=-\mathbf{1}$.

Major axis is obtained as:

$$\boldsymbol{r_{max}}=\mathbf{3}\boldsymbol{U}\sqrt{\boldsymbol{I_l}^2+\boldsymbol{I_r}^2+\mathbf{2}\,\boldsymbol{I_r I_l}}=\mathbf{3}\boldsymbol{U}\sqrt{(\boldsymbol{I_r}+\boldsymbol{I_l})^2}=\mathbf{3}\boldsymbol{U}(\boldsymbol{I_r}+\boldsymbol{I_l}) \quad (86)$$

and short axis as:

$$\boldsymbol{r_{min}}=\mathbf{3}\boldsymbol{U}\sqrt{\boldsymbol{I_l}^2+\boldsymbol{I_r}^2-\mathbf{2}\,\boldsymbol{I_r I_l}}=\mathbf{3}\boldsymbol{U}\sqrt{(\boldsymbol{I_r}-\boldsymbol{I_l})^2}=\mathbf{3}\boldsymbol{U}|\boldsymbol{I_r}-\boldsymbol{I_l}| \quad (87)$$

The angle θ between the major axis and the center of ellipse is given by the following relation:

$$\mathbf{tan}(\boldsymbol{\theta})=\frac{\mathbf{Y}}{\mathbf{X}}=\frac{\mathbf{I_l}\,\mathbf{sin}(2\mathbf{s\omega_I t}+\boldsymbol{\alpha}_\mathbf{l})-\mathbf{I_r}\,\mathbf{sin}(2\mathbf{s\omega_I t}-\boldsymbol{\alpha}_\mathbf{r})}{\mathbf{I_l}\,\mathbf{cos}(2\mathbf{s\omega_I t}+\boldsymbol{\alpha}_\mathbf{l})+\mathbf{I_r}\,\mathbf{cos}(2\mathbf{s\omega_I t}-\boldsymbol{\alpha}_\mathbf{r})}=\mathbf{tan}\left(\frac{\boldsymbol{\alpha}_\mathbf{l}+\boldsymbol{\alpha}_\mathbf{r}}{\mathbf{2}}\right) \quad (88)$$

As result $\boldsymbol{\theta}=\frac{\boldsymbol{\alpha_l}+\boldsymbol{\alpha_r}}{\mathbf{2}}$

As it was discussed before, induction generator faults diagnosis based on, power system model with a minimal influence of the load can be obtained only when using appropriate PQ ellipse characteristics. Longest and shortest radius

together with the angle between the longest radius and the ellipse center represent the main parameters that a diagnostic system can be based on.

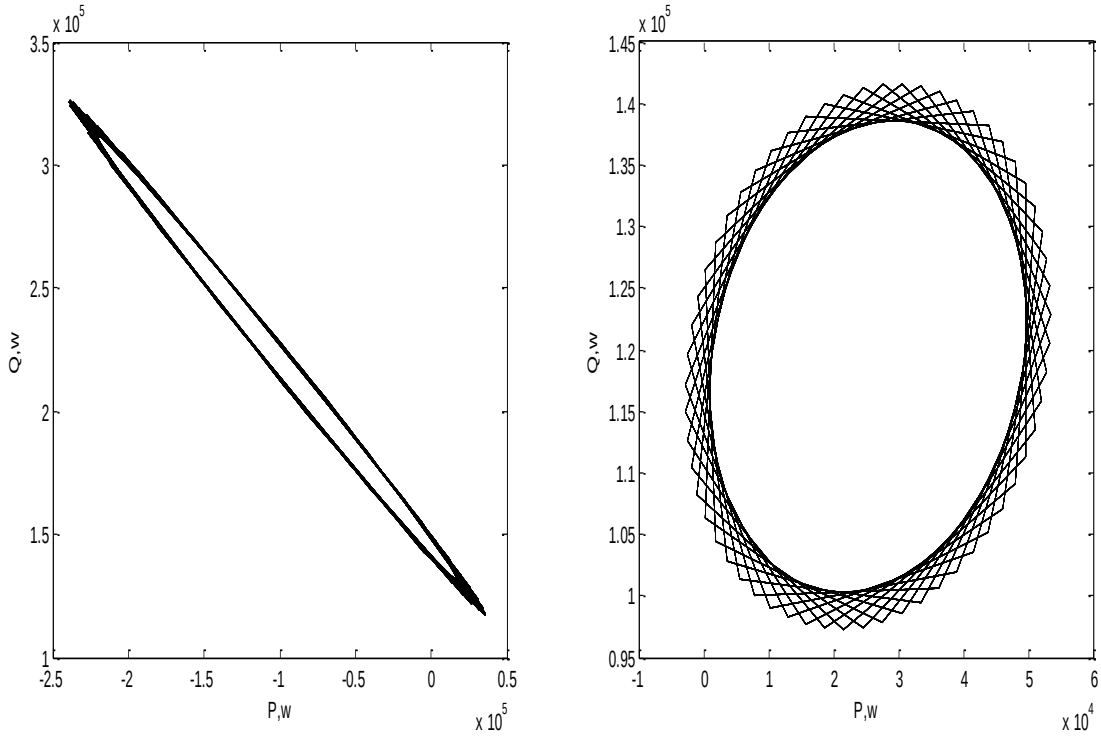

-a-under faulty condition **-b-**under load condition

Fig.8 PQ power ellipse for faulty and under load conditions

The left form represents PQ ellipse that the generator suffer from rotor faults, $\alpha > 90$ represents the ellipse angle. Conversely, the right form correspond to under load situation when$\alpha < 90$.

This result has been carried out for rotor broken bars only, introducing stator faults will makes this results erroneous as it is illustrated in Fig9.

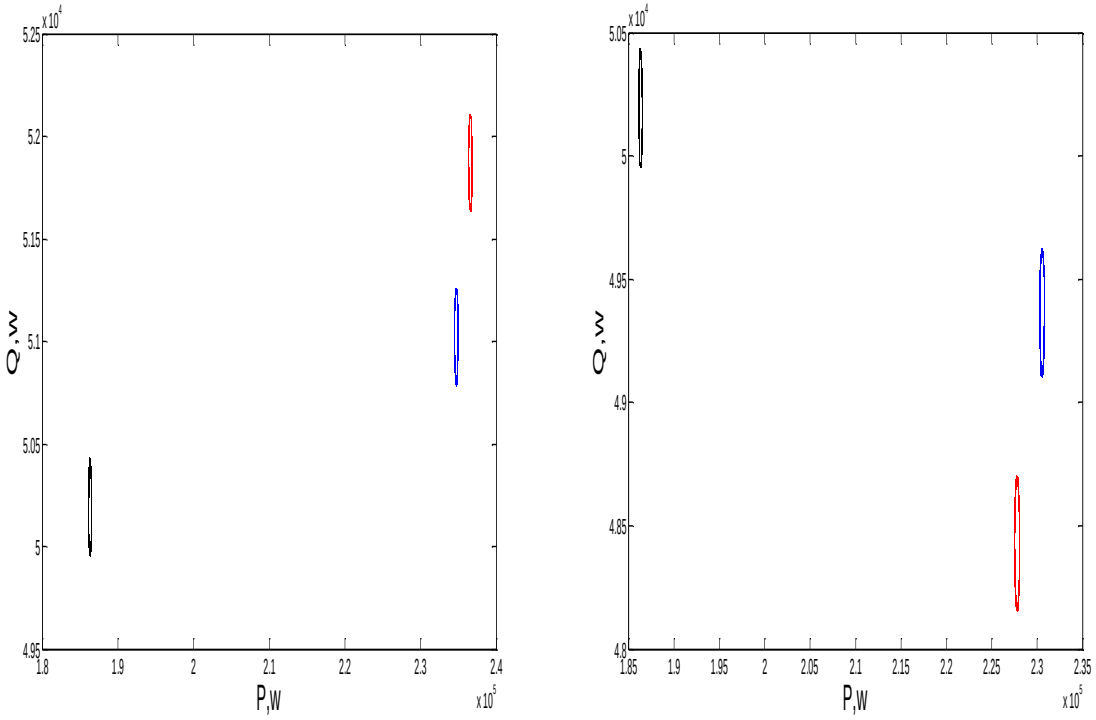

STATOR ROTOR

Fig.9 PQ power ellipse for healthy (Black), faulty (Red) and under load (Bleu) conditions.

A combination of active and reactive power will leads to PQ ellipses, fig. 9. One can see that the orientation of faulty together with under load ellipse hasn't changed only the position; they were displaced compared to the healthy ellipse. In addition, it is really difficult task to extract the exact practically occurred fault, from the other ordinary behaviors of induction machine or external phenomena (Leksir and Bensaker 2009). Moreover, through the PQ transformation it is really difficult task to distinguish the different levels of fault, and more complicated concerning the separation of the interaction of other faults or transitory behavior levels.

However, industrial environment together with the internal behavior of induction generator illustrate that, there are multiple problems that can occur and lead to total or partial damage of induction generator, these problems come up from output measurements, which lead to deformation of ellipse shape. The

complexity of IG diagnosis is the idea that different damages and other influences, have impacts on the ellipse angle orientation, which will make confusion and the application of the previous method will be difficult task. Consequently, rotor faults, stator faults and load influences, ellipse my take place in the same trigonometric quarter. A new approach is proposed in this thesis, instead of using the raw active and reactive power, the evolution of these parameters due to changes introduced by faults is proposed to be analyzed in order to diagnosis induction machine situation.

In this thesis a severity factor (SF) has been proposed. Load has been introduced into induction generator behavior in both stator and rotor faults conditions, results confirm that SF proposed in Eq.78 is independent from load influences,

Chapter3: Induction Generator Powers Fault based Diagnosis Methods.

3.1 Healthy Induction Generator Powers Modeling

The process of abnormalities detection is based on the fact that they cause periodic disturbance of generator's variables, such as current, flux, torque, speed and hence the induced powers as active, reactive, total and partial instantaneous, complex and power transferred from stator to rotor. Thus, spectral analysis of those variable or related quantities may yield a warning about incipient failure of the drive system. Although, the traditional diagnostics method are mostly based on the signature analysis of the stator current, this is because its availability in the major systems of the induction generators applications. Other media can also be employed, as the total and partial instantaneous power, active and reactive power, complex apparent power and transformed from mechanical to electrical power form.

The fundamental of any condition monitoring depends on understanding the electric, magnetic and mechanical behavior of the machine in both healthy and faulty states. An induction machine is a highly symmetrical system and the presence of any kind of fault modifies its symmetry and produces changes in the measured sensor signals, or more precisely, in the magnitude of certain fault frequencies (Intesar et all. 2010).

The signal characteristics (such as magnitude of a frequency component) for indicating existence or level of fault magnitude is named a fault indicator. Ideal fault indicator should exhibit a measurable change when the imbalance level increases with the size of the fault. In addition, a fault indication should have small or otherwise non consistent variation with load and should be independent of other faults (Drif, M. and Cardoso, M. A. J. 2012).

In this study, a deep analysis of induction generator behavior in healthy conditions and under fault's circumstances taking into account the load influences is carried out in the following.

3.1.1 Healthy Partial and Total Power

In order to make comprehensive analysis of induction generator defects, it is necessary to analyze total instantaneous power of three phase induction generator in the (*a*, *b*, *c*) reference frame.
First the instantaneous power of one phase is classically given by:

$$\boldsymbol{P_a(t) = v_a(t) i_a(t)} \tag{89}$$

The total instantaneous power of a healthy induction generator can be calculated by the Eq. (90) using the three phase measured instantaneous voltages and currents (Kucukerand Bayrak, 2013):

$$\boldsymbol{P_t(t) = v_a(t)i_a(t) + v_b(t)i_b(t) + v_C(t)i_C(t) = 3UI\cos(\alpha)} \quad (90)$$

Where *U* and *I* are the maximum values of voltage and current respectively, and $\boldsymbol{\alpha}$is the phase angle.

The instantaneous partial power of the generator between the phases *a* and *b* is (Trzynadlowski, 1999):

$$\mathbf{P_{ab}(t) = v_{ab}(t)i_a(t)} \quad (91)$$

$$\mathbf{v_{ab}} = \sqrt{2}\mathbf{U}\cos(\mathbf{wt}) - \sqrt{2}\mathbf{U}\cos\left(\mathbf{wt} - \frac{2\pi}{3}\right)$$

$$= \sqrt{2}\mathbf{U}\left(\cos(\mathbf{wt}) - \cos\left(\mathbf{wt} - \frac{2\pi}{3}\right)\right)$$

$$= \sqrt{2}\mathbf{U}\left(\cos(\mathbf{wt}) - (\cos(\mathbf{wt})\cos\left(\frac{2\pi}{3}\right) + \sin(\mathbf{wt})\sin\frac{2\pi}{3})\right)$$

$$= \sqrt{2}\mathbf{U}\left(\cos(\mathbf{wt}) - (\cos(\mathbf{wt})\left(-\frac{1}{2}\right) + \sin(\mathbf{wt})\left(\frac{\sqrt{3}}{2}\right))\right)$$

$$= \sqrt{2}\mathbf{U}\left(\frac{3}{2}\cos(\mathbf{wt}) - \frac{\sqrt{3}}{2}\sin(\mathbf{wt})\right)$$

$$= \sqrt{6}\mathbf{U}\left(\frac{\sqrt{3}}{2}\cos(\mathbf{wt}) - \frac{1}{2}\sin(\mathbf{wt})\right)$$

$$= \sqrt{6}\mathbf{U}\left(\cos(\mathbf{wt})\cos\left(\frac{\pi}{6}\right) - \sin\left(\frac{\pi}{6}\right)\sin(\mathbf{wt})\right)$$

$$= \sqrt{6}\mathbf{U}\cos\left(\mathbf{wt} + \frac{\pi}{6}\right) \quad (92)$$

Here $\mathbf{v_{ab}} = \sqrt{6}\mathbf{U}\cos\left(\boldsymbol{\omega}\mathbf{t} + \frac{\pi}{6}\right)$is line to line voltage between the phase *a* and *b*

Applying the Park transformation the above relations for healthy system yields to:

$$\boldsymbol{P_t(t) = \left(v_{dq}\right)^T P(\theta)^{-1} P(\theta)\left(i_{dq}\right) = \left(v_{dq}\right)^T\left(i_{dq}\right) = 3UI\cos(\alpha)} \quad (93)$$

In the case where the Park reference frame (*d*, *q*) is aligned with the stator axes, the inverse Park matrix reduces to:

$$\boldsymbol{P(\theta)^{-1}} = \sqrt{\frac{2}{3}}\begin{bmatrix} \mathbf{1} & \mathbf{0} & \frac{\mathbf{1}}{\sqrt{\mathbf{2}}} \\ -\frac{\mathbf{1}}{\mathbf{2}} & \frac{\sqrt{\mathbf{3}}}{\mathbf{2}} & \frac{\mathbf{1}}{\sqrt{\mathbf{2}}} \\ -\frac{\mathbf{1}}{\mathbf{2}} & -\frac{\sqrt{\mathbf{3}}}{\mathbf{2}} & \frac{\mathbf{1}}{\sqrt{\mathbf{2}}} \end{bmatrix} \quad (94)$$

Following the same way, as total power, the partial power expression using the Eq. 91 can be written as:

$$\mathbf{P_{ab}(t)} = (\mathbf{v_a} - \mathbf{v_b})\mathbf{i_a} = \mathbf{i_d}\left(\frac{\mathbf{1}}{\mathbf{3}}\mathbf{v_d} - \frac{\mathbf{1}}{\sqrt{\mathbf{3}}}\mathbf{v_q}\right) = \sqrt{\mathbf{3}}\mathbf{U\ I}\ \mathbf{cos}(\boldsymbol{\alpha}) \quad (95)$$

which instantaneous electric power, partial or total, is better as a diagnostic medium for induction generator faults diagnosis is more difficult to answer. A profounder study of the capability of each power to detect faults should carry out.

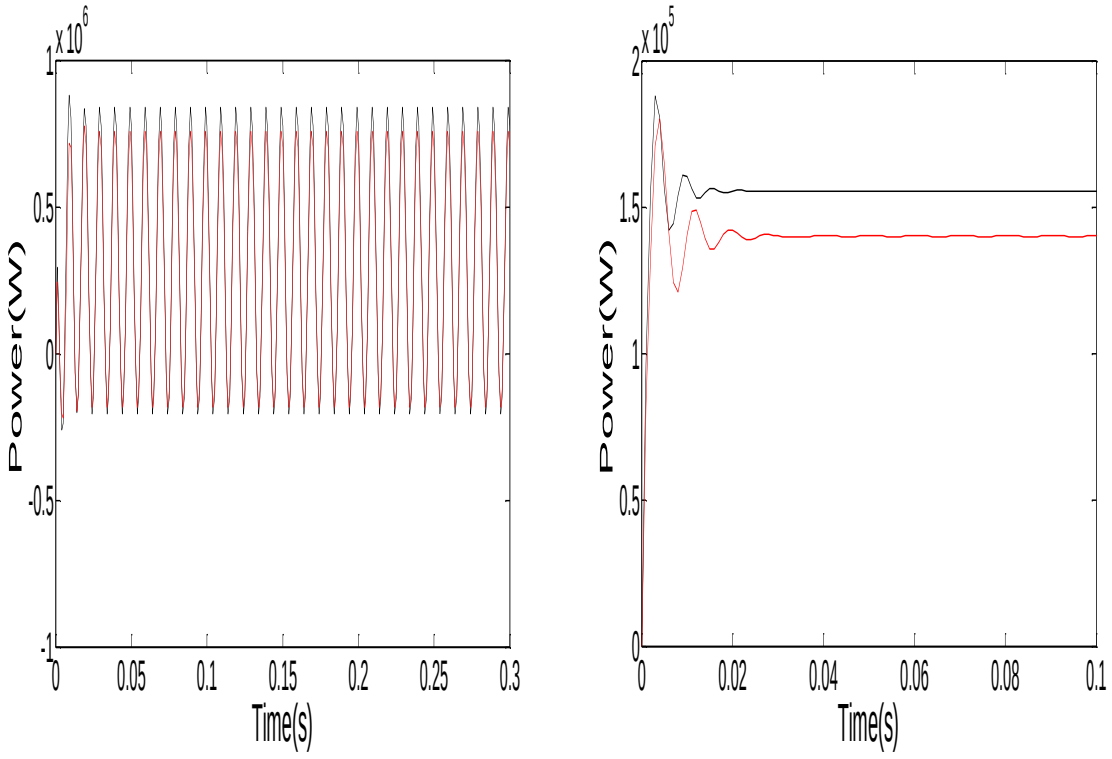

-a- Partial power -b- Total power

Fig.10 Total and partial instantaneous power

The use of instantaneous power offers certain advantages over the stator current approach, especially under noisy conditions.

Some advantages of using instantaneous power spectrum are given as follows (Benbouzid, 2000; Didier et all., 2006):

- Presence of additional components in frequencies domain;
- First low frequency component is positioned directly at the speed oscillation frequency;
- Easier filtering of the DC component in the power spectrum than to remove the 50 Hz fundamental component in the current spectrum without affecting the faults components, in case of a very small slip.

Under ideal conditions, the total and partial powers spectrum consists of a dc component and a sinusoidal component whose frequency equal to two times the fundamental frequency.

3.1.2 Healthy Complex Apparent Power and Active-Reactive Power

It is generally accepted that under sinusoidal conditions, with the combination of active power and the reactive power, a new power concept appear as complex apparent power.

The instantaneous complex apparent power is defined in three phase system (*a*, *b*, *c*) and Park's reference frame (*d*, *q*) respectively as the following (Drif and Cardoso 2012; Fiorucci 2015):

$$\mathbf{S} = \mathbf{v_a i_a} + \mathbf{v_b i_b} + \mathbf{v_c i_c} + \mathbf{j}\frac{\mathbf{1}}{\sqrt{\mathbf{3}}}[(\mathbf{v_a} - \mathbf{v_b})\mathbf{i_c} + (\mathbf{v_b} - \mathbf{v_c})\mathbf{i_a} + (\mathbf{v_c} - \mathbf{v_a})\mathbf{i_b}] \quad (96)$$

$$\boldsymbol{S} = \frac{\mathbf{3}}{\mathbf{2}}\left[\boldsymbol{v_d i_d} + \boldsymbol{v_q i_q} + \boldsymbol{j}\left(\boldsymbol{v_q i_d} - \boldsymbol{v_d i_q}\right)\right] \quad (97)$$

Let$\boldsymbol{P} = \boldsymbol{v_d i_d} + \boldsymbol{v_q i_q}$ and $\boldsymbol{Q} = \boldsymbol{v_q i_d} - \boldsymbol{v_d i_q}$then the apparent power is given by:

$$\boldsymbol{S} = \boldsymbol{P} + \boldsymbol{jQ} = \boldsymbol{3UI} \quad (98)$$

Here $\boldsymbol{P}$ and $\boldsymbol{Q}$ are known as the active and reactive power respectively.

Notice that the apparent power is the sum of active and reactive power parts. Active power $\boldsymbol{P}$ and the reactive power $\boldsymbol{Q}$ represent the real and imaginary parts of the apparent power respectively.

A matrix representation of the active and reactive powers can be as:

$$\begin{bmatrix} \boldsymbol{P} \\ \boldsymbol{Q} \end{bmatrix} = \begin{bmatrix} \boldsymbol{v_{sd}} & \boldsymbol{v_{sq}} \\ -\boldsymbol{v_{sq}} & \boldsymbol{v_{sd}} \end{bmatrix} \begin{bmatrix} \boldsymbol{i_{sd}} \\ \boldsymbol{i_{sq}} \end{bmatrix} \quad (99)$$

The negative sign of the reactive power has no physical meaning. It only defines the direction of the energy flow. To obtain positive value an automatic negative multiplication is needed (Liu et all., 2007).

These concepts are in the evaluation and design of induction generator, some modifications are necessary, and when stator or rotor fault takes place, additional components must be introduced (Bitoleanu et all., 2007).

For healthy three phases system active power is given by:

$$\boldsymbol{P} = (\boldsymbol{v_{abc}})^{\boldsymbol{T}} \boldsymbol{I_s} = \boldsymbol{v_a i_a} + \boldsymbol{v_b i_b} + \boldsymbol{v_c i_c} \quad (100)$$

$$\boldsymbol{P} = \boldsymbol{v_{sd} i_{sd}} + \boldsymbol{v_{sq} i_{sq}} \quad (101)$$

$$\boldsymbol{Q} = (-\boldsymbol{H}(\boldsymbol{v_{sd}}))\boldsymbol{i_{sd}} + (-\boldsymbol{H}(\boldsymbol{v_{sd}}))\boldsymbol{i_{sq}} \quad (102)$$

Using the park transformation the voltage and current are $\boldsymbol{v_{dq}} = \boldsymbol{P}(\boldsymbol{\theta})(\boldsymbol{v_{abc}})$ and $\boldsymbol{i_{dq}} = \boldsymbol{P}(\boldsymbol{\theta})(\boldsymbol{i_{abc}})$

Where$\boldsymbol{P}(\boldsymbol{\theta})^{\boldsymbol{T}} = \boldsymbol{P}(\boldsymbol{\theta})^{-\boldsymbol{1}}$,

The active power Eq.102 will be

$$\mathbf{P} = \left(\mathbf{v_{dq}}\right)^{\mathbf{T}}\mathbf{P(\theta)^{-1}P(\theta)}\left(\mathbf{i_{dq}}\right) =$$

$$\left(\boldsymbol{v_{dq}}\right)^{\boldsymbol{T}}\left(\boldsymbol{i_{dq}}\right)=\left(\sqrt{\mathbf{3}}\boldsymbol{U} \quad \mathbf{0}\right)\begin{pmatrix}\sqrt{\mathbf{3}}\boldsymbol{I}\,\mathbf{cos(\alpha)}\\ \sqrt{\mathbf{3}}\,\boldsymbol{I}\mathbf{sin(\alpha)}\end{pmatrix} \quad (103)$$

$$\mathbf{P} = \mathbf{3UI\,cos(\alpha)} \quad (104)$$

Following the same way we obtain the reactive power relation.

$$\boldsymbol{Q} = (-\boldsymbol{H}(\boldsymbol{v_{abc}}))^{\boldsymbol{T}}\boldsymbol{i_s} \quad (105)$$

Using the characteristic of HILBERT transformation H [B] =AH [B] =H [A] B.

$$\boldsymbol{H}(\boldsymbol{v_{abc}}) = \boldsymbol{H}(\boldsymbol{P}(\boldsymbol{\theta})\boldsymbol{v_{dq}}) = \boldsymbol{P}(\boldsymbol{\theta})\boldsymbol{H}(\boldsymbol{v_{dq}}) \quad (106)$$

$$\boldsymbol{H}(\boldsymbol{v_{abc}})^{\boldsymbol{T}} = \boldsymbol{H}(\boldsymbol{v_{dq}})^{\boldsymbol{T}}\boldsymbol{P}(\boldsymbol{\theta})^{\boldsymbol{T}} = \boldsymbol{H}(\boldsymbol{v_{dq}})^{\boldsymbol{T}}\boldsymbol{P}(\boldsymbol{\theta})^{\mathbf{-1}} \quad (107)$$

$$\boldsymbol{Q} = \left(-\boldsymbol{H}(\boldsymbol{v_{dq}})\right)^{\boldsymbol{T}}\boldsymbol{P}(\boldsymbol{\theta})^{\mathbf{-1}}\boldsymbol{P}(\boldsymbol{\theta})\boldsymbol{i_{dq}} = \left(-\boldsymbol{H}(\boldsymbol{v_{dq}})\right)^{\boldsymbol{T}}\boldsymbol{i_{dq}} \quad (108)$$

$$\boldsymbol{Q} = \mathbf{3}\boldsymbol{UI}\,\mathbf{sin}(\boldsymbol{\alpha}) \quad (109)$$

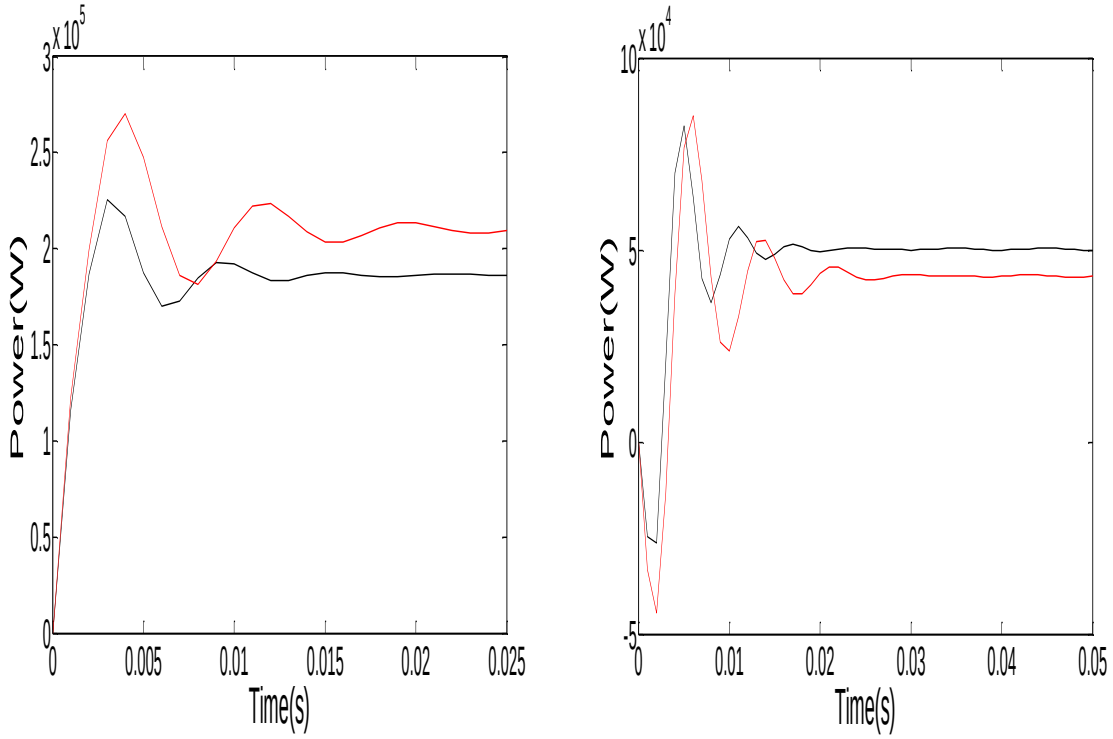

-a- Active power -b- Reactive power

Fig.11 Active and reactive power

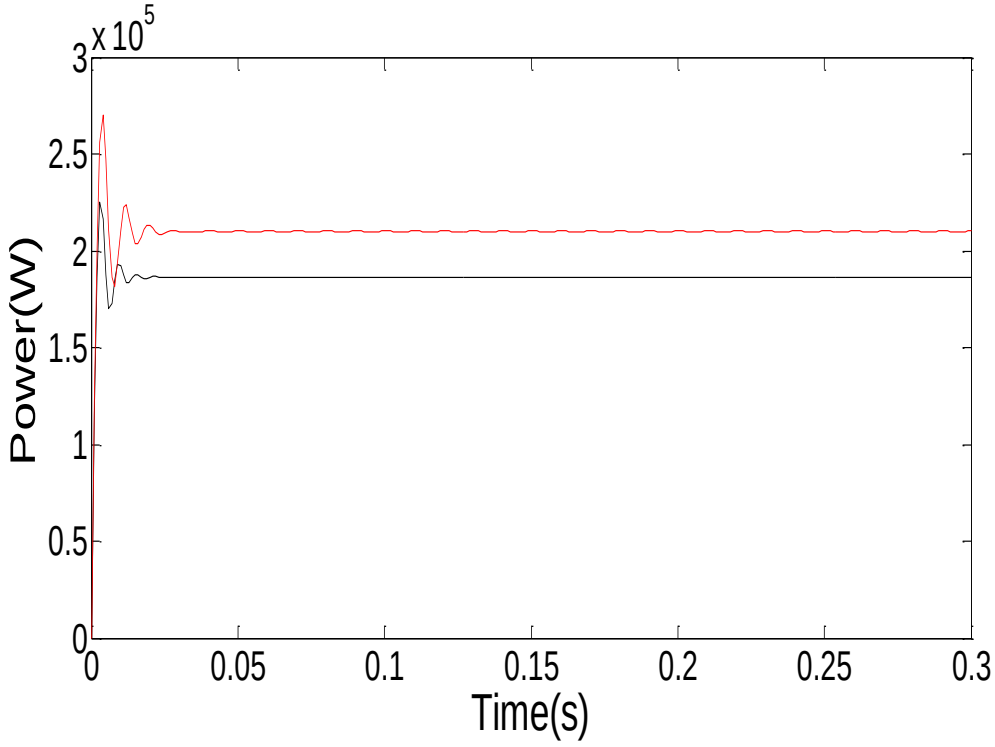

Fig.12 The complex apparent power

The black curve represents the system in healthy conditions and the red one represents the system in faulty conditions in, figure (11) and figure (12), complex power and both active and reactive power. It can be clearly seen that

faulty and healthy curves follow almost the same evolution, and then induction generator complex, active and reactive power diagnosis based on time domain leads to inaccurate results.

The use of active and reactive power for induction machine faults diagnosis isincreasing rapidly. This is due to their capability to differentiate between the machine faults and the load variation (Drif and Cardoso2012).

3.1.3 Healthy Mechanic to Electric Transformed Power

It is well known that the active power Eq.103, of the induction generator is the product of voltage and current. Using the equations of the induction generator model, relations Eq.9 and Eq.10, the active power expression can be written as :

$$\boldsymbol{P_{ac} = \left[r_s i_{sd}^2 + r_s i_{sq}^2\right] + \left[\frac{d}{dt}\varphi_{sd} i_{sd} + \frac{d}{dt}\varphi_{sq} i_{sq}\right] + \left[\omega_s\left(\varphi_{sd} i_{sq} - \varphi_{sd} i_{sd}\right)\right]} \quad (110)$$

It can be clearly seen that the relation Eq.110 is divided to three components. The first component represents Joule losses; the second one is the electromagnetic power stored by the field. The third part corresponds to the power transferred from mechanical nature to electric nature.

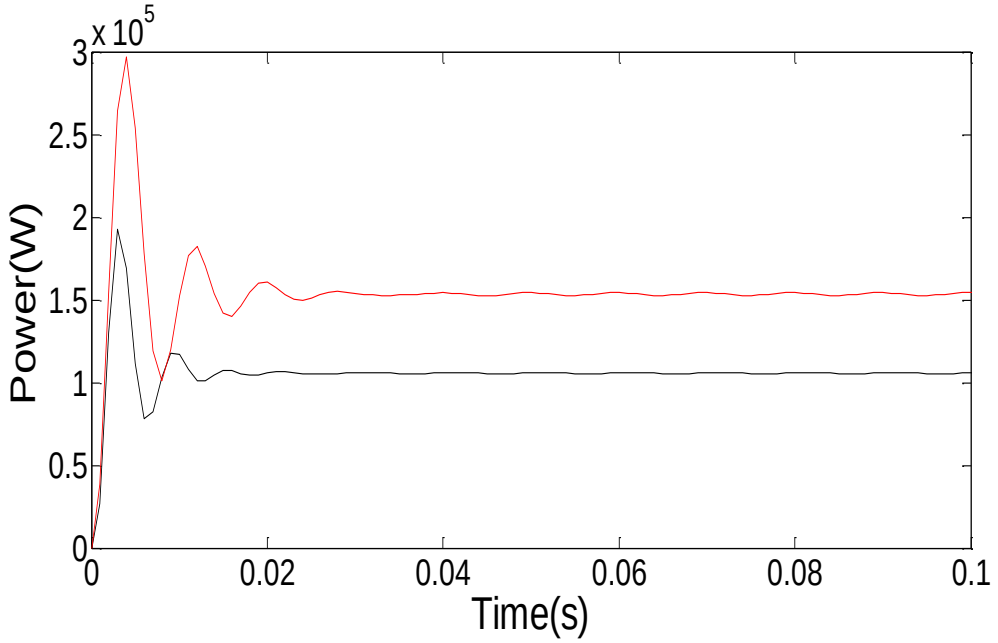

Fig.13 Transformed power

In Figure (13) the black curve represents the healthy system and the red one represents the faulty system. The interaction between the two curves, healthy and faulty, makes induction generator diagnostic based on transformed power in time domain hard task.

3.2. Induction Generator Fault Modeling

The only practically accessible signals of the induction generator system are the currents and the supply voltages. The availability of these currents is allowed through current clips or current sensors, not requiring any disconnection in power supply circuit.

Generator modeling in the presence of faults, stator current contains a new left and right side band components which can be expressed as (Liu et all. 2007):

$$\boldsymbol{i_f(t) = \sqrt{2} I \cos(\omega t - \alpha) + \sqrt{2} I_l \cos\big((1-2s)\omega t - \alpha_l\big) + \sqrt{2} I_r \cos\big((1+2s)\omega t - \alpha_r\big)} \quad (111)$$

Where s is the slip of the induction generator. $\boldsymbol{I_l}$ and $\boldsymbol{I_r}$ are the magnitudes of the left and right sideband current components respectively. $\boldsymbol{\alpha_l}$ and $\boldsymbol{\alpha_r}$ are the phases of the left and right sideband current components respectively.

In the case of rotor faults we notice the appearance of two sideband harmonic components, in the stator current spectrum, located at the frequency of $\boldsymbol{(1 \pm 2s)f}$(Bellini et All. 2001). The well known motor current signature analysis (MCSA) method is based on the detection of these sidebands harmonic components.

Similarly, stator short turns can be found via the MCSA. The objective is to identify current components in the stator winding that are function of shorted

turns. It has been proven in several papers, using MCSA, that the following equation gives the frequency components of shorted turns (Chilengue, et all., 2011; Elayaraja, Natarajan, 2015; Da Silva et all., 2008):

$$\boldsymbol{f_{st} = f\left\{\frac{n}{p}(1-s) \pm k\right\}} \quad (112)$$

Where f_{st} represent the frequency components that are function of shorted turns, f is the supply frequency, n =1,2,3…, k=1,3,5…, p is the number pole-pairs, and$s$ is the slip.

Full details of the theory and application of MCSA to diagnose shorted turns can be found in (Thomson, W. and Fenger, M., 2001).
This means that the fault characteristic frequency is very close to the supply frequency, and the amplitude of the fault harmonics in currents spectrum is very small. As a result, the fault characteristic frequency is almost always submerged by the fundamental component, which makes the fault diagnosis a difficult task.
Generator power signature analysis considered as a more convenient and reliable method for induction machine fault detection (Benbouzid 2000).

3.2.1. Faulty Partial and Total Power Model

The method presented in this thesis, uses all components created by the rotor/stator fault in the instantaneous power spectrum for the final diagnosis. We show that additional information carried by the instantaneous power in frequency domain improves the diagnosis of broken rotor bars and or stator short cut.

The instantaneous power of the generator can be used to detect wide range of abnormalities. Power contains more diagnostic information that allows analyzing and detecting defects caused by supply asymmetry.

In this case of faulty generator the total power can be expressed as (leksir and bensaker 2019):

$$\boldsymbol{P_t = 3UI\,cos(\alpha) + 3U[I_l\,cos(2s\omega t + \alpha_l) + I_r\,cos(2s\omega t - \alpha_r)]} \qquad (113)$$

One can see that the first term represents healthy power and the second term represents the faulty components of the power. Notice that in the power spectrum one can see the appearance of two components superposed and located at the frequency of$2sf$. In a similar way the partial power of the faulty generator can be expressed as:

$$\boldsymbol{P_p = \sqrt{3}\,(UI\,cos(\alpha)) + \sqrt{3}U[I_l\,cos(2s\omega t + \alpha_l) + I_r\,cos(2s\omega t - \alpha_r)]} \quad (114)$$

Once again one can see the appearance of the sideband components in the second term that represents the effect of the appearance of a fault.

In case of symmetrical phase generator, the spectrum of total instantaneous power signal contains only the main component. Thus, every kind of generator fault asymmetry leads to appearance of harmonic components in the spectrum. For a healthy generator, the partial power spectrum contains in addition of a dc component another component oscillating at twice the supply frequency *f*. Consequently, the total and partial instantaneous power spectra are powerful means to diagnose induction generator faults because they contain information that concern phase defects and supply voltage asymmetry (Zagirnyak, et all., 2013;Trzynadlowski,1999*)*.

Total faulty power is given by:

$$\boldsymbol{[P'] = [P] + 3U[I_l\,cos(2s\omega_l t + \alpha_l) + I_r\,cos(2s\omega_l t - \alpha_r)]} \qquad (115)$$

$$\mathbf{P_{totpar} = P_{par} + P_{parfault}}$$

$$\mathbf{= UI[cos(wt) + cos(3wt)]}$$

$$\mathbf{+UI_l[cos(2swt + \alpha_l) + cos(2(s-1)wt + \alpha_l)]}$$

$$\mathbf{+UI_r[cos(2swt - \alpha_r) + cos(2(s+1)wt - \alpha_l)]} \qquad (116)$$

It is found that the use of partial power signatures gives more information about faults than the use of stator current signatures. Hence, the partial power spectrum will contain additional components which express fault types. The magnitude of these components with respect to the DC component (or twice the supply frequency component) will express fault severity.

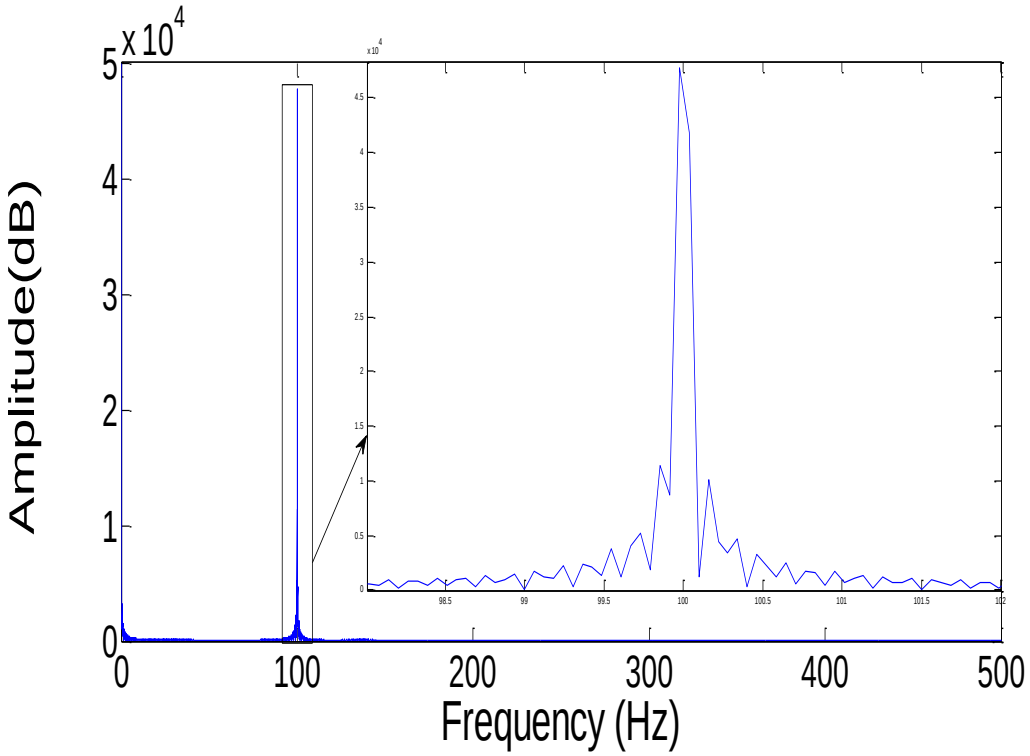

Fig.14 Partial power Spectrum

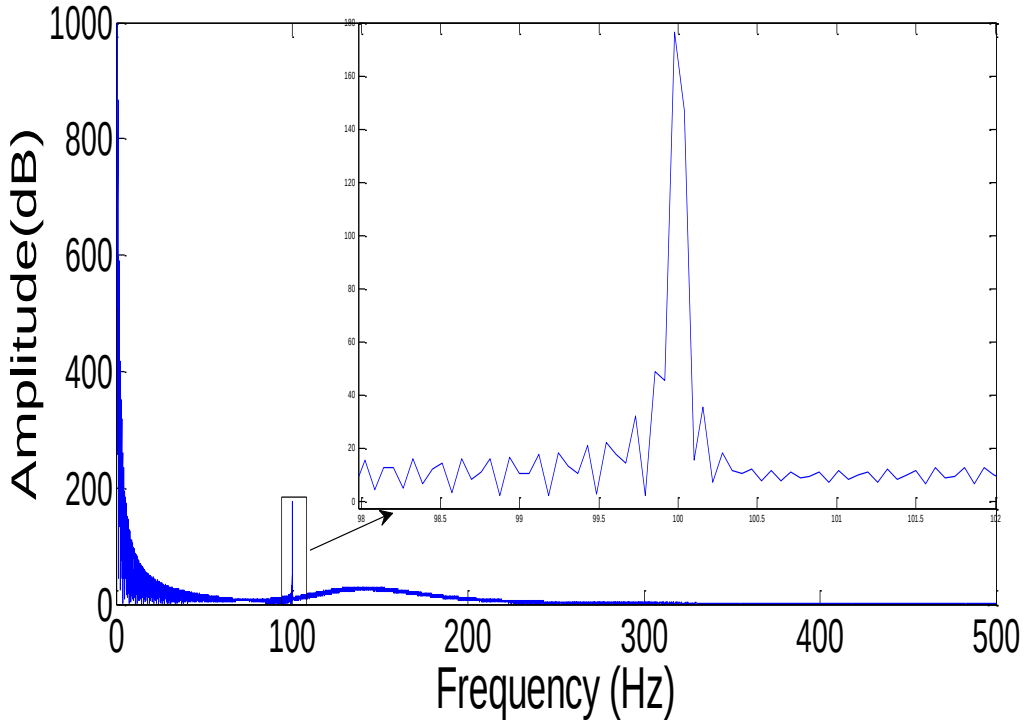

Fig.15 Total power Spectrum

Figure 14 and figure 15 represent partial and total spectrum of faulty induction generator. In both total and partial power a zoom has been taken out to point out the influence of fault. Two additional sideband components left and right take place are clearly seen in both spectrum of total and partial power.

3.2.2 Faulty Active and Reactive Power model

The faulty three phases system active power is given by:

$$\boldsymbol{P = (v_{abc})^T I_s{}' = v_a i_a{}' + v_b i_b{}' + v_c i_c{}'} \qquad (117)$$

Given that the three phase currents for fault system are $\boldsymbol{i_a{}' = i_{a+} i_{af}, i_b{}' = i_{b+} i_{bf}, i_c{}' = i_{c+} i_{cf}}$.

$$\boldsymbol{i_{af} = \sqrt{2} I_l \cos((1-2s)wt - \alpha_l) + \sqrt{2} I_r \cos((1+2s)wt - \alpha_r)} \qquad (118)$$

$$\mathbf{i_{bf}} = \sqrt{2}\mathbf{I_l}\cos((\mathbf{1-2s})\mathbf{wt} - \boldsymbol{\alpha}_\mathbf{l} - \frac{\mathbf{2\pi}}{\mathbf{3}}) + \sqrt{2}\mathbf{I_r}\cos((\mathbf{1+2s})\mathbf{wt} - \boldsymbol{\alpha}_\mathbf{r}\frac{\mathbf{2\pi}}{\mathbf{3}}) \quad (119)$$

$$\mathbf{i_{cf}} = \sqrt{2}\mathbf{I_l}\cos((\mathbf{1-2s})\mathbf{wt} - \boldsymbol{\alpha}_\mathbf{l} + \frac{\mathbf{2\pi}}{\mathbf{3}}) + \sqrt{2}\mathbf{I_r}\cos((\mathbf{1+2s})\mathbf{wt} + \boldsymbol{\alpha}_\mathbf{r}\frac{\mathbf{2\pi}}{\mathbf{3}}) \quad (120)$$

$\mathbf{i_{af}}, \mathbf{i_{bf}}, \mathbf{i_{cf}}$ are the induced currents by the defect, taking into account the induced current. The new formula of active power is

$$\boldsymbol{P} = \boldsymbol{v_a i_a}' + \boldsymbol{v_b i_b}' + \boldsymbol{v_c i_c}' = \boldsymbol{v_a}(\boldsymbol{i_{a+} i_{af}}) + \boldsymbol{v_b}(\boldsymbol{i_{b+} i_{bf}}) + \boldsymbol{v_c}(\boldsymbol{i_{c+} i_{cf}}) \quad (121)$$

$$\boldsymbol{P} = (\boldsymbol{v_a i_a} + \boldsymbol{v_b i_b} + \boldsymbol{v_c i_c}) + \left(\boldsymbol{v_a i_{af}} + \boldsymbol{v_b i_{bf}} + \boldsymbol{v_c i_{cf}}\right) \quad (122)$$

$$\boldsymbol{P'} = \boldsymbol{P_{healthy}} + \boldsymbol{P_{faulted}} \quad (123)$$

$$\boldsymbol{P} = \left(\boldsymbol{v_{dq}}\right)^{\boldsymbol{T}} \boldsymbol{P(\theta)}^{-1} \boldsymbol{P(\theta)} \left(\boldsymbol{i_{dq}} + \boldsymbol{i_{dqfaulted}}\right) \quad (124)$$

$$\boldsymbol{P} = \left(\boldsymbol{v_{dq}}\right)^{\boldsymbol{T}} \left(\boldsymbol{i_{dq}}\right) + \left(\boldsymbol{v_{dq}}\right)^{\boldsymbol{T}} \left(\boldsymbol{i_{dqfaulted}}\right) \quad (125)$$

$$\boldsymbol{I_{dqfaulted}} = \boldsymbol{P(\theta)} \boldsymbol{I_{abcfaulted}} \quad (126)$$

$$\boldsymbol{I_{dqfaulted}} = \begin{bmatrix} \boldsymbol{i_{dfaulted}} \\ \boldsymbol{i_{qfaulted}} \end{bmatrix} = \begin{bmatrix} \boldsymbol{i_{dlfaulted}} + \boldsymbol{i_{drfaulted}} \\ \boldsymbol{i_{qlfaulted}} + \boldsymbol{i_{qrfaulted}} \end{bmatrix} \quad (127)$$

$$\boldsymbol{i_{dlfaulted}} = \sqrt{\frac{\mathbf{2}}{\mathbf{3}}} \boldsymbol{I}\sqrt{\mathbf{2}} \left[\boldsymbol{\cos}(\boldsymbol{w_s t})\, \boldsymbol{\cos}\left((\mathbf{1-2s})\boldsymbol{w_s t} - \boldsymbol{\alpha_l}\right) + \boldsymbol{\cos}\left(\boldsymbol{w_s t} - \frac{\mathbf{2\pi}}{\mathbf{3}}\right) \boldsymbol{\cos}(\mathbf{1-2s})\boldsymbol{w_s t} - \boldsymbol{\alpha_l} - \frac{\mathbf{2\pi}}{\mathbf{3}}) + \boldsymbol{\cos}\left(\boldsymbol{w_s t} + \frac{\mathbf{2\pi}}{\mathbf{3}}\right) \boldsymbol{\cos}\left((\mathbf{1-2s})\boldsymbol{w_s t} - \boldsymbol{\alpha_l} + \frac{\mathbf{2\pi}}{\mathbf{3}}\right) \quad (128)$$

$$\boldsymbol{i_{dlfaulted}} =$$

$$\frac{\mathbf{2}}{\sqrt{\mathbf{3}}}\boldsymbol{I}\left[\frac{\mathbf{1}}{\mathbf{2}}\{\boldsymbol{cos}(\boldsymbol{w_s t}+(\mathbf{1}-\mathbf{2}\boldsymbol{s})\boldsymbol{w_s t}-\boldsymbol{\alpha_l})+\boldsymbol{cos}(\boldsymbol{w_s t}-(\mathbf{1}-\mathbf{2}\boldsymbol{s})\boldsymbol{w_s t}+\boldsymbol{\alpha_l})\}+\frac{\mathbf{1}}{\mathbf{2}}\right.$$

$$\left\{\boldsymbol{cos}\left(\boldsymbol{w_s t}+(\mathbf{1}-\mathbf{2}\boldsymbol{s})\boldsymbol{w_s t}-\boldsymbol{\alpha_l}-\frac{\mathbf{2\pi}}{\mathbf{3}}\right)+\boldsymbol{cos}\left(\boldsymbol{w_s t}-\frac{\mathbf{2\pi}}{\mathbf{3}}-(\mathbf{1}-\mathbf{2}\boldsymbol{s})\boldsymbol{w_s t}+\boldsymbol{\alpha_l}+\right.\right.$$

$$\left.\left.\frac{\mathbf{2\pi}}{\mathbf{3}}\right)\right\}+\frac{\mathbf{1}}{\mathbf{2}}\left\{\boldsymbol{cos}\left(\boldsymbol{w_s t}+\frac{\mathbf{2\pi}}{\mathbf{3}}+(\mathbf{1}-\mathbf{2}\boldsymbol{s})\boldsymbol{w_s t}-\boldsymbol{\alpha_l}+\frac{\mathbf{2\pi}}{\mathbf{3}}\right)+\boldsymbol{cos}(\boldsymbol{w_s t}+\frac{\mathbf{2\pi}}{\mathbf{3}}-\right.$$

$$\left.\left.(\mathbf{1}-\mathbf{2}\boldsymbol{s})\boldsymbol{w_s t}+\boldsymbol{\alpha_l}-\frac{\mathbf{2\pi}}{\mathbf{3}})\right\}\right] \quad (129)$$

$$\mathbf{i_{dlfaulted}} = \frac{\mathbf{I}}{\sqrt{\mathbf{3}}}[\{\mathbf{cos}(\mathbf{2}(\mathbf{1}-\mathbf{2s})\mathbf{w_s t}-\boldsymbol{\alpha_l})+\mathbf{cos}(\mathbf{2w_s t}+\boldsymbol{\alpha_l})\}+$$

$$\left\{\mathbf{cos}(\mathbf{2}(\mathbf{1}-\mathbf{2s})\mathbf{w_s t}-\boldsymbol{\alpha_l})\mathbf{cos}\left(\frac{\mathbf{4\pi}}{\mathbf{3}}\right)+\mathbf{sin}(\mathbf{2}(\mathbf{1}-\mathbf{s})\mathbf{w_s t}-\boldsymbol{\alpha_l})\,\mathbf{sin}\left(\frac{\mathbf{4\pi}}{\mathbf{3}}\right)+\right.$$

$$\mathbf{cos}(\mathbf{2sw_s t}+\boldsymbol{\alpha_l})+\mathbf{cos}(\mathbf{2}(\mathbf{1}-\mathbf{2s})\mathbf{w_s t}-\boldsymbol{\alpha_l})\mathbf{cos}\left(\frac{\mathbf{4\pi}}{\mathbf{3}}\right)-$$

$$\left.\mathbf{sin}(\mathbf{2}(\mathbf{1}-\mathbf{2s})\mathbf{w_s t}-\boldsymbol{\alpha_l})\,\mathbf{sin}\left(\frac{\mathbf{4\pi}}{\mathbf{3}}\right)+\mathbf{cos}(\mathbf{2sw_s t}+\boldsymbol{\alpha_l})\right\}\Big] \quad (130)$$

$$\mathbf{i_{dlfaulted}} = \sqrt{\mathbf{3}}\mathbf{I_l}\,\mathbf{cos}(\mathbf{2sw_s t}+\boldsymbol{\alpha_l}) \quad (131)$$

Following the same way we can obtain

$$\mathbf{i_{drfaulted}} = \sqrt{\mathbf{3}}\mathbf{I_r}\,\mathbf{cos}(\mathbf{2sw_s t}+\boldsymbol{\alpha_r}) \quad (132)$$

$$\mathbf{i_{qlfaulted}} = -\sqrt{\mathbf{3}}\mathbf{I_l}\,\mathbf{sin}(\mathbf{2sw_s t}+\boldsymbol{\alpha_l}) \quad (133)$$

$$\mathbf{i_{qrfaulted}} = \sqrt{\mathbf{3}}\mathbf{I_r}\,\mathbf{sin}(\mathbf{2sw_s t}-\boldsymbol{\alpha_l}) \quad (134)$$

$$\begin{bmatrix}\mathbf{P'}\\ \mathbf{Q'}\end{bmatrix} = \begin{bmatrix}\mathbf{P}\\ \mathbf{Q}\end{bmatrix} + \mathbf{3U}\begin{bmatrix}\mathbf{I_l}\,\mathbf{cos}(\mathbf{2s\omega_I t}+\boldsymbol{\alpha_l})+\mathbf{I_r}\,\mathbf{cos}(\mathbf{2s\omega_I t}-\boldsymbol{\alpha_r})\\ -\mathbf{I_l}\,\mathbf{sin}(\mathbf{2s\omega_I t}+\boldsymbol{\alpha_l})+\mathbf{I_r}\,\mathbf{sin}(\mathbf{2s\omega_I t}-\boldsymbol{\alpha_r})\end{bmatrix} \quad (135)$$

In the faulty case the active (P_f) and reactive (Q_f) powers can be expressed as:

$$\begin{bmatrix} \mathbf{P_f} \\ \mathbf{Q_f} \end{bmatrix} = \begin{bmatrix} \boldsymbol{P} \\ \boldsymbol{Q} \end{bmatrix} + \mathbf{3}\boldsymbol{U} \begin{bmatrix} \boldsymbol{I_l}\cos(\mathbf{2}\boldsymbol{s\omega t} + \boldsymbol{\alpha_l}) + \boldsymbol{I_r}\cos(\mathbf{2}\boldsymbol{s\omega t} - \boldsymbol{\alpha_r}) \\ \boldsymbol{I_l}\sin(\mathbf{2}\boldsymbol{s\omega t} + \boldsymbol{\alpha_l}) - \boldsymbol{I_r}\sin(\mathbf{2}\boldsymbol{s\omega t} - \boldsymbol{\alpha_r}) \end{bmatrix} \quad (136)$$

The first part of this equation Eq.136 corresponds to the healthy behavior of the induction generator system, and the second part represents the faulty behavior. For a healthy generator, the spectrum of the apparent power contains only the main component. When a fault takes place in the system, the apparent power spectrum shows in addition to the main component harmonic components at the frequencyof2s*f*. These additional components, called characteristic components, provide an extra index of diagnostic information about the condition of the machine. In (Bitoleanu et all., 2007) a third part of the apparent power is introduced to represent the power distortion that appears only once the system is damaged. The approach that deals with the active and reactive power is known as the PQ transformation (Liu et all., 2007). It presents the main advantage to overcome or at least to limit the load influence.

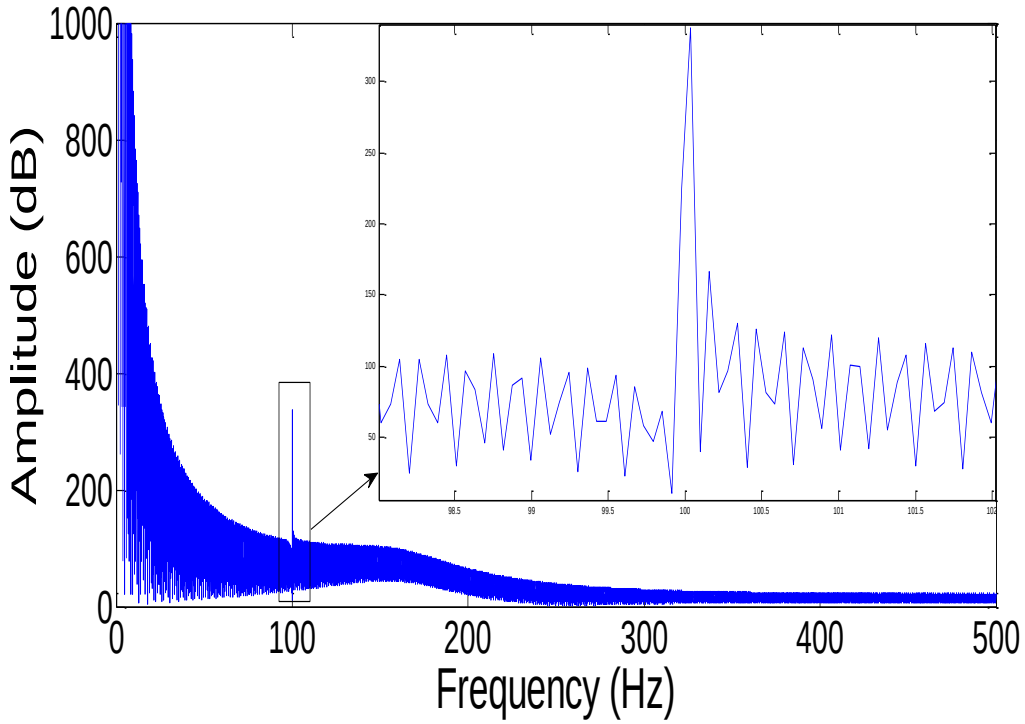

Fig.16 Active power Spectrum

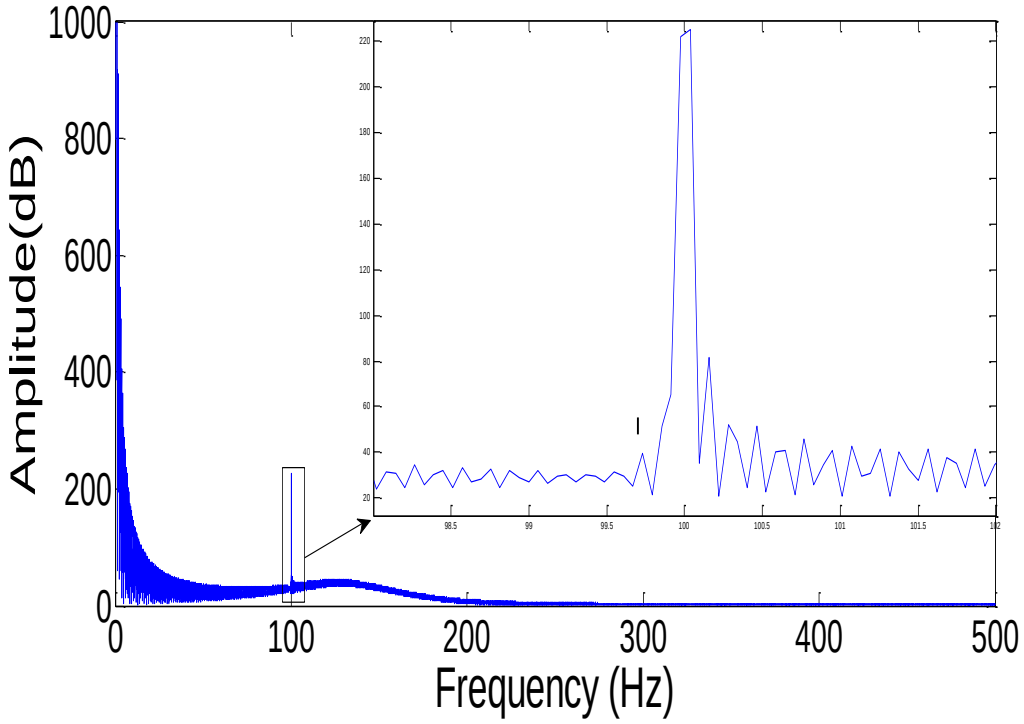

Fig.17 Reactive power spectrum

Figure 16 and Figure 17 present active and reactive power curves corresponding to faulty behavior of induction generator. A zoom has been taken in order to either eliminate the direct component and to confirm the apparition of fault side band component at the right and left side of the fundamental component.

3.2.3 Faulty Mechanic to Electric Transformed Power Model

Through the same way, the faulty system can be given by:

$$\mathbf{P_{ac}} = \left[\mathbf{r_s i_{sd}^2} + \mathbf{r_s i_{sq}^2}\right] + \left[\frac{\mathbf{d}}{\mathbf{dt}}\boldsymbol{\varphi}_{\mathbf{sd}}\mathbf{i} + \frac{\mathbf{d}}{\mathbf{dt}}\boldsymbol{\varphi}_{\mathbf{sq}}\mathbf{i_{sq}}\right] + \left[\boldsymbol{\omega}_{\mathbf{s}}\left(\boldsymbol{\varphi}_{\mathbf{sd}}\mathbf{i_{sq}} - \boldsymbol{\varphi}_{\mathbf{sd}}\mathbf{i_{sd}}\right)\right] + \left[\mathbf{r_s i_{sdfl}^2} + \mathbf{r_s i_{sqfl}^2}\right] + \left[\frac{\mathbf{d}}{\mathbf{dt}}\boldsymbol{\varphi}_{\mathbf{sd}}\mathbf{i_{sdfl}} + \frac{\mathbf{d}}{\mathbf{dt}}\boldsymbol{\varphi}_{\mathbf{sq}}\mathbf{i_{sqfl}}\right] + \left[\boldsymbol{\omega}_{\mathbf{s}}\left(\boldsymbol{\varphi}_{\mathbf{sd}}\boldsymbol{i}_{\mathbf{sqfl}} - \boldsymbol{\varphi}_{\mathbf{sd}}\boldsymbol{i}_{\mathbf{sdfl}}\right)\right] + \left[\mathbf{R_s}\boldsymbol{i}_{\mathbf{sdfr}}^{\mathbf{2}} + \mathbf{R_s}\boldsymbol{i}_{\mathbf{sqfr}}^{\mathbf{2}}\right] + \left[\frac{\mathbf{d}}{\mathbf{dt}}\boldsymbol{\varphi}_{\mathbf{sd}}\boldsymbol{i}_{\mathbf{sdfr}} + \frac{\mathbf{d}}{\mathbf{dt}}\boldsymbol{\varphi}_{\mathbf{sq}}\boldsymbol{i}_{\mathbf{sqfrl}}\right] + \left[\boldsymbol{\omega}_{\mathbf{s}}\left(\boldsymbol{\varphi}_{\mathbf{sd}}\boldsymbol{i}_{\mathbf{sqfr}} - \boldsymbol{\varphi}_{\mathbf{sd}}\boldsymbol{i}_{\mathbf{sdfr}}\right)\right] \quad (137)$$

It can be clearly seen that relation Eq.137 contains three parts. The first part corresponds to the healthy induction generator power. The second and the third parts correspond to the left and the right sideband faulty component power respectively. Each part contains three components. The first component represents Joule losses, the second component represents the electromagnetic power produced by the electromagnetic field, and the third component corresponds to the transformed power from mechanical form to electrical form. The main advantage of using power signature analysis is the availability of both, stator voltage and current measurements. However, the use of this last expression of the power to diagnose induction generator faults, is the necessity of stator flux measurements, which is a difficult task in real conditions. This difficulty can be avoided with the help of a state observer design (Bourbia et all. 2014).

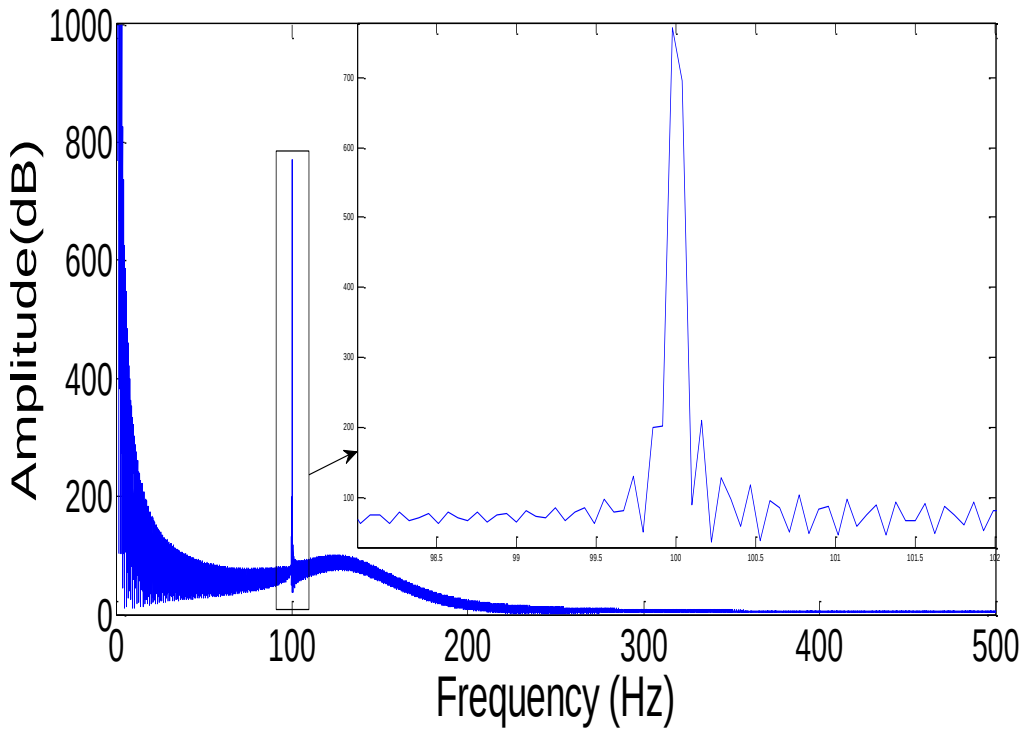

Fig.18 Transformed power Spectrum

Figure 18 represents faulty transformed power spectrum, a zoom has been taken to point out the apparition of side band components which are the main characteristics of faults.

3.2.4 Faulty Complex Apparent Power Model

Instantaneous complex apparent power is decomposed on two components, real part named active power and imaginary part called reactive power. That variation introduced to induction generator by a faults, leads to a distortion in power that appears and can be defined as the root mean square value of instantaneous complex distortion power modulus. Below is the equation that represents the complex apparent power under faulty conditions (Bitoleanu et all., 2007).

$$\mathbf{S} = \sqrt{\boldsymbol{P^2 + Q^2 + D^2}} = \sqrt{\boldsymbol{6}}\boldsymbol{UI} \qquad (138)$$

Where **P** is active power, **Q** is the reactive power and **D** is the distortion power introduced by fault.

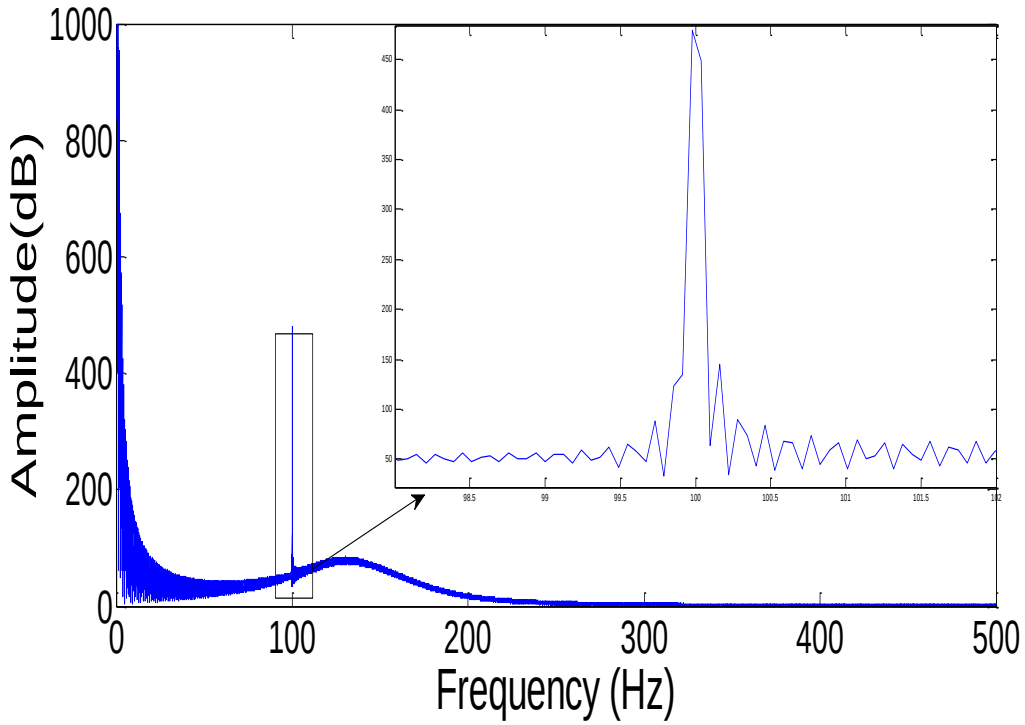

Fig.19 Complex apparent power Spectrum

Figure19 represents the complex apparent power variations under the presence of fault, a zoom have been taken which confirm the apparition of the two side band component corresponds to the fault.

3.3 Load Influences

Load and inertia influences represent the main problem encountered while analyzing induction generator behavior. Distinguish between the faults pattern and other deformations related to the system open a large window to new researches. The combined analysis of the amplitude and frequency spectra of the induction generator different powers can be used with great success in the discrimination of rotor and/or stator faults from load influences (De Angelo et all., 2010; Drif and Cardoso, 2012). In that case supply current will contain spectral components related to load torque variability, (Zeraoulia. Et all., 2005). Variability in load torque at multiple of rotational speed $m\boldsymbol{f}_r$produces stator currents components at frequencies $\boldsymbol{f}_{load}$as described in Eq.139:

$$\mathbf{f}_{\text{load}} = \mathbf{f}_{\text{s}} \pm \text{m}\mathbf{f}_{\text{r}} = \mathbf{f}_{\text{s}}\left[1 \pm \text{m}\left(\frac{1-\text{s}}{\text{p}}\right)\right] \quad (139)$$

Where:

$\boldsymbol{f}_{load}$is the frequency related to load variation, $\boldsymbol{f}_s$is the electrical supply (grid) frequency, $\boldsymbol{f}_r$is the rotational frequency, p is the number of pole pairs, s is the induction generator slip. m=1, 2, 3, ...

Based on the faults frequency for rotor presented in Eq.1 and faults frequency of stator shortcut given in Eq.2, together with the interaction of load that appears at the frequency illustrated in Eq.139, it can be concluded that all frequencies either of faults or load are close to fundamental component. Accordingly, any separation between them based only on the spectral analysis will be useless.

3.4Induction Generator Power Faults Diagnosis Approach

In this thesis the process of obtaining correlation for fault diagnosis from signal analysis is summarized as follows:

First a usable raw signal was extracted by means of induction generator model proposed in (Bensaker et all., 2003) and estimator proposed in (Bourbia et all.,

2014), the time domain representation of the power will not give a helpful tools in diagnosis process as it is illustrated in Fig.20.

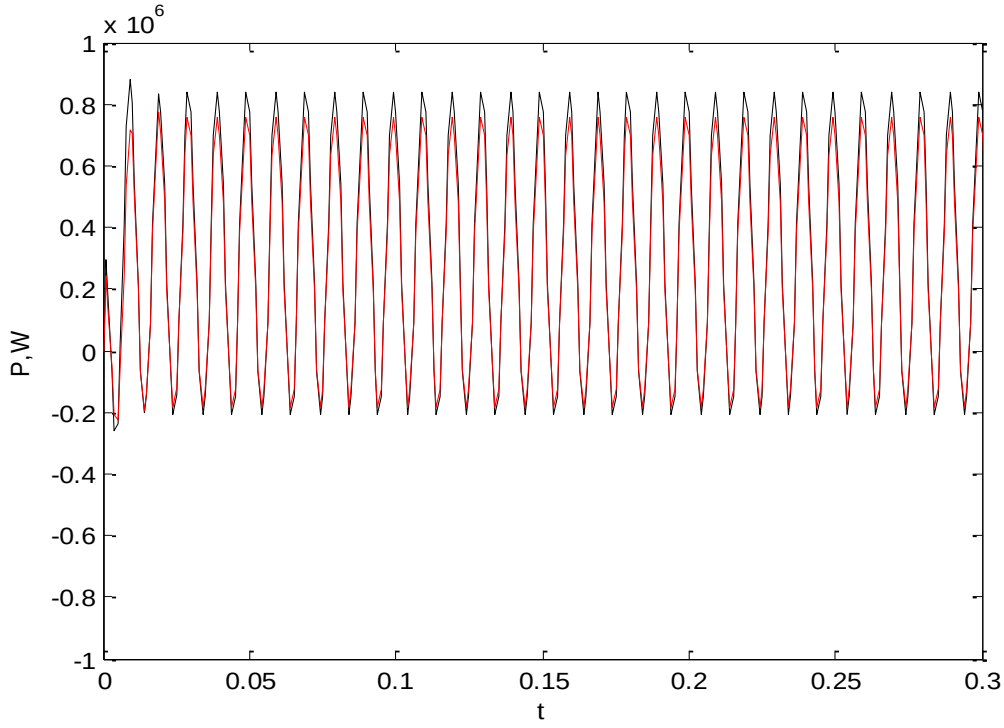

Fig.20 Partial power

It can be clearly seen in figure above that distinguishing between the faulted signal (red one) and the healthy ones (the black one) isn't an easy task, the two signals appear to be superposed. Moreover, there is no specific characteristics that can be followed to detect faults.

The diagnosis and fault detection methods used in this research are based on the effective analysis of the frequency domain; this analysis is performed by Fast Fourier Transformation (FFT) and PQ transformation. The FFT performs the fault characterization by representing the power signals as the sum of sine and cosine functions, which transforms a time domain signal into frequency domain signal. It can be mentioned that, in original power specter, all information are presented.

The task of distinguishing faulty conditions from normal conditions based on the FFT can be done accurately as long as the signals are stationary. But the FFT is

notable to reveal the inherent features of non-stationary signals and is not suitable for non-stationary signal analysis.

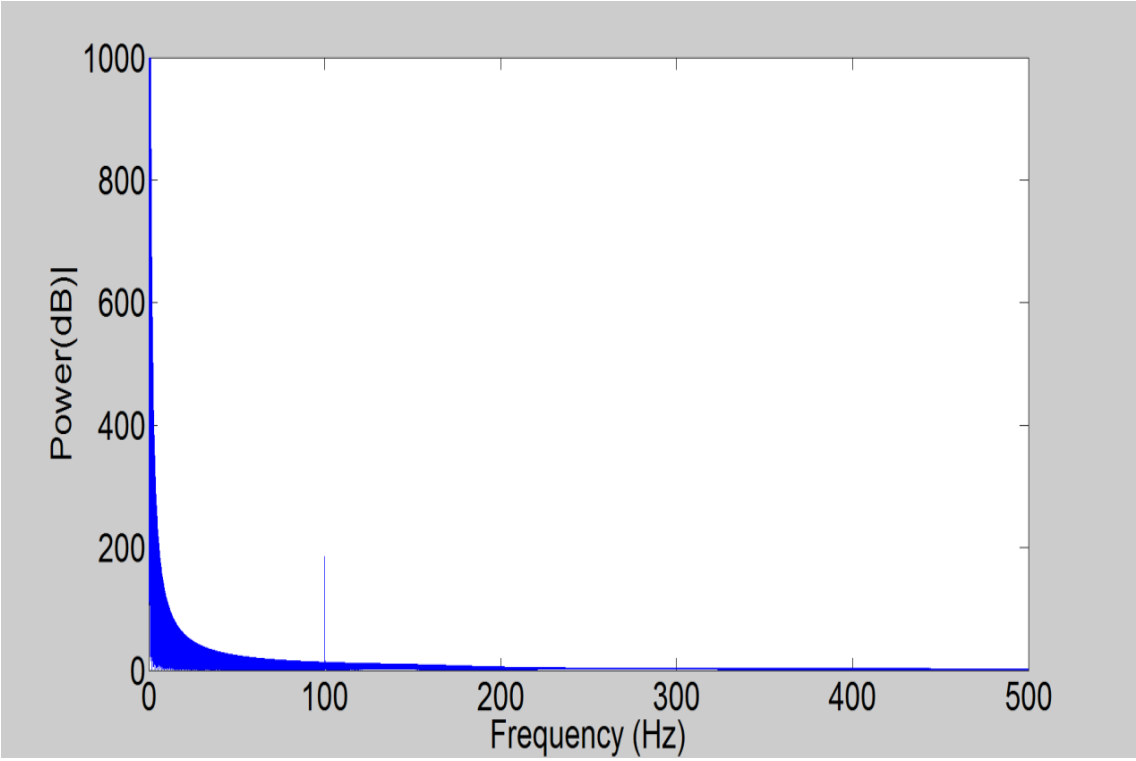

Fig.21 Partial power Spectrum

Fig.21 points out the difficulties faced to find the main component of specter that can be followed in diagnosis process; however the FFT has difficulties in early fault detection due to the small amplitude of the failure components. Consequently, the fault components are hidden by not diagnosable signals introduced by data acquisition process. To overcome these problems a new diagnosis process was proposed in this thesis. The process efficiencies evaluated based on the capability to extract the purely faulty signal from all unwanted signals as noise, harmonics, non-sinusoidal signals and even healthy system should be omitted. Induction machine fault diagnosis based on power analysis minimizes the influences of noise and harmonics, which make the diagnosis more efficient (Trzynadlowski, 1999).

Fig.21 presents the hole partial power specter that contains the DC component, it can be clearly seen that only a pick appears at twice the fundamental frequency

(100HZ). There is no trace of faults indicator that should occur in the two sideband components at left and right of the fundamental pick (100HZ), in addition, the DC component of the specter does not contains any information concerning faults, which make theme not beneficial in induction generator diagnosis.

A zoom has been realized to point out the diagnosable part alone, the DC component has been omitted too, and figure below presents the results of the previous treatments.

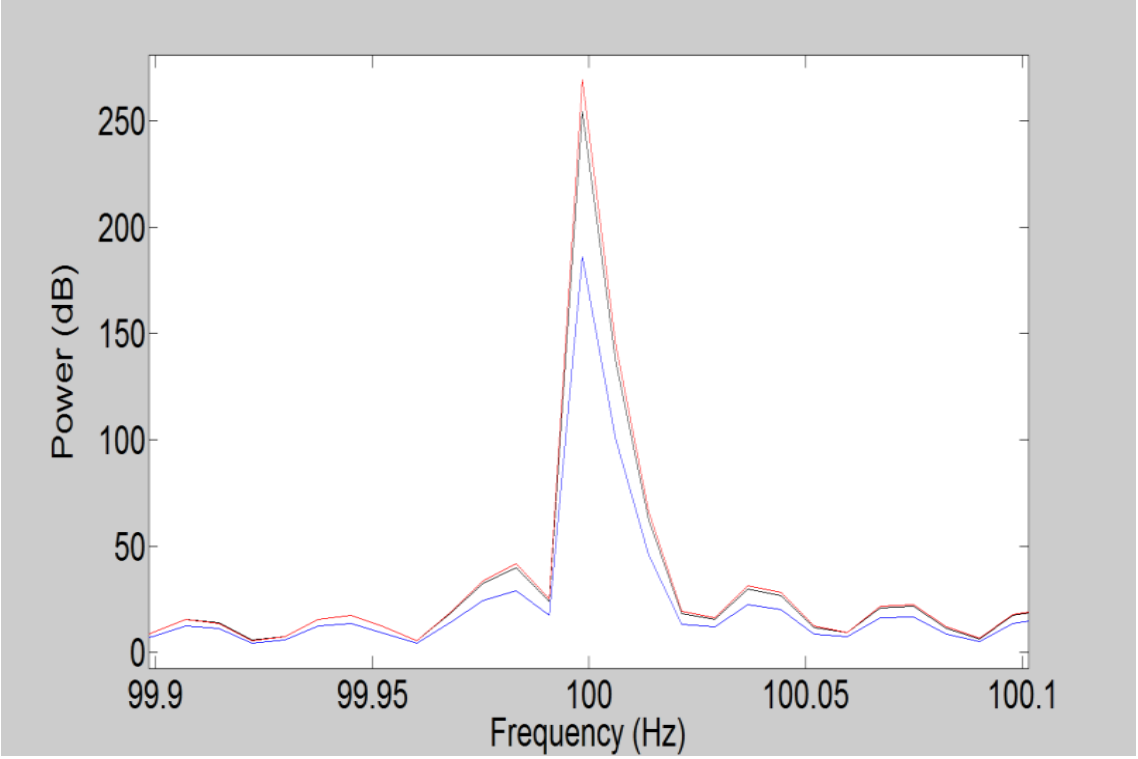

Fig.22 partial power for Rotor BB vs healthy

It can be clearly seen in Fig.22 that the two curves of rotor broken bars are separated from the healthy one. In contrast, the two specters of faults are almost superposed, this will make diagnosis difficult task. Fig22 confirm that even if the ordinary specter hide the progress of fault, the removal of healthy behavior will clearly reveals the difference between the two specters. In addition to the fundamental component (2f), two sideband components appear at (1±2s)f. This makes faults diagnosis process not easy task, but gives the possibility to select

the suitable power form to diagnose induction generator fault. Generally, if the two specters corresponding to one and two broken bars (BB) or stator short cut (CC) are superposed or even, in order to obtain high specter fault amplitude in (1±2s)f for (2BB) / (2CC) compared to (1BB)/(1CC), a deficiency in specter amplitude of faults for the two sideband (1±2s)f appears, then the selected power method used will be unusable to diagnose induction generator specific faults.

Furthermore, the simplification proposed before, in the evolution method, the healthy signal is takenout of the analysis. This later technique has the benifite to dealdirectly with faulty behavior. Other characteristics as DC components dont have wealthy information concerning fault, moreover they can make the power specter doughty and consequently diagnosis process hard task.

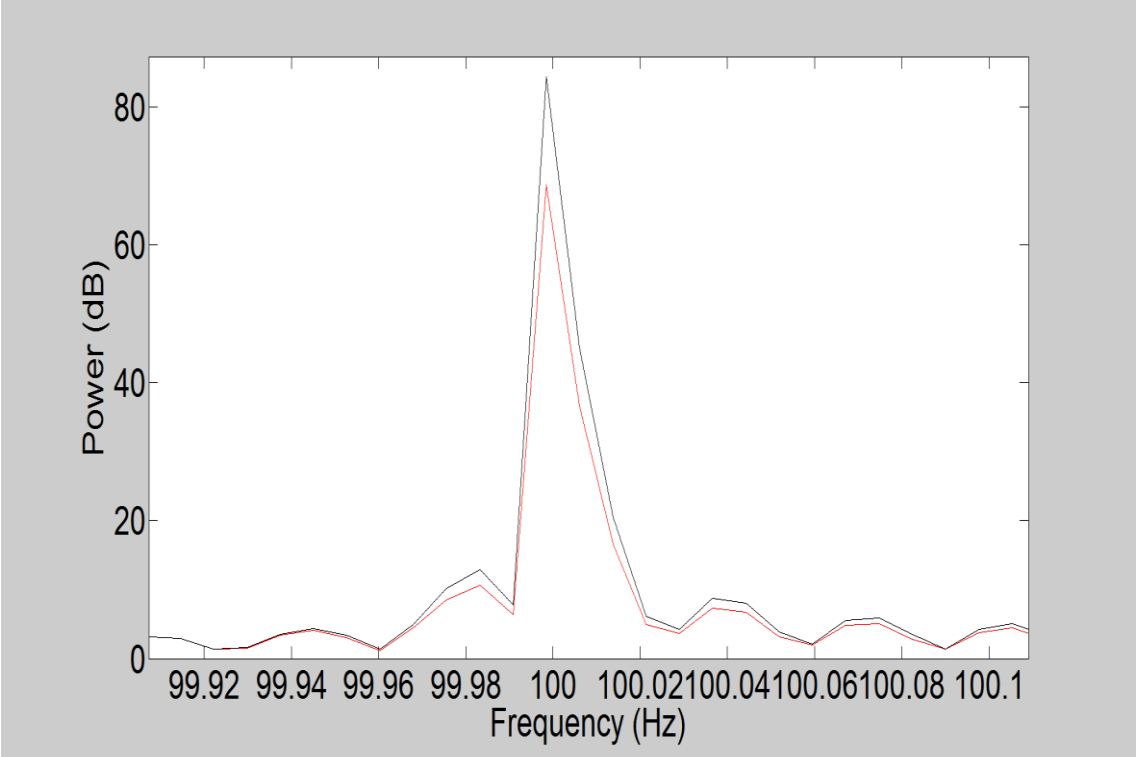

Fig.23 Evolution of rotor faults for Partial power

The specter of power presented in Figure 23 above summarizes the evolution method, the two specters are separated and the progression of fault can be quantified in the two sideband components.

Catch a fault characteristics through power specter is not the only objective via the evolution method, selection of the suitable power for diagnosing each induction generator fault is one of the main ideas of this thesis.

Chapter4Induction Generator Fault Diagnosis Simulation Results

In this simulation experiments the instantaneous partial and total power, the active and reactive power, the complex power and the transformed mechanical power into electrical power are investigated to diagnose rotor and stator faults of an induction generator.

The different characteristics of the considered induction generator are listed in the Table 1. Induction generator state model and observer based system are mediums to simulate different powers.

Table 1: Characteristics of the considered induction generator

Symbol	Quantity	Unit
P	Electric power	11 Kw
F	Supply frequency	50 Hz
U	Supplyvoltage	220 Volt
P	Numberof pair pole	2
ω_r	Rotor angularspeed	1440 rpm
R_s	Stator resistance	0.5 Ohm
R_r	Rotor resistance	0.5 Ohm
L_s	Stator inductance	0.0069 Henry
L_r	Rotor inductance	0.0069 Henry
M	Mutualinductance	0.0067 Henry
n	Numberof rotor bar	42
N_s	Number of turns by slots.	22

The MATLAB control toolbox support is used to perform different simulation experiments.

4.1 Simulation Results of Selected Model

The simulation of the selected model, stator current and rotor flux signals are given in the following Fig24.

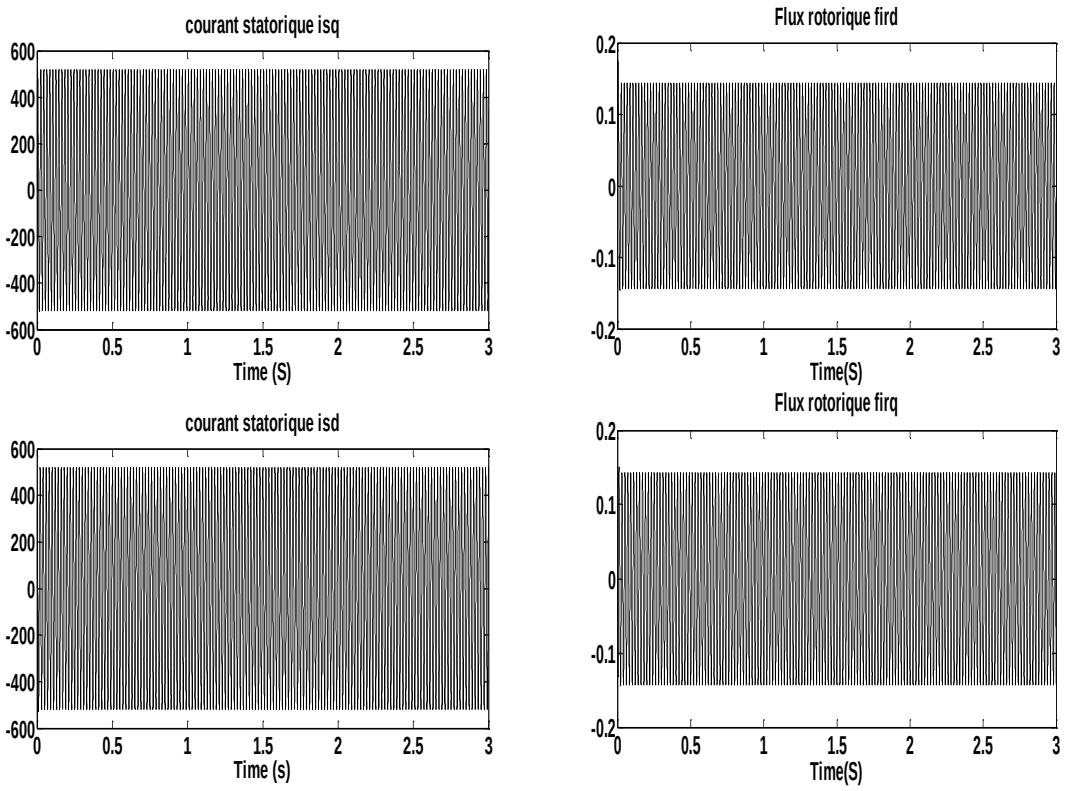

Fig.24 Stator current and rotor flux signals of induction generator.

Based on the above induction generator selected model and the powers modeling detailed in chapter two, simulation of different power such as instantaneous partial and total power, active and reactive power, complex apparent power and transformed power from mechanic to electric nature is given in the following.

First, the different power signals are presented in the figure 25.

The Blue line represents the active power;

The Green line represents the reactive power;

The Red line represents the partial power;

The Cyan line represents the power transformed from mechanic to electric nature;

The Magenta line represents the complex apparent power;

The Black line represents the total power.

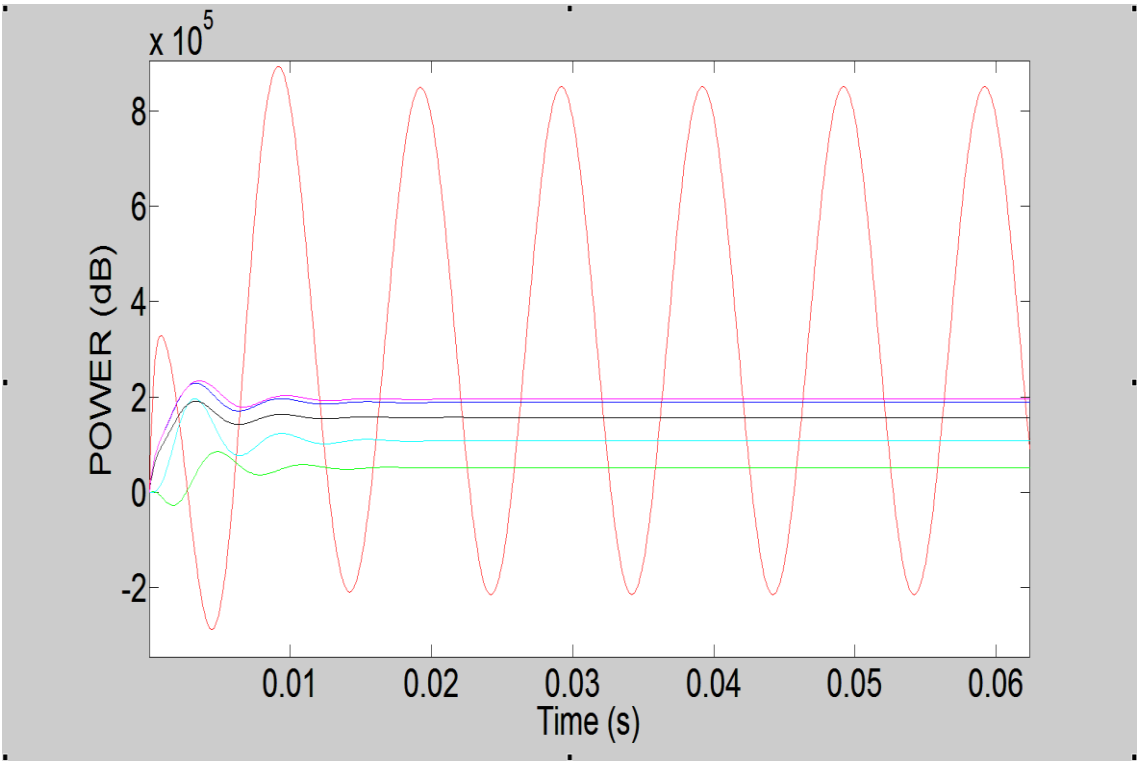

Fig.25 Induction generator different power presentations.

4.2 Induction Generator Faults Simulation

4.2.1 Rotor Fault Simulation

In order to simulate induction generator rotor faults, a fault is introduced in the rotor resistance as in (Calıs and Cakır, 2007) by the following relation:

$$\Delta \boldsymbol{R} = \left(\frac{\boldsymbol{n}}{\frac{\boldsymbol{z_r}}{\boldsymbol{3}}} - \boldsymbol{n} \right) \boldsymbol{r_r} \qquad (140)$$

Here $\Delta \boldsymbol{R}$ represents the increase in rotor resistance introduced by the simulated defect and $\boldsymbol{z_r}$ represents the number of broken rotor bars.

4.2.2 Stator Fault Simulation

In the same way, stator faults are simulated by using a similar estimation (Chilengue et All., 2011). In this assumption the stator phase contains N_s turns

that are disposed as two windings in series, more details can be found in (ArkanetAll.,2005).

$$\boldsymbol{R_{ph} = \left(1 - \frac{N_{sc}}{N_s}\right) r_s} \qquad (141)$$

Here R_{ph} is the faulty phase stator resistance andN_{sc} is the number of short cuts.

4.3 Simulation of Induction Generator Faults Detection under Load Variations

In real conditions some interactions of other faults, induction generator self-undesirable behavior or environment affection could have significant influence on faults diagnosis. Load variation is a well-known problem which can make the situation doubt, and consequently fault detection a hard task. Below are simulations which point out the influence of load on diagnosis process. Healthy or faulty generator, under half or full load are all studied to clarify the interaction of load with faults.

4.3.1 Load Influence on Partial and Total Power

In real conditions induction generators are exposed to external and internal influences that can change their behavior significantly. The main function of induction generator is to convert mechanical torque to electrical energy. Torque changes due to load fluctuation, causes mechanical unbalance that appears as oscillations proportional to the induction generator speed.

This engenders important change in induction generator healthy conditions, as well as in partial and total power harmonics.

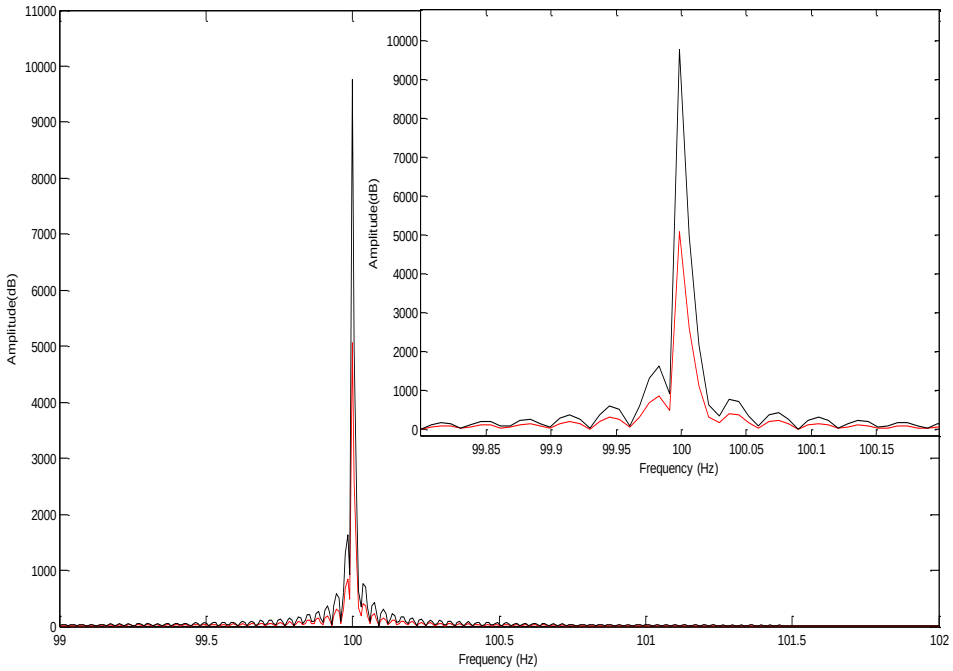

Fig.26 Healthy induction generator half and full load for partial power

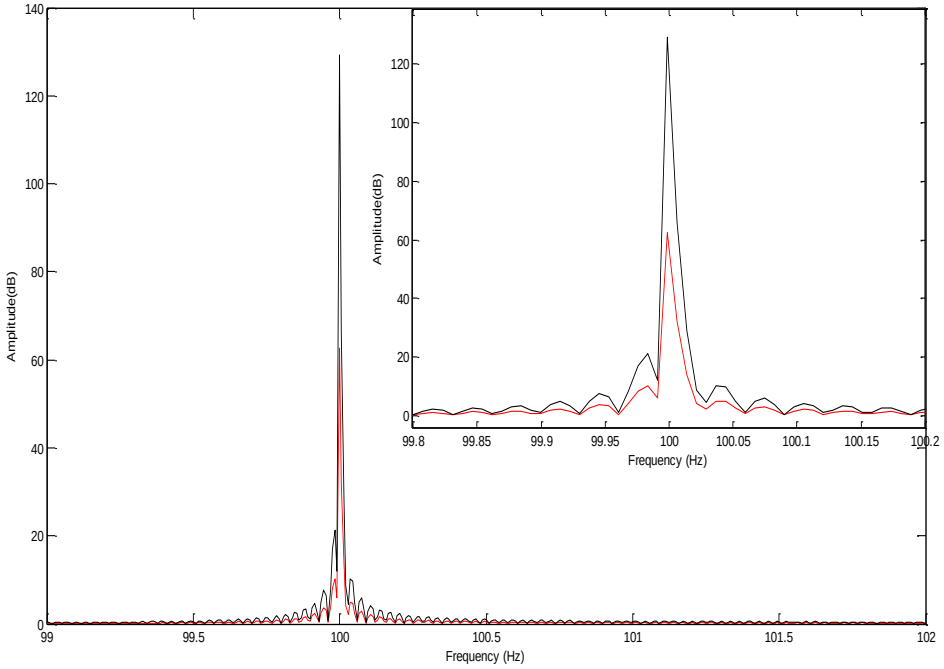

Fig.27 Healthy induction generator half and full load for total power

The black line represents the full load conditions and the red line represents the half load ones for both partial and total power. One can see, in zoom taken out for spectrum correspond to partial and total power, that both partial power Eq.

114 and total power Eq. 113 spectrums receive large change in terms of either main spectrum component or left and right side band components. This later will leads to a confusing situation while diagnosing induction generator situation. Deeper the interaction of load with partial and total power signals will leads to lose the difference between diverse induction generator situation.

Figures (28-31) below present the interaction of half and full load conditions and rotor induction generator's faults. The red line represents the faulty system and the black line represents the load influence.

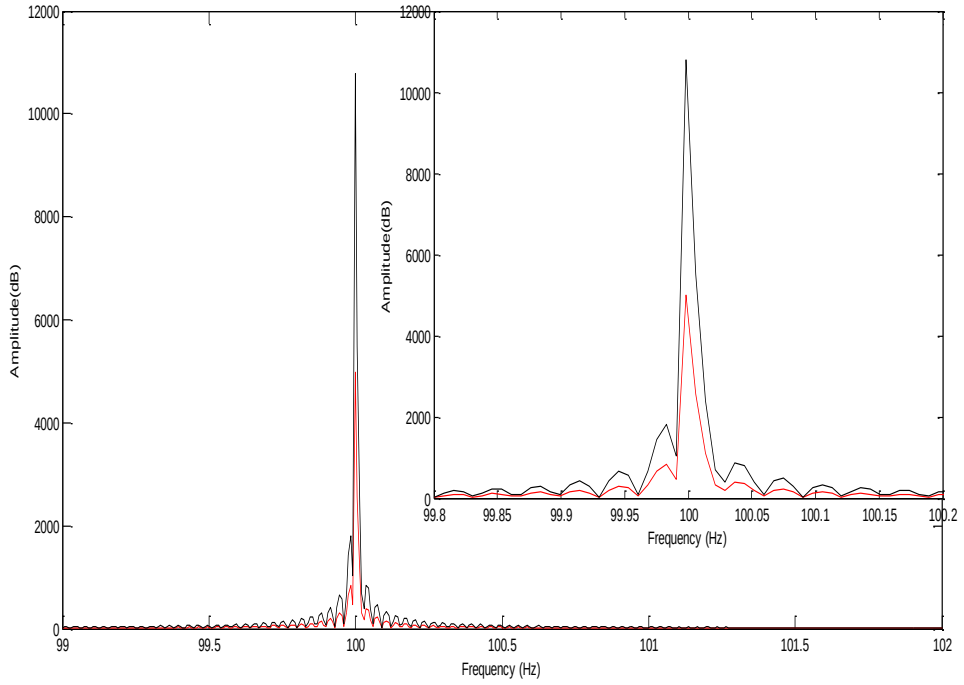

Fig.28 Rotor faulty induction generator under half load for partial power

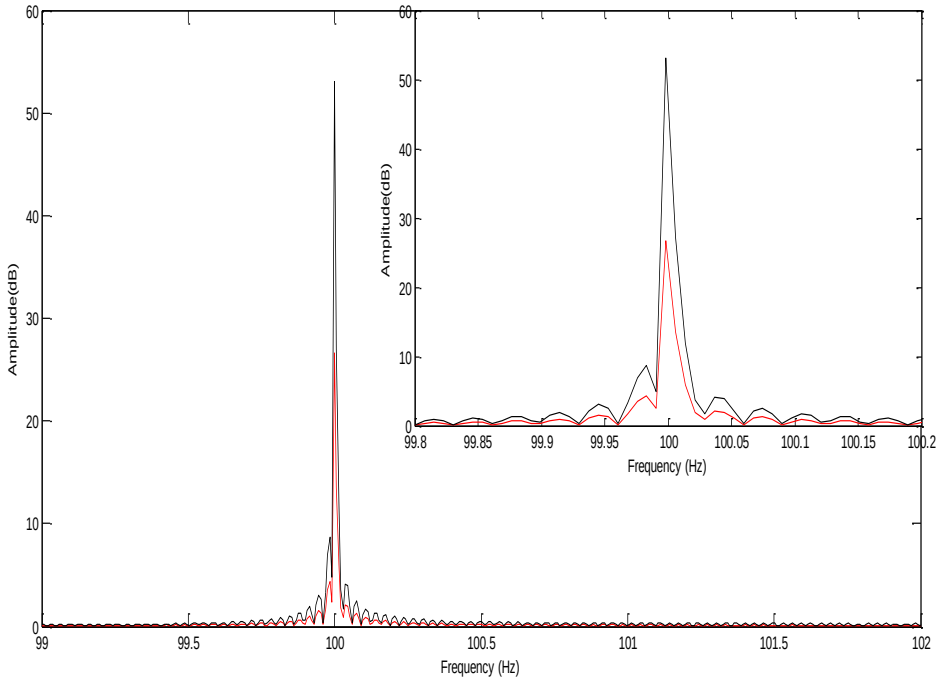

Fig.29 Rotor faulty induction generator under half load for total power

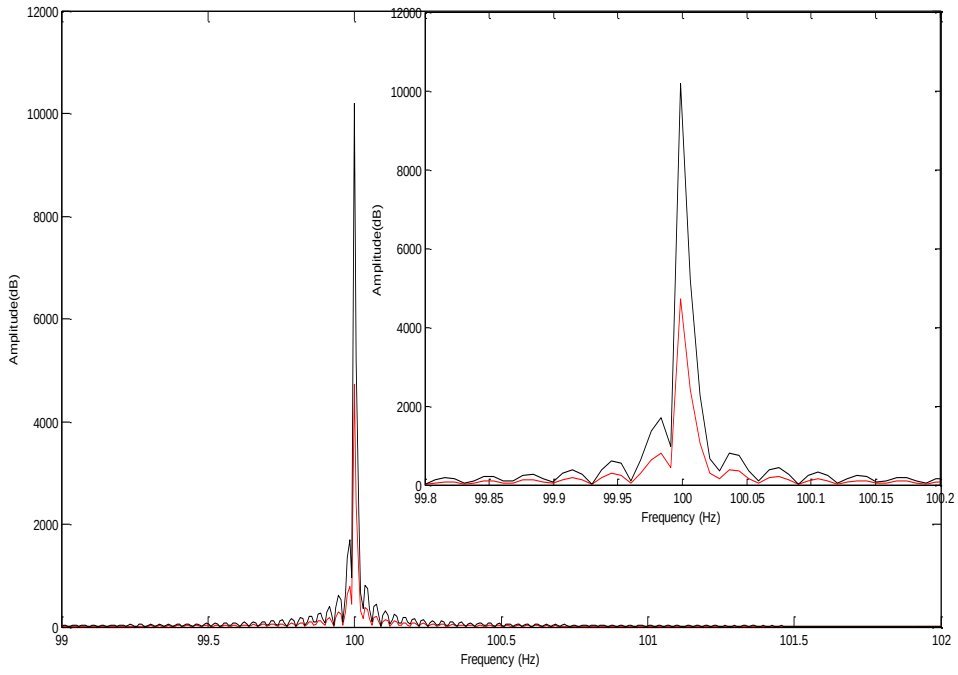

Fig.30 Rotor induction generator under full load for partial power

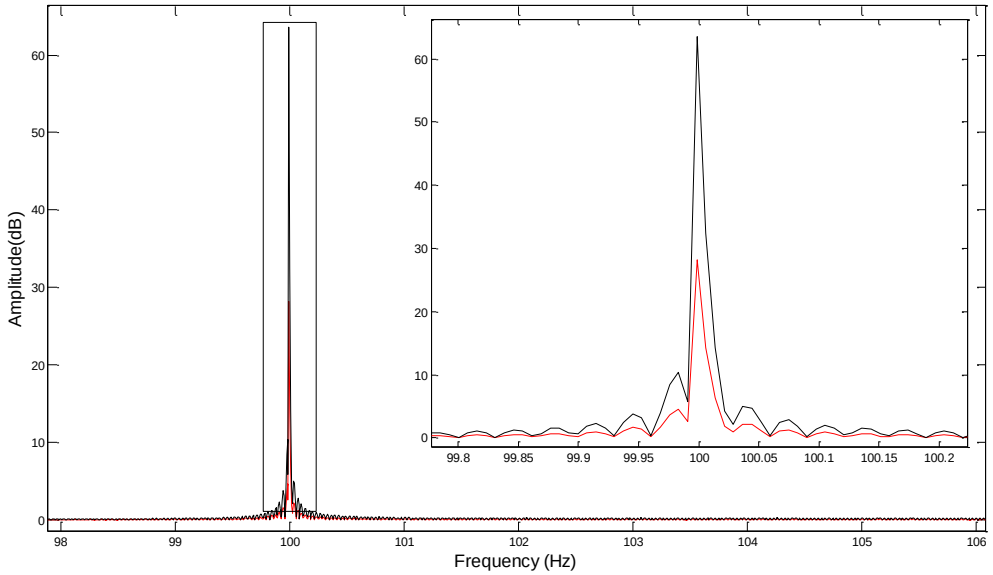

Fig.31 Rotor faulty induction generator under full load for total power

Figures (28-31) present faulty total and partial powers under load variation (half to full load conditions), all figures obtain more or less variation due to load variations. The zoom taken out for spectrums of total and partial power under both half or full load confirms that the load variations can lead to doubt situation. Then diagnosis process can guide to inaccurate decision in presence of load.

Figures (32-35) below present the interaction of half and full load conditions and rotor induction generator's stator faults. The red line represents the faulty system and the black line represents the load influence for both total and partial power.

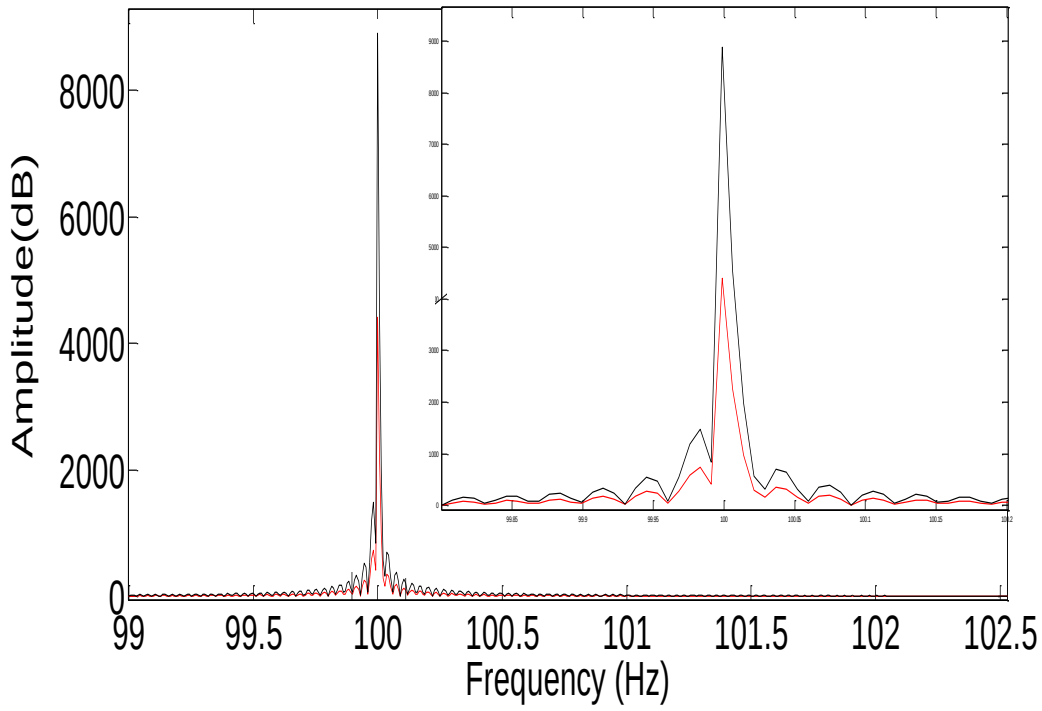

Fig.32 Stator faulty induction generator under half load for partial power

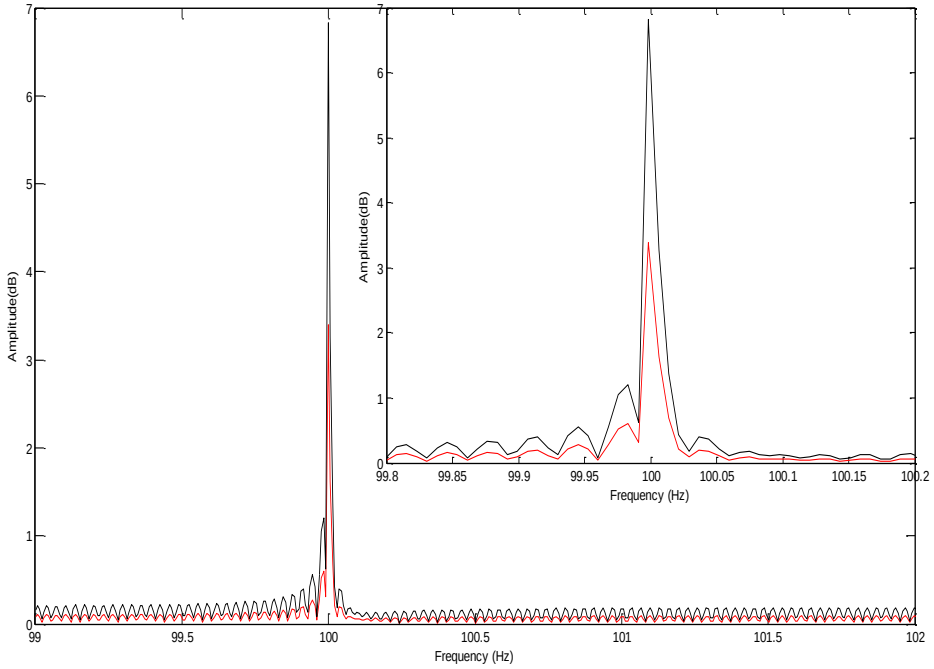

Fig.33 Stator faulty induction generator under half load for total power

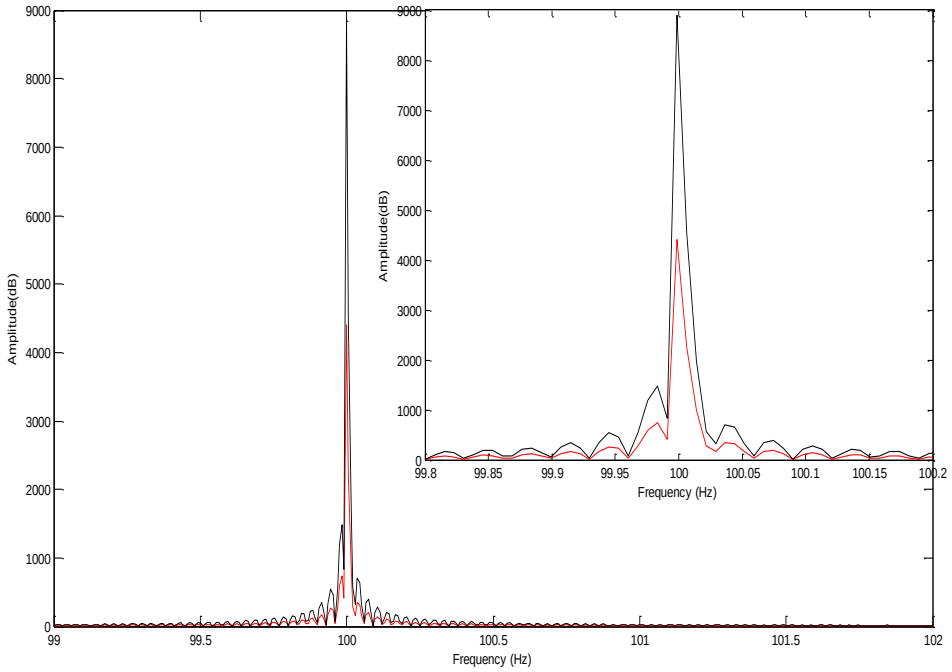

Fig.34 Stator induction generator under full load for partial power

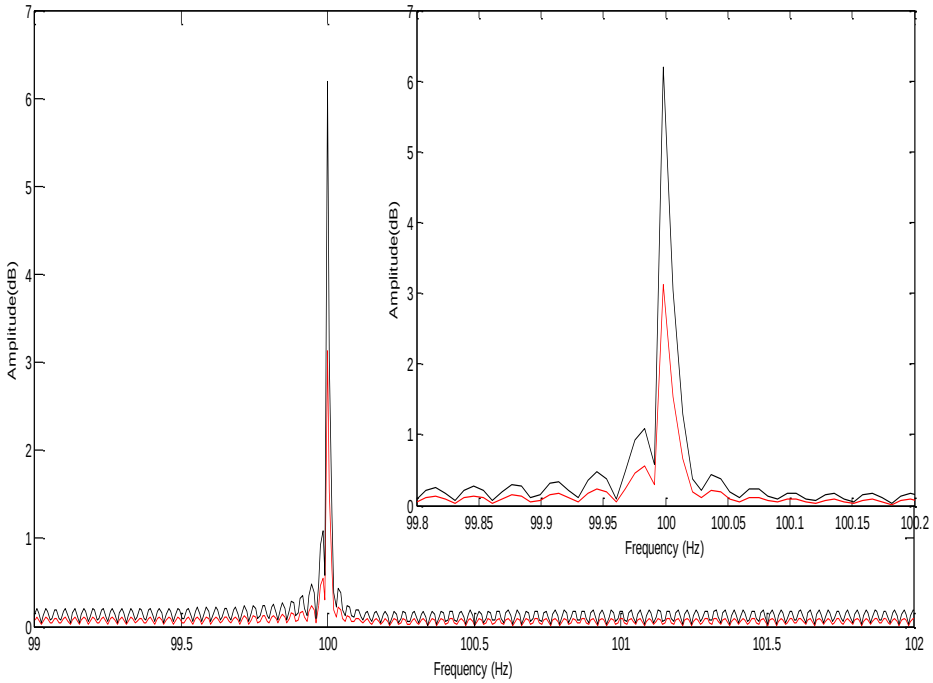

Fig.35 Stator induction generator under full load for total power

Figures (32-35) present induction generator spectrums for total and partial power in presence of either half or full load.

Interaction of rotor and stator fault with load variation, point out that diagnosis based on total and partial power spectrum receives enormous changes or either for the main or lateral harmonics which can lead to confusion situation

4.3.2 Load Influence on Active and Reactive Powers

Active and reactive powers are largely used in induction generator faults diagnosis; they can be used separately or in combination as it is presented in PQ transformation. The introduction of load to the healthy active and reactive power mechanism is presented in figures below.

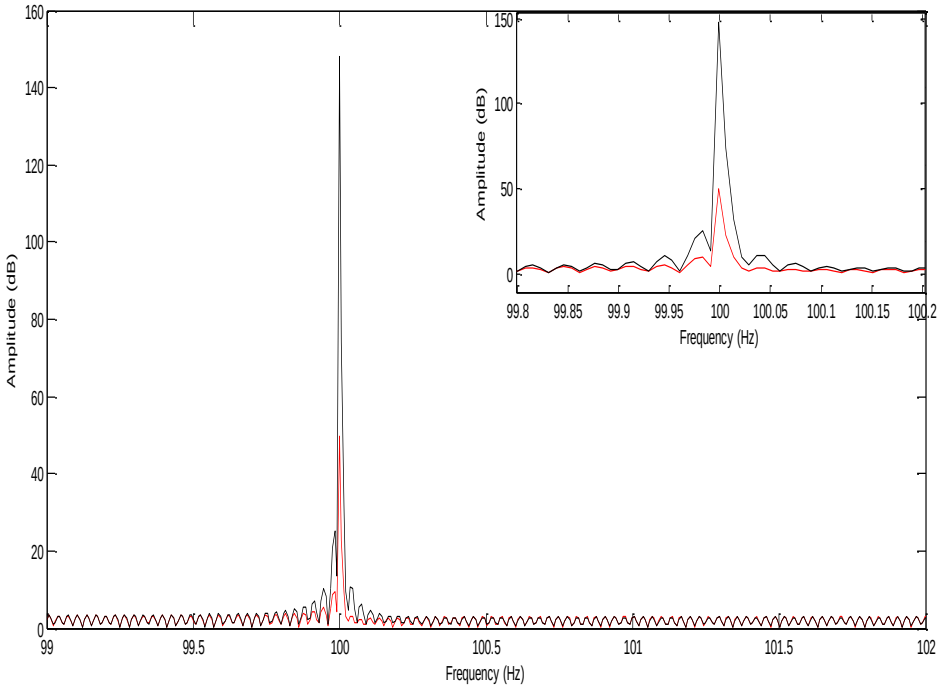

Fig.36 Healthy induction generator under half and full load for active power

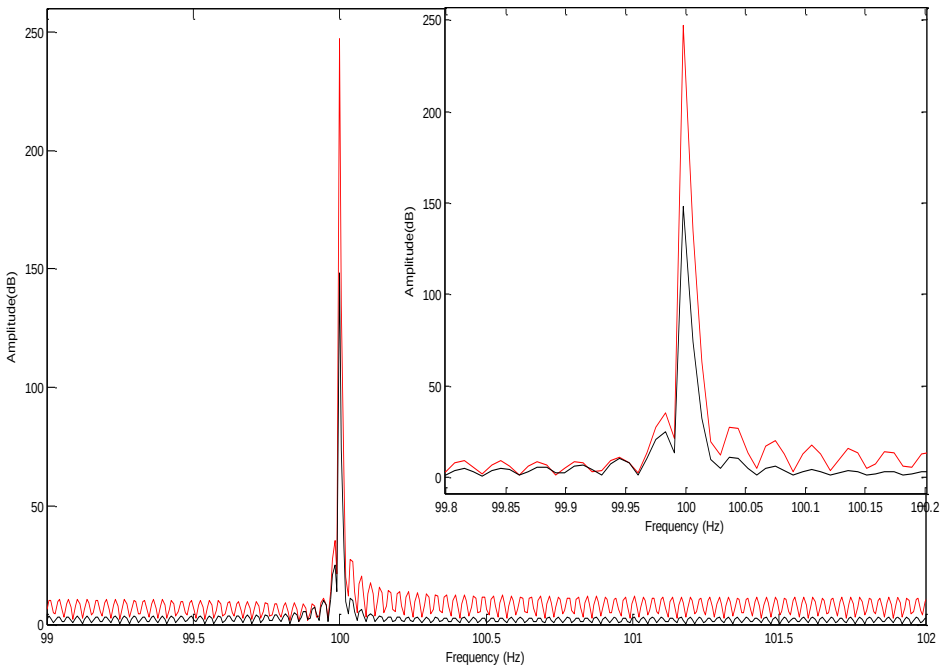

Fig.37 Healthy induction generator under half and full load for reactive power

The black line represents induction generators spectrum under full load conditions and the red line represents the half load one for both active and reactive power.

It can be clearly seen in figure 36 and figure 37 correspond to both active and reactive power spectrum that load will bring some changes to the keys of faults detection. Inversely to active power figure 36 where spectrum magnitude increase remarkably from half to full load, reactive power figure 37 spectrum magnitude decrease. Accordingly, diagnosis process via spectrum analysis and under load variation is a difficult task.

The influences of load change on diagnosis process can be cleared out by the following figures, which present the interaction of load in one hand and rotor fault on the other hand.

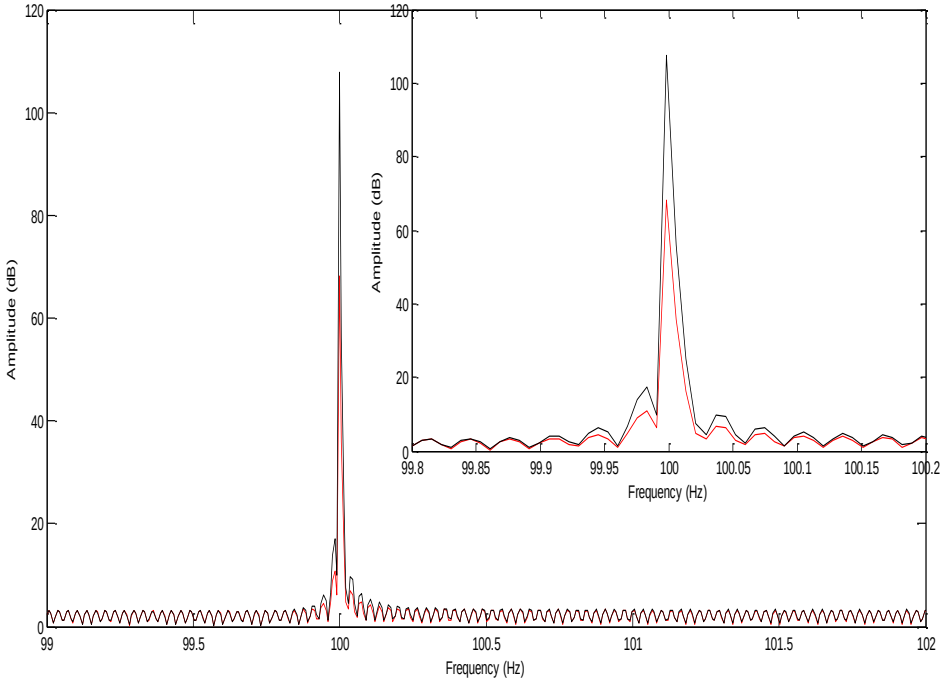

Fig.38 Rotor faulty induction generator under half load for active power

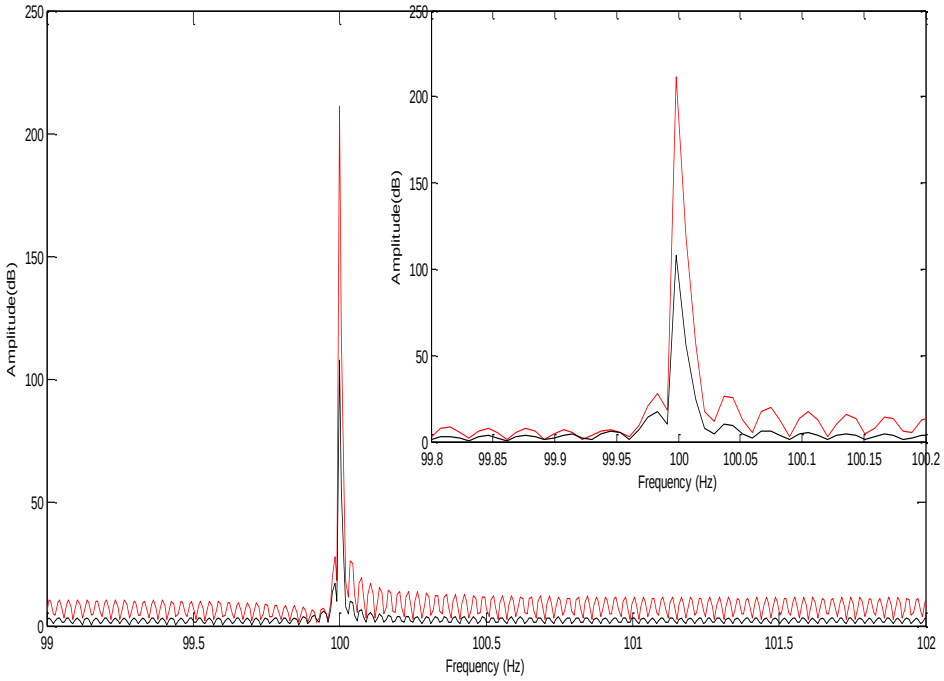

Fig.39 Rotor faulty induction generator under half load for reactive power

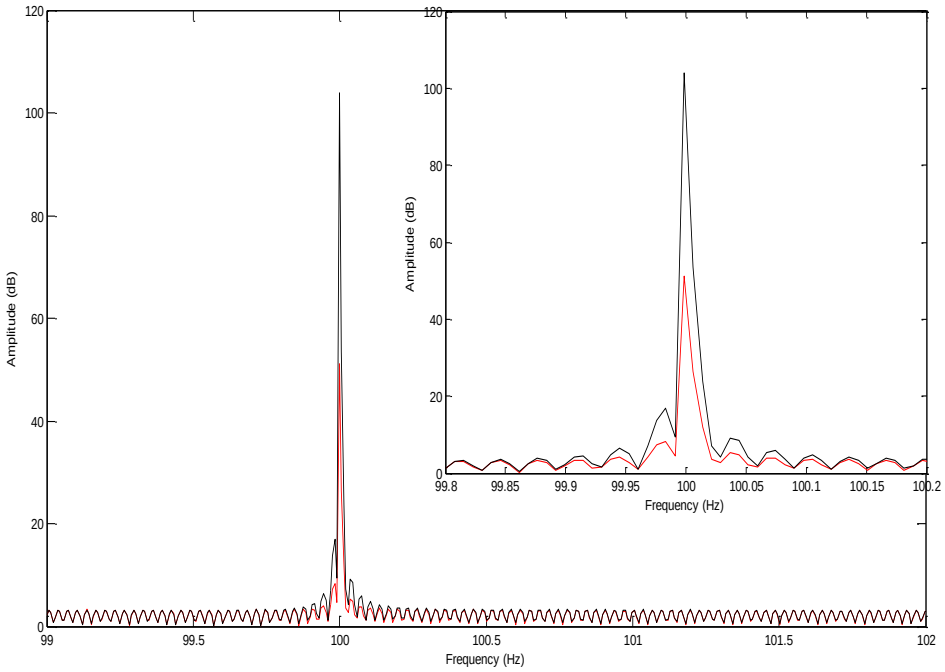

Fig.40 Rotor faulty induction generator under full load for active power Spectrum

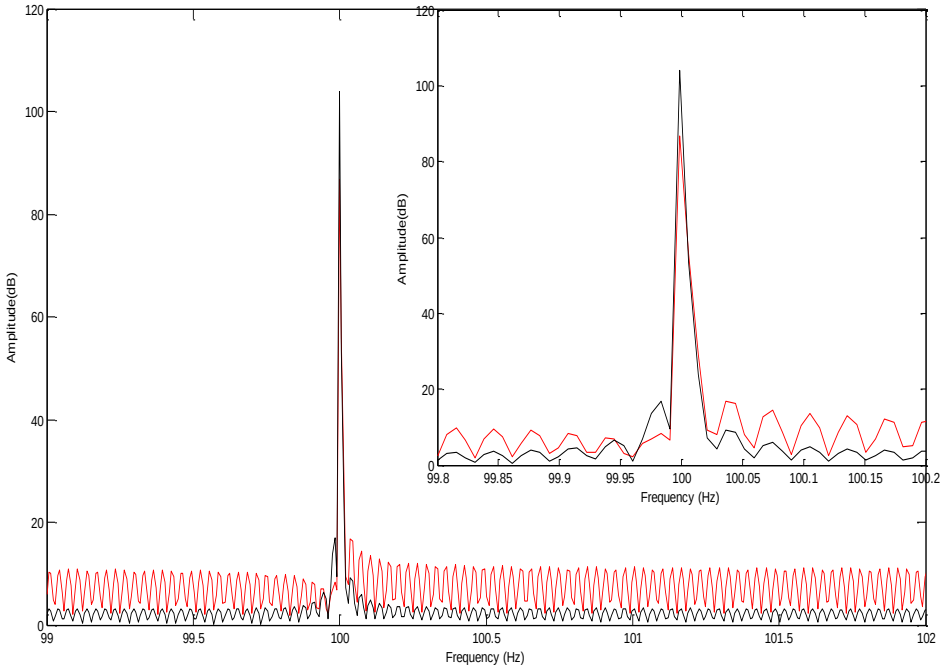

Fig.41 Rotor faulty induction generator under full load for reactive power

Induction generator active and reactive power's spectrum under half and full load represented in figures above (figure 38-41) present interaction between

faulty and under load curves. This later makes diagnosis process in doubted situation.

The influences of load change on diagnosis process can be cleared out by the following figures, which present the interaction of load in one hand and stator fault on the other hand.

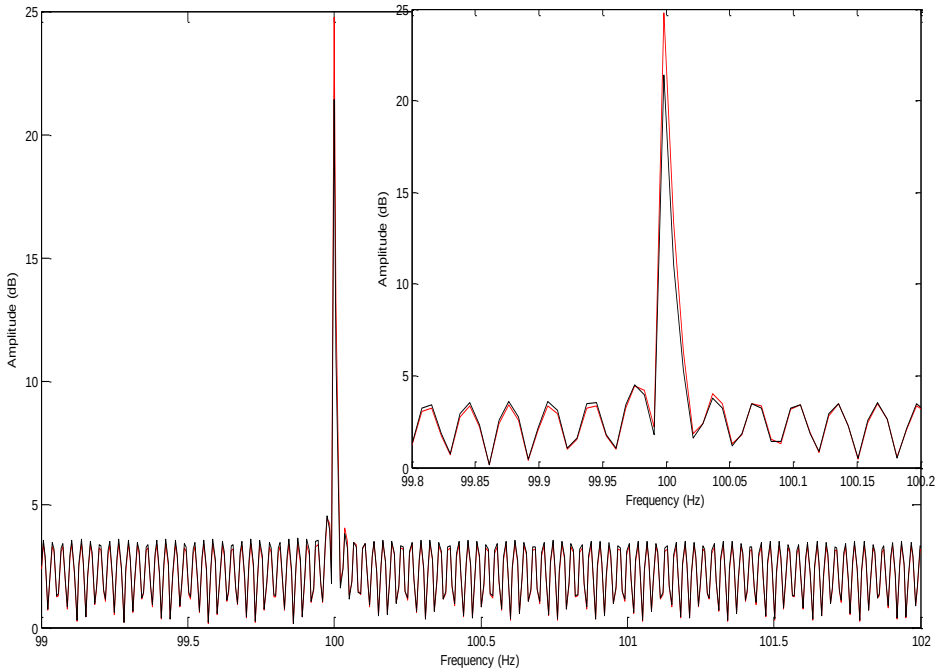

Fig.42 Stator faulty induction generator under half load for active power.

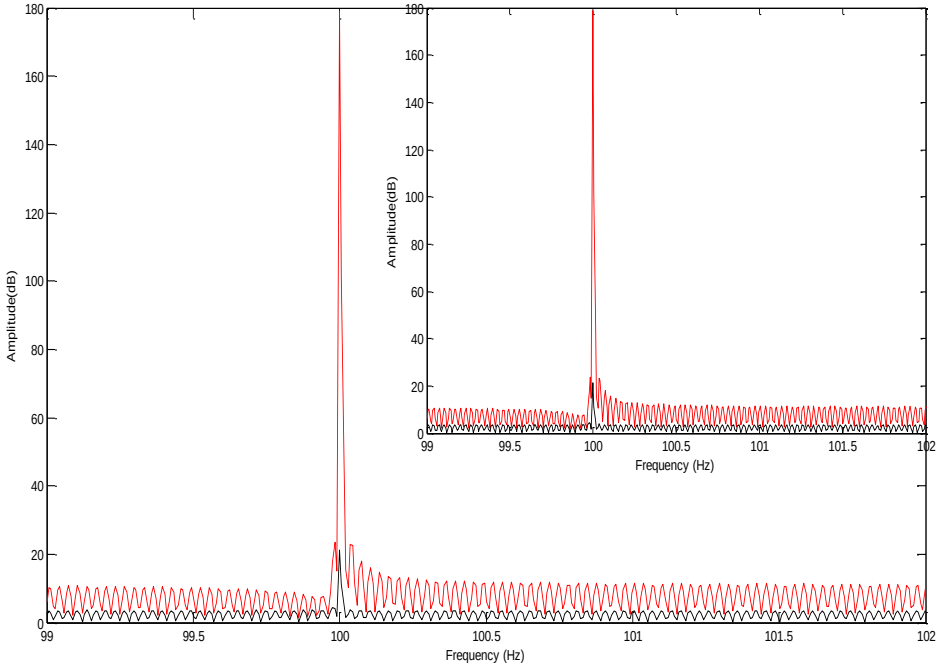

Fig.43 Stator faulty induction generator under half load for reactive power

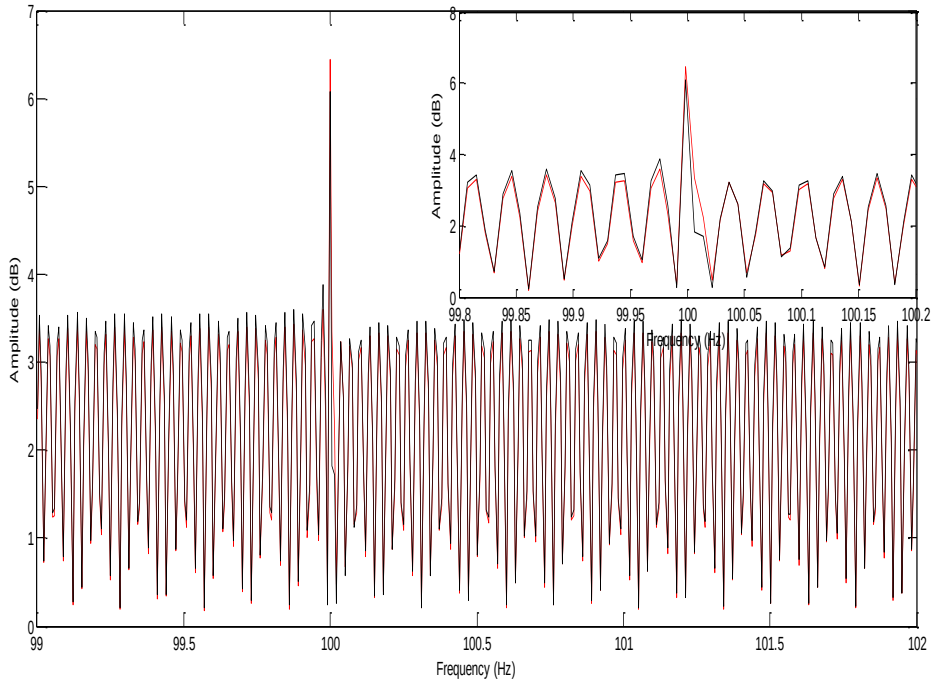

Fig.44 Stator faulty induction generator under full load for active power

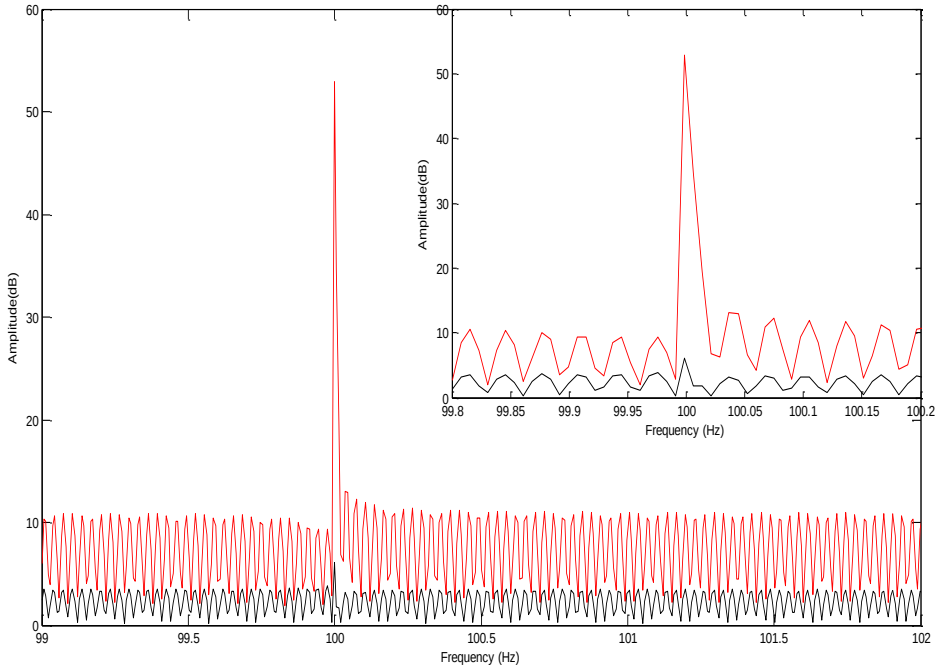

Fig.45 Stator faulty induction generator under full load for reactive power

Then in any induction generator diagnosis, the effect of load should be taken into account to be close to the real system in one hand and to get high sensitive diagnosing system in the other hand. Inversely to rotor one, stator faulty

induction generator under load variation (half and full load) for active and reactive powers present a decrease in power magnitude spectrum with load increase from half to full load. This later makes active and reactive power usable for diagnosing induction generator stator faults.

4.3.3 Load Influence on Mechanic to Electric Transformed Power Based Diagnostic

Transformation of power from mechanic to electric represents the main role of induction generator and it can be a key in diagnosis process. Load variation is one of the most common problems faced in the accurate faults detection in industrial environment.

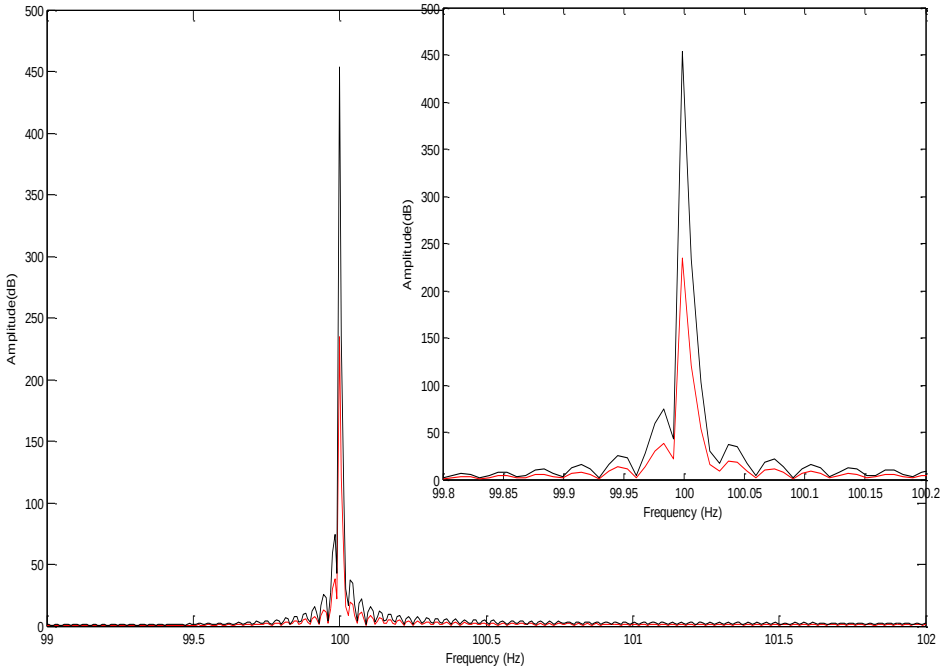

Fig.46 Healthy induction generator under half and full load for transformed power

The red line represents induction generator under half load condition and the black line represents induction generator under full load condition. The figure (46) above is points out the changes introduced by load to the healthy induction

generator. In order to clearly seen the fault variation as side band components, a zoom has been taken out for both healthy under half and full load.

Even that the system is in healthy conditions, either fundamental component of spectrum or side bands ones correspond to fault receive remarkable variations. Consequently, induction generator diagnosis process based on transformed power analysis presents doubt situation in presence of load.

Interaction of load and rotor fault for transformed power diagnosis is presented in figures (47-50) below.

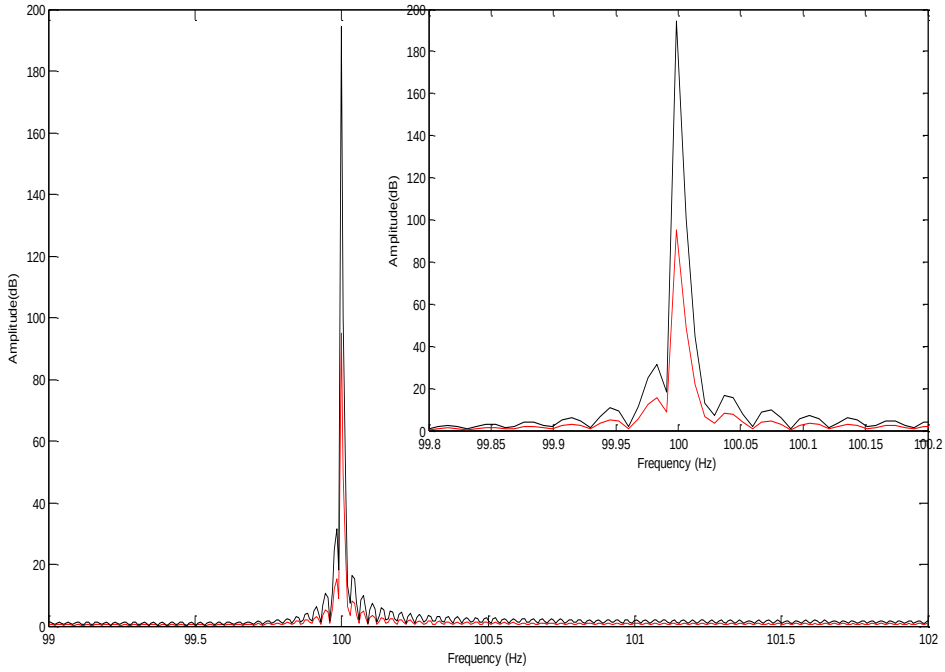

Fig. 47 Rotor faulty induction generator under half load for transformed power

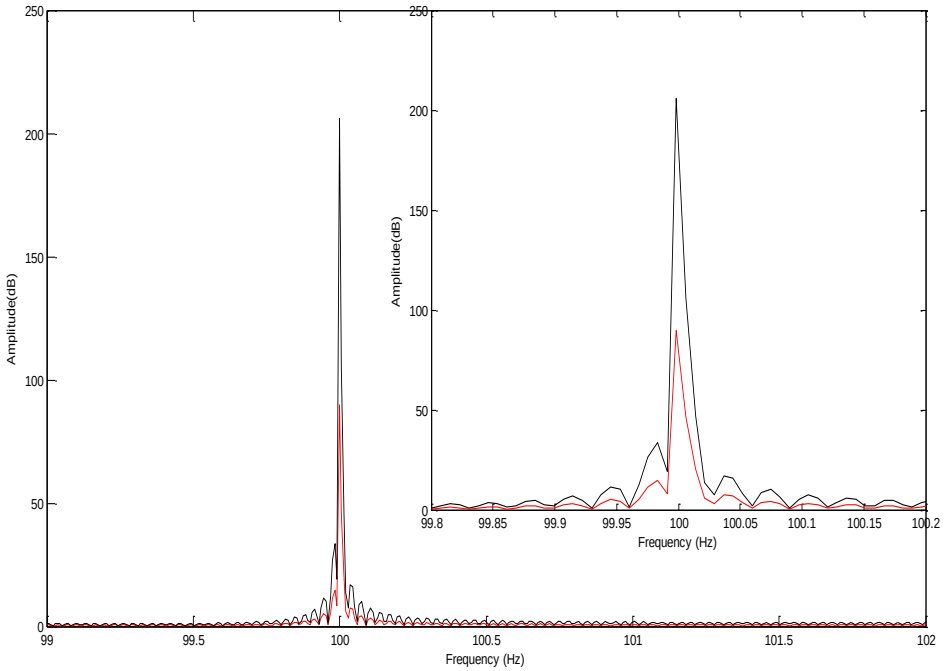

Fig.48 Rotor faulty induction generator under full load for transformed power

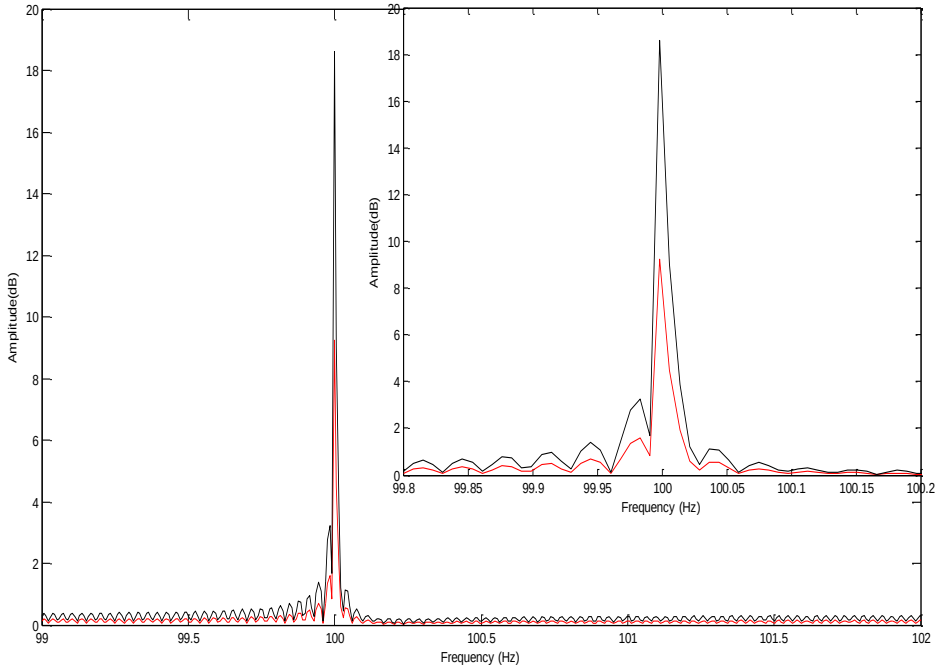

Fig.49 Stator faulty induction generator under half load for transformed power

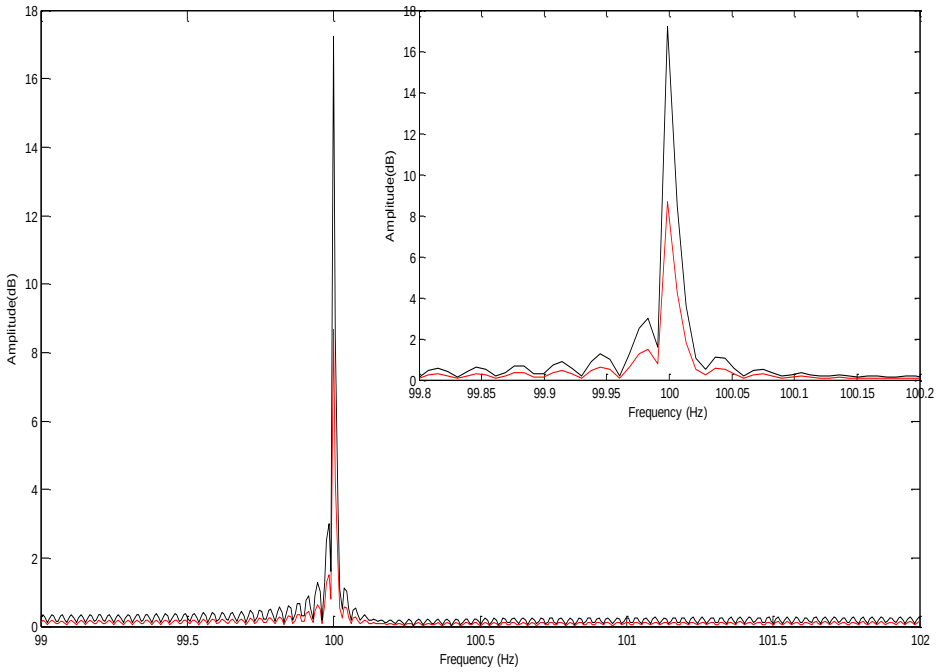

Fig.50 Stator faulty induction generator under full load for transformed power

It can be clearly seen in all spectrums above and confirmed by zoom out corresponding, either for rotor or stator fault spectrum, under load variations bring by load appears at the same frequency of fault, which can hide faults features and makes diagnosis process in doubted situation.

4.3.4 Load Influence on Complex Apparent Power

Complex apparent power encloses active and reactive power together and can be useful tool in induction generator faults diagnosis. Many phenomena can interact with generator behaviors and leads to erroneous diagnosis. Figure 51 below presents the influence of load variations on the healthy generator.

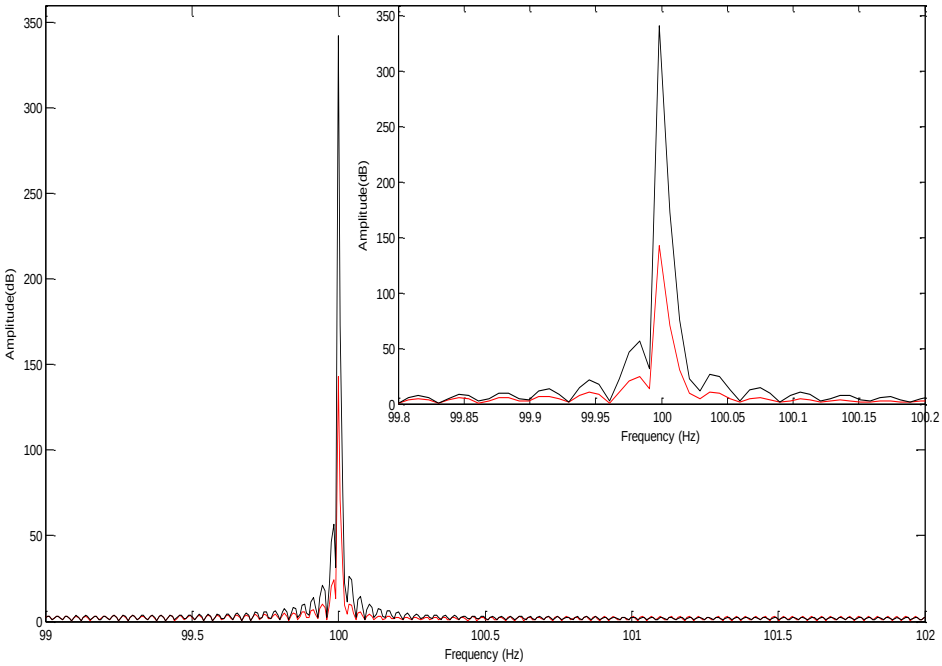

Fig.51 Healthy induction generator under half and full load for Complex apparent power

The black line represents healthy induction generator under full load for Complex apparent power.

The red line represents healthy induction generator under half load for Complex apparent power.

One can see that, even that the system is in healthy conditions, load variation influence affects the side band component correspond to the faults frequency in addition to the main specter component. A zoom has been taken out and presented in the same figure confirms the variation of the fundamental component of spectrum and the side band components.

Deeper, interaction of load and stator or rotor faults could be presented in the figures (52-55) below.

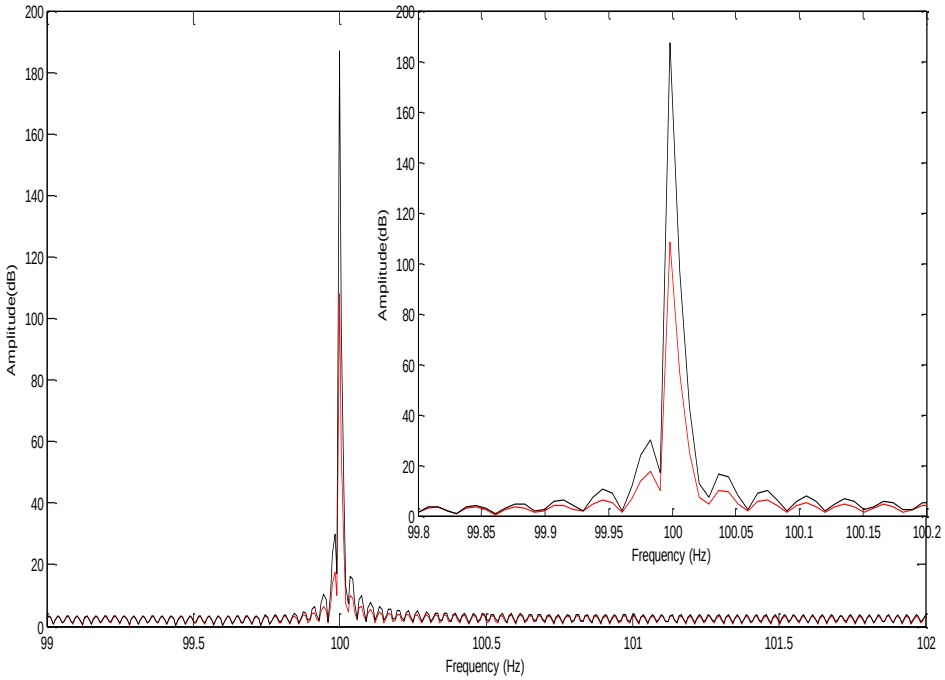

Fig.52 Rotor faulty induction generator under half load for Complex apparent power

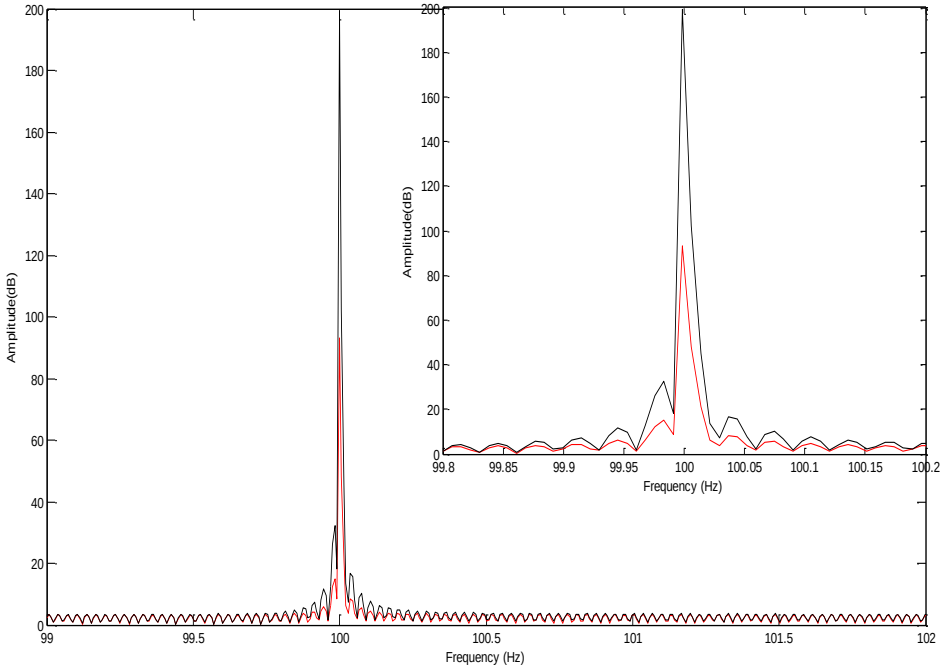

Fig.53 Rotor faulty induction generator under full load for Complex apparent power

The black line represents the rotor faulty induction generator.

The red line represents the rotor faulty induction generator under load variations.

Figures (52-53) represent spectrum of rotor faulty induction generator under half and full load for Complex apparent power, one can see that load variation can modify the results and may hide the fault characteristics, either fundamental or the two side band components vary with load variation. These outcomes are confirmed by zooms which are taken out for each spectrum to points out the influence of load variation on the faulty system.

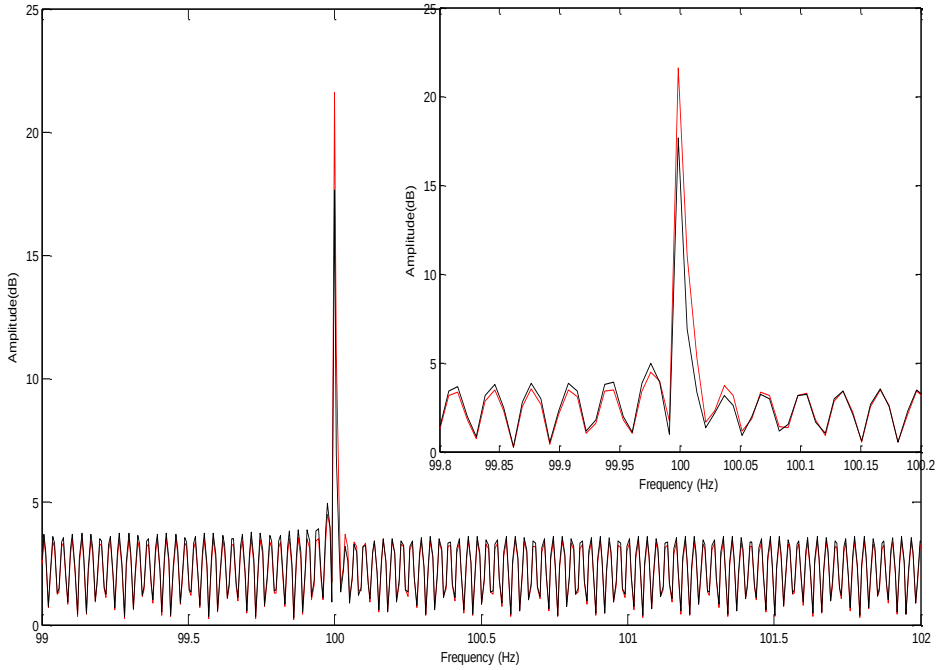

Fig.54 Stator faulty induction generator under half load for Complex apparent power

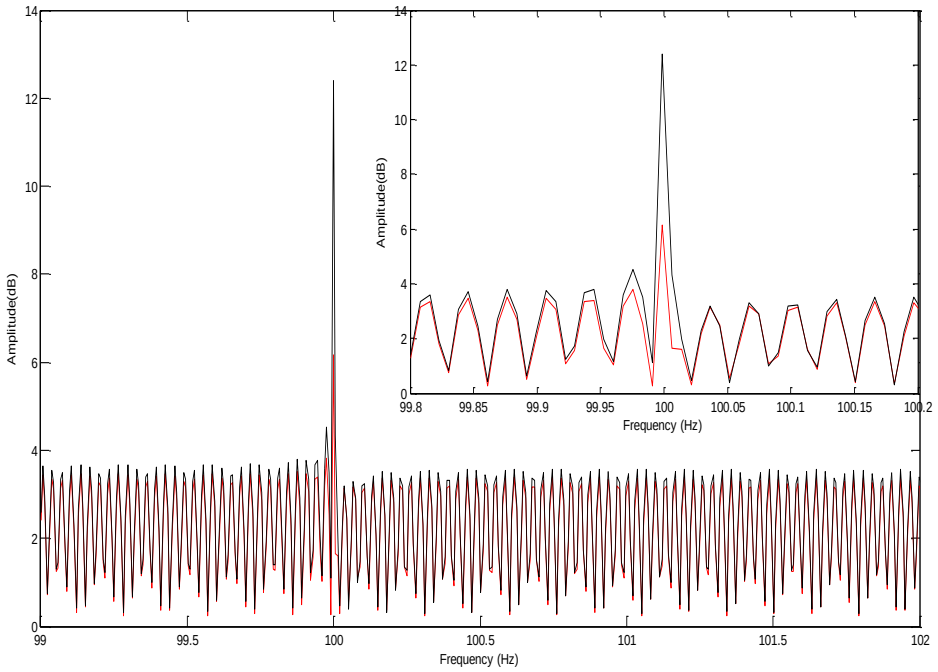

Fig.55 Stator faulty induction generator under full load for Complex apparent power

The black line represents the stator faulty induction generator.

The red line represents the stator faulty induction generator under load variations.

Figures (52-53) correspond to complex apparent power for stator faulty induction generator under half and full load. Even that the side bands components of stator faulty complex apparent power spectrum under half or full appear to be practically unchangeable, the fundamental ones receive remarkable changes which make diagnosis process in doubt situation.

Specters analysis all powers of induction generator investigated in this thesis shows that all powers analysis suffer from load influence, more over specter analysis clarify that changes received can lead to wrong diagnosis. An accurate faults analysis should pass through minimizing load influences.

4.4 Different Powers Simulation Results Based on Faults Evolution Technique

In the following, simulation results are presented. The blue spectrum component represents the one rotor broken bar (1BB) and one stator short cut (1SC) respectively. The red spectrum component represents two rotor broken bars (2BB) and two stator short cuts (2SC) respectively. Figure (a) represent the no load faulty rotor case and (b) represents the full load faulty rotor case. Similarly; figure (c) and (d) represent the no load faulty stator case and the full load faulty stator case respectively. Notice that all figures present only the frequency band in which the fault is expected.

4.4.1 Instantaneous Partial and Total Power Spectra

Fig.56 and Fig.57 represent the instantaneous partial and total power spectra of rotor and stator fault respectively. To highlight the spectrum components a zoom has been drawn around the fundamental component which appears at the frequency of 100 Hz. One can see the appearance of side-band components, called harmonics, at the frequency of $(1 \pm 2s)f$ around the fundamental component. These harmonics represent the faulty behavior that increases remarkably with the rotor and stator defect without a significant load effect. Load effect influences only the amplitude of spectrum and hence cannot lead to erroneous diagnosis. Generally, all faults can be easily separated, 1BB from 2BB and 1SC from 2SC, which makes partial and total power usable for detecting faults in induction generator.

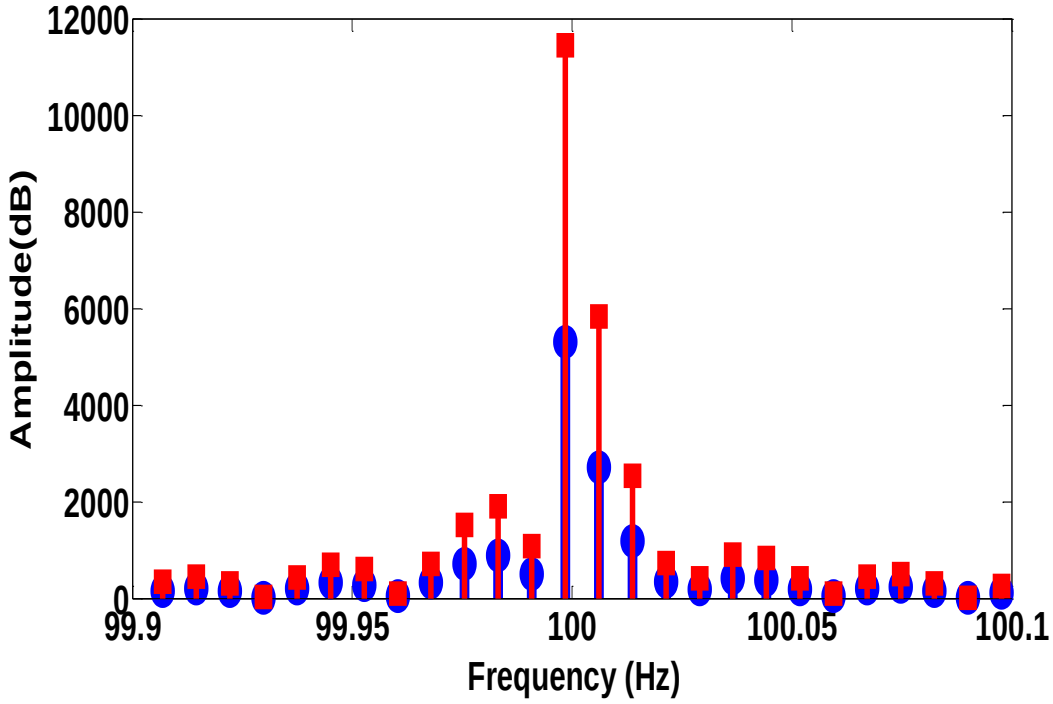

a. No load rotor power spectrum

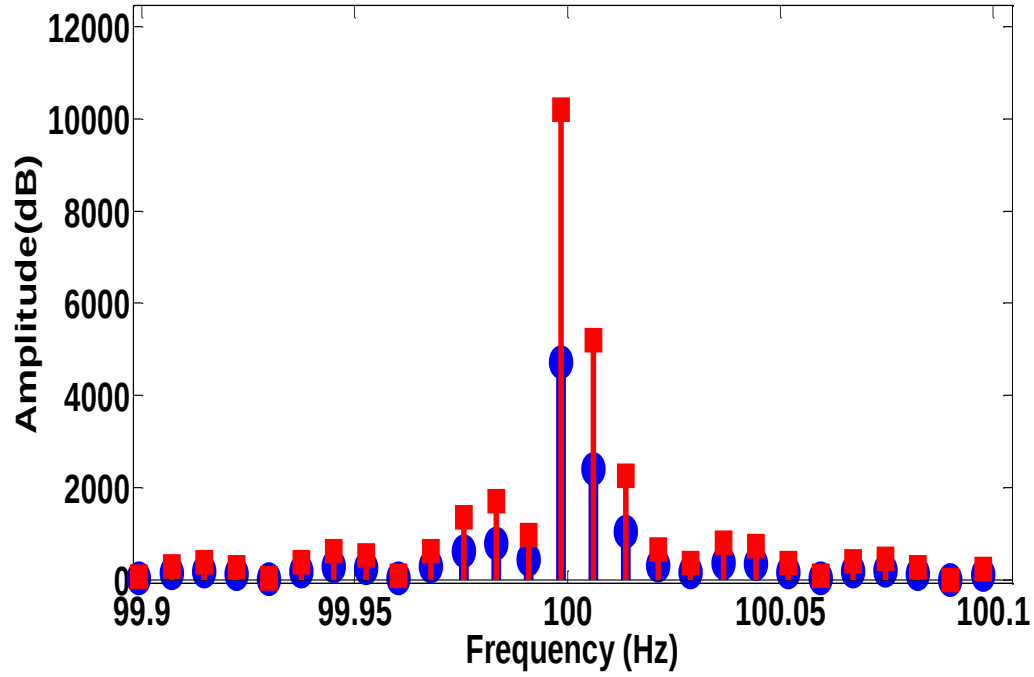

b. Full load rotor power spectrum

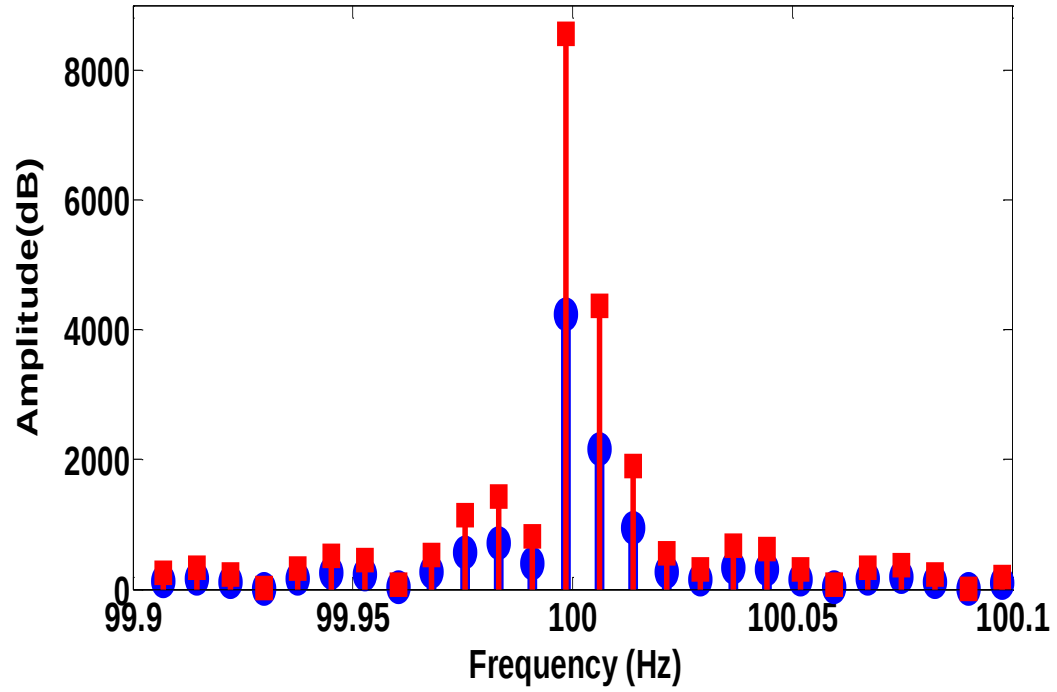

c. No load stator power spectrum

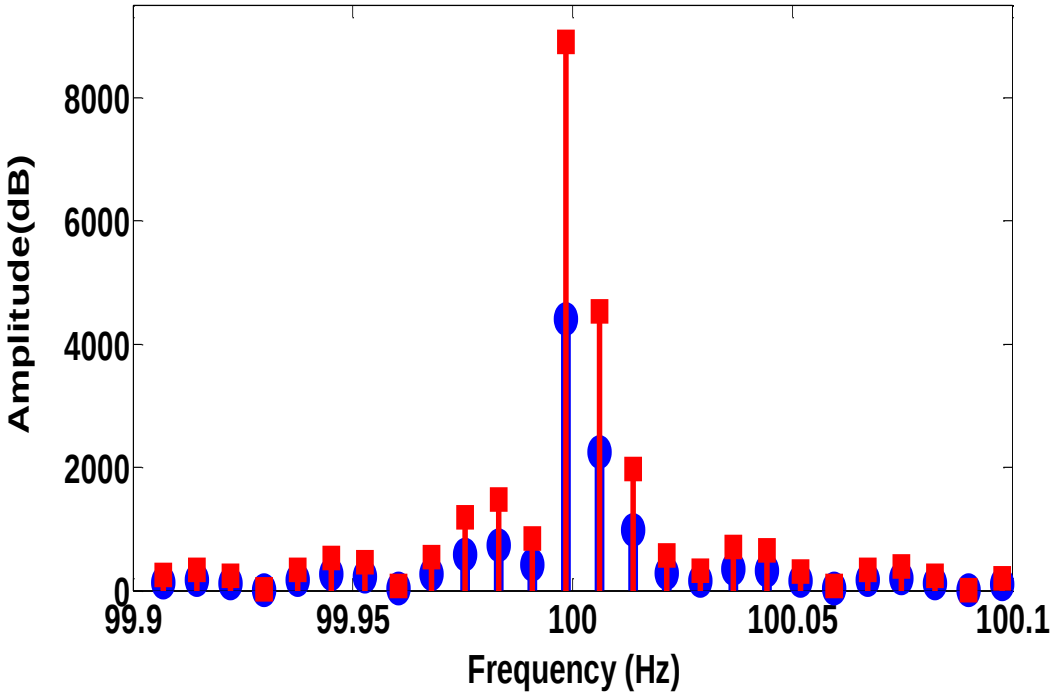

d. Full load stator power spectrum

Figure. 56 Rotor and stator spectra curves for partial power experiments

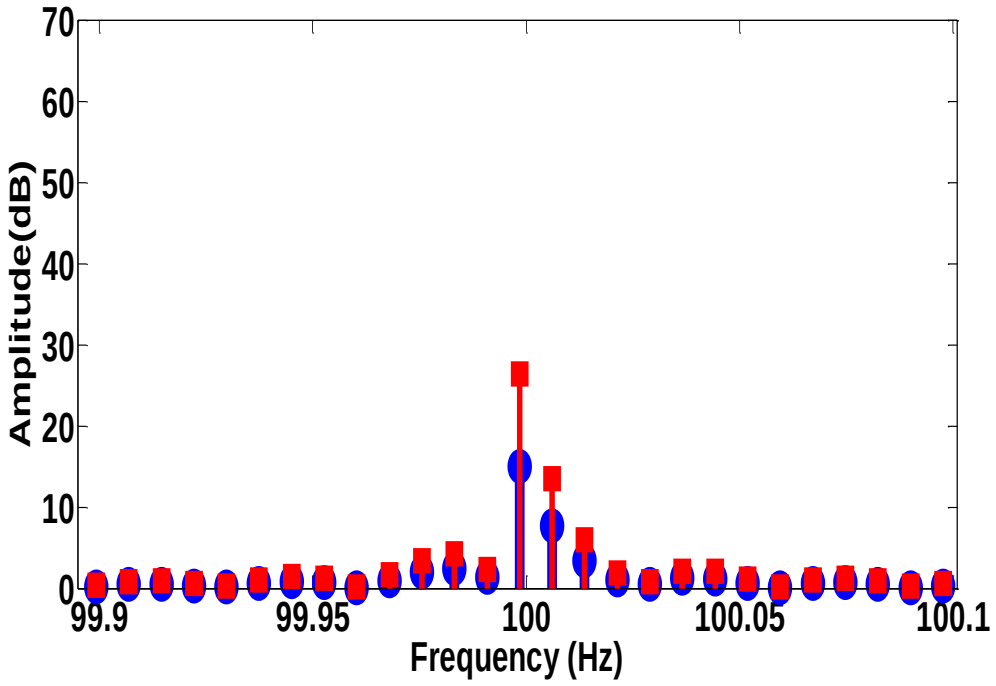

a. No load rotor power spectrum

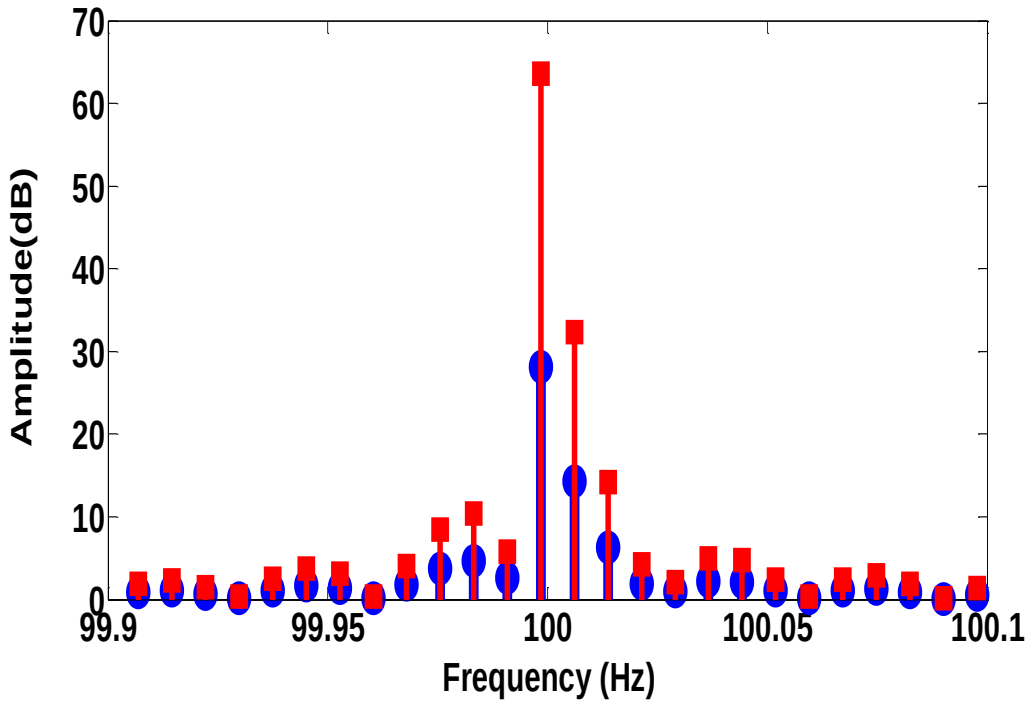

b. Full load rotor power spectrum

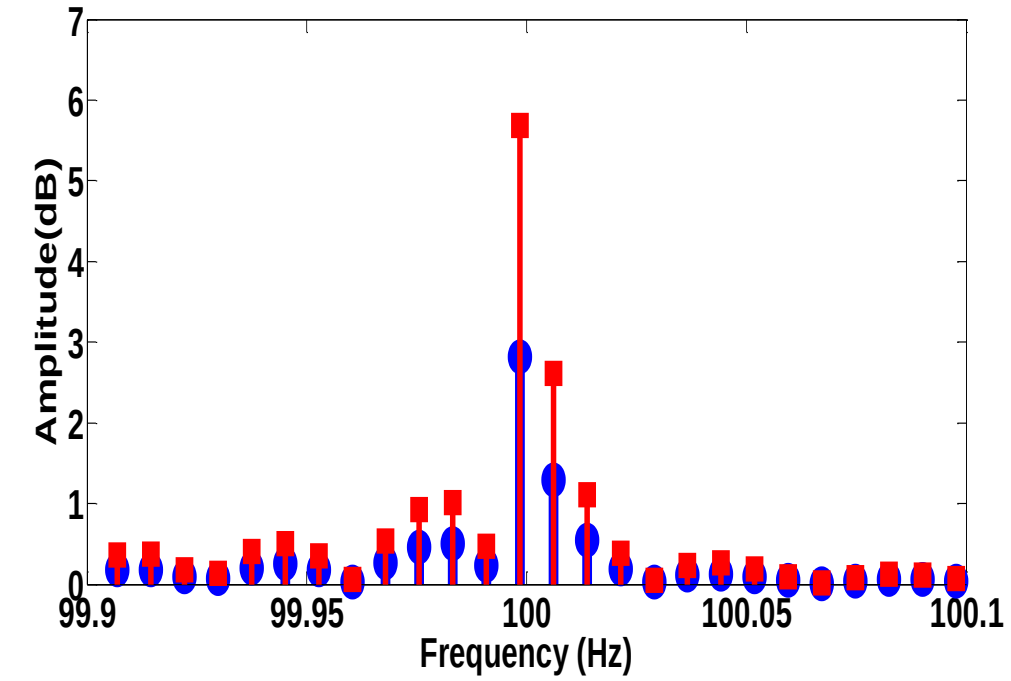

c. No load stator power spectrum

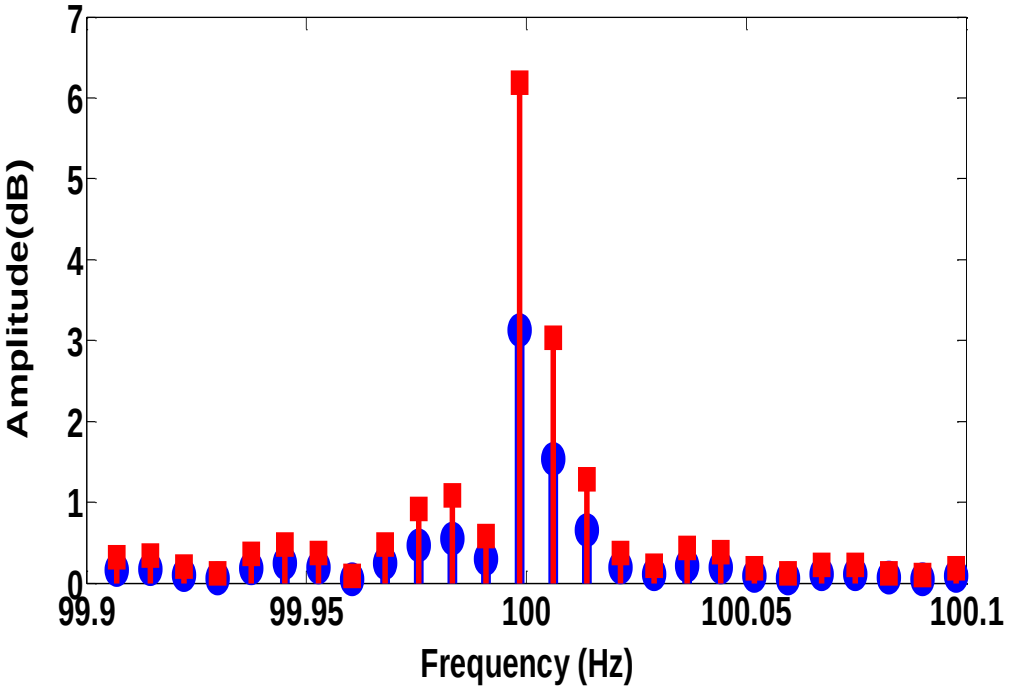

d. Full load stator power spectrum

Figure.57 Rotor and stator spectra for total power experiments

4.4.2 Simulation Results for Active and Reactive Power

Fig.58 and Fig.59 present the simulation results for active and reactive power experiments. One can see in Fig.58.a and Fig.58.b that rotor fault evolution is detectable and the results are similar to the partial and total power discussed before. Conversely, the stator fault signatures, Fig.58.c and Fig.58.d, are practically superposed thus makes faults evolution diagnosis useless. For the reactive power analysis, Fig.59.a and Fig.59.b, one can notice while the rotor fault severity is increasing from 1BB to 2BB, the spectrum amplitude decreases abnormally, consequently, thus hide the fault effect. The load influence for rotor fault is not considerable and the main component for 1BB is practically superposed upon the 2BB, this makes the fault evolution diagnosis useless.

In the case of stator faults, Fig.59.c and Fig.59.d, one can see that the main fault characteristics are lost and as a consequence the reactive power spectrum method cannot be used to diagnose stator faults.

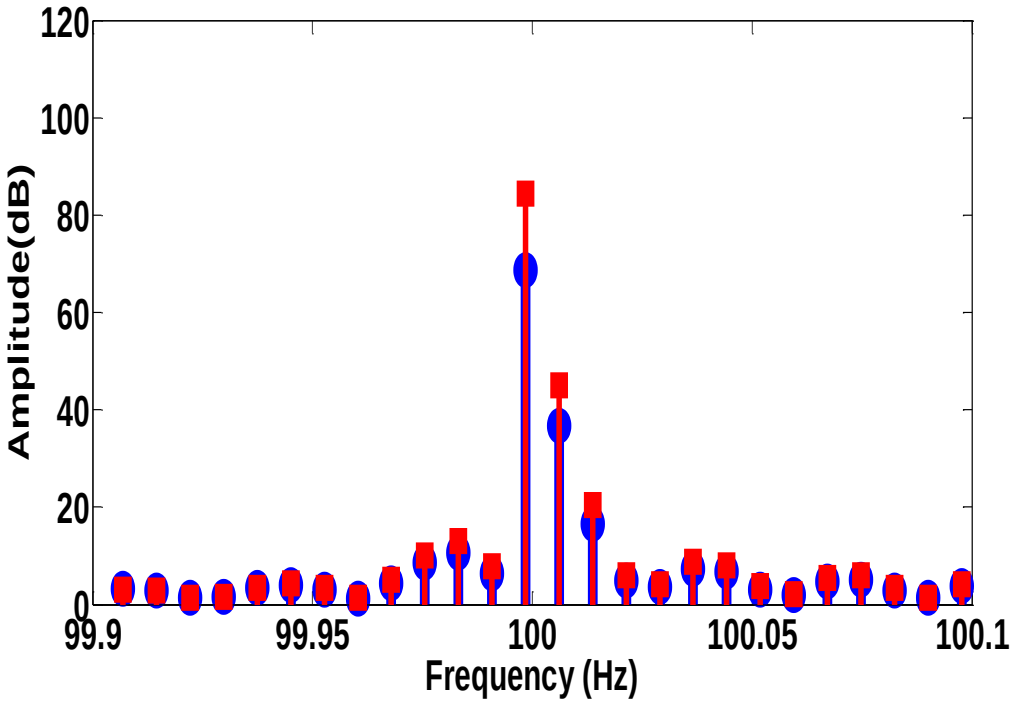

a. No load rotor power spectrum

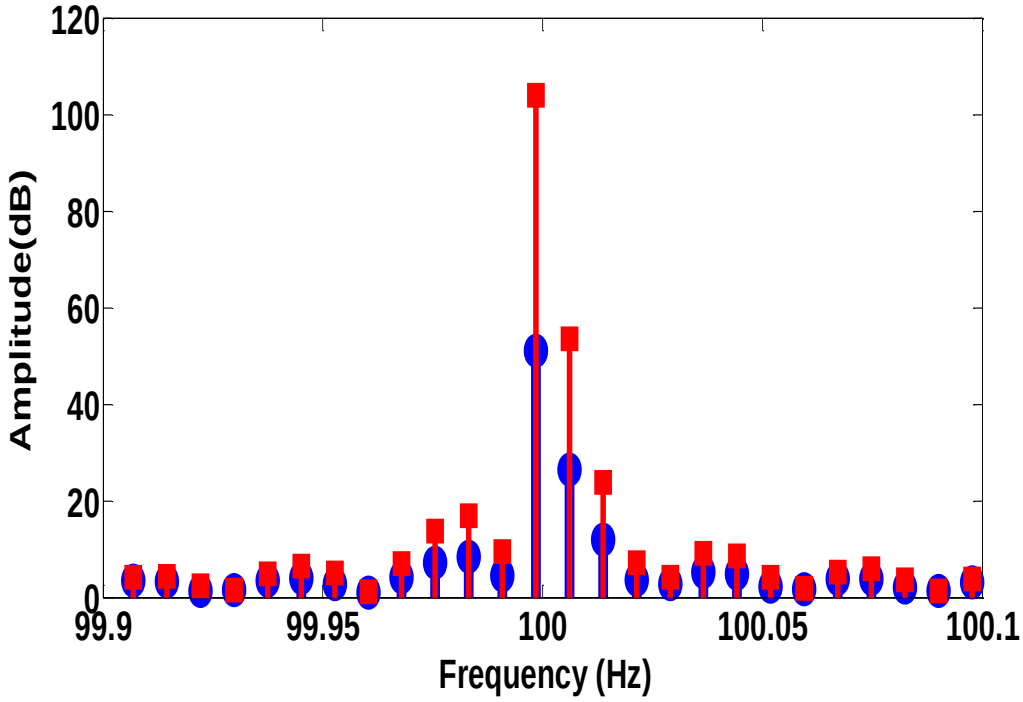

b. Full load rotor power spectrum

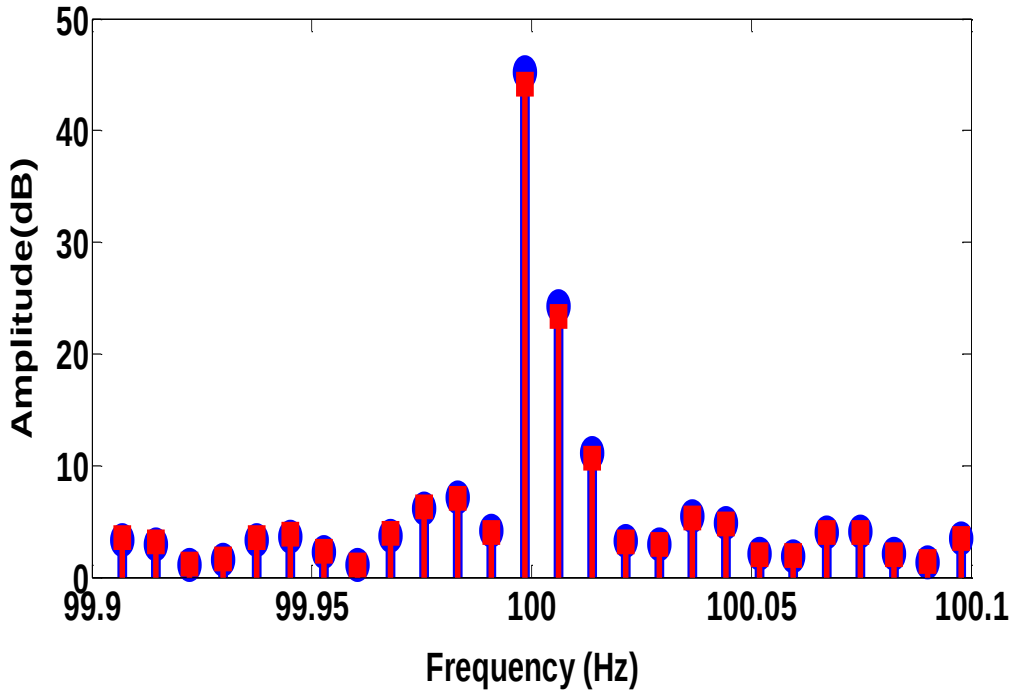

c. No load stator power spectrum

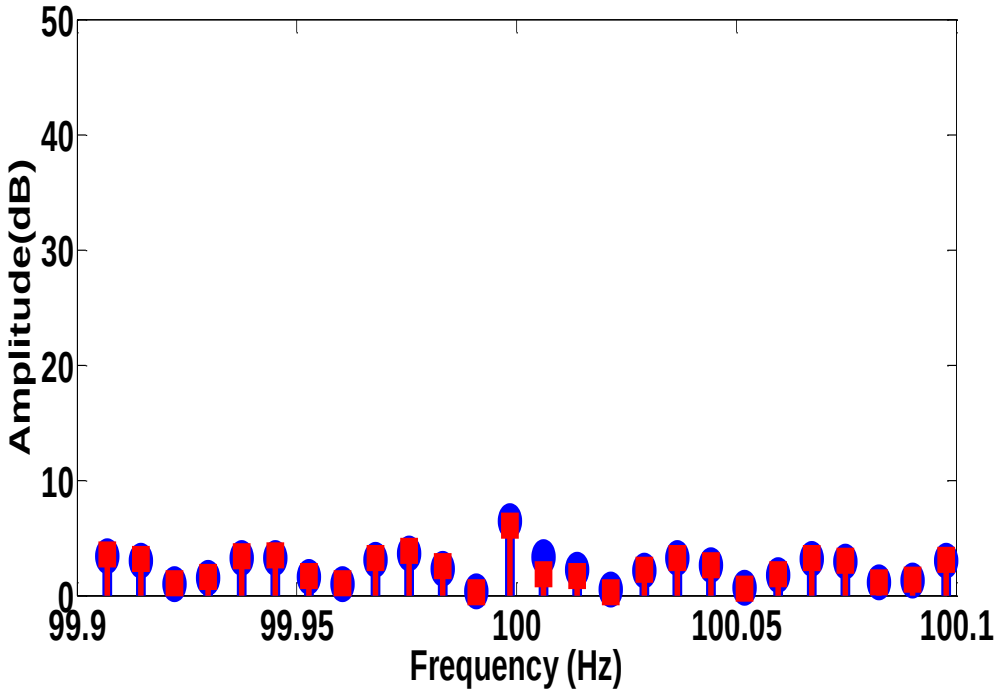

d. Full load stator power spectrum

Figure. 58 Rotor and stator spectra for active power experiments

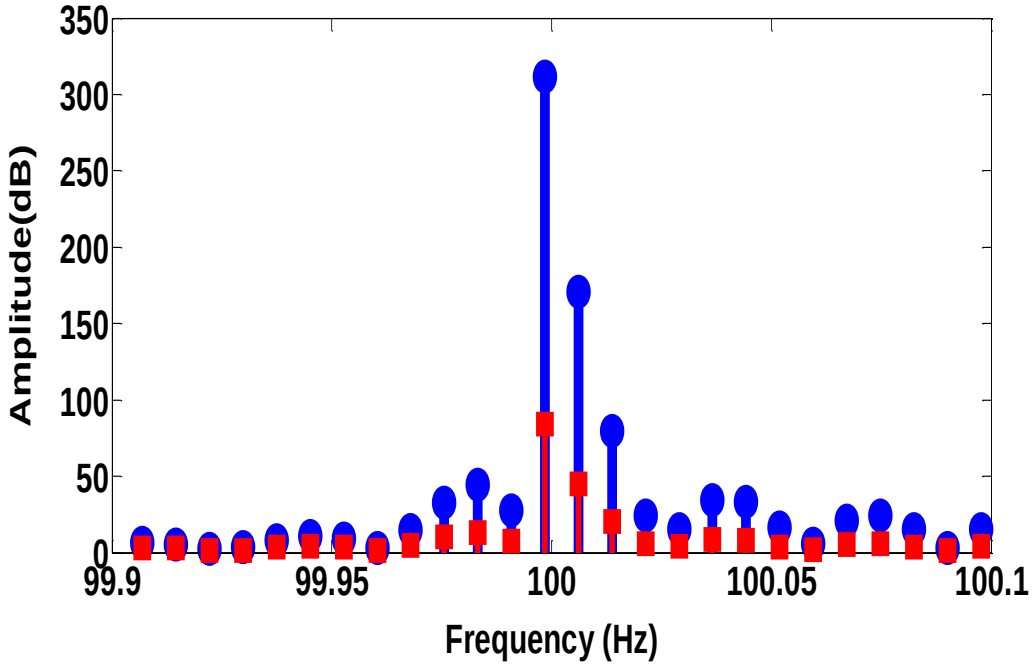

a. No load rotor power spectrum

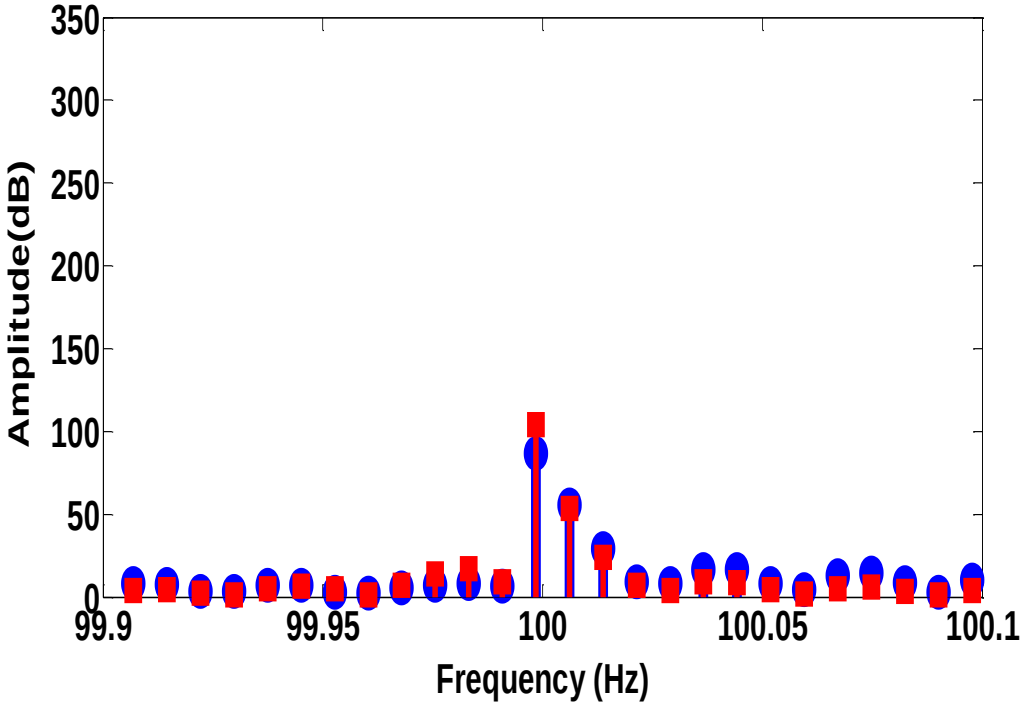

b. Full load rotor power spectrum

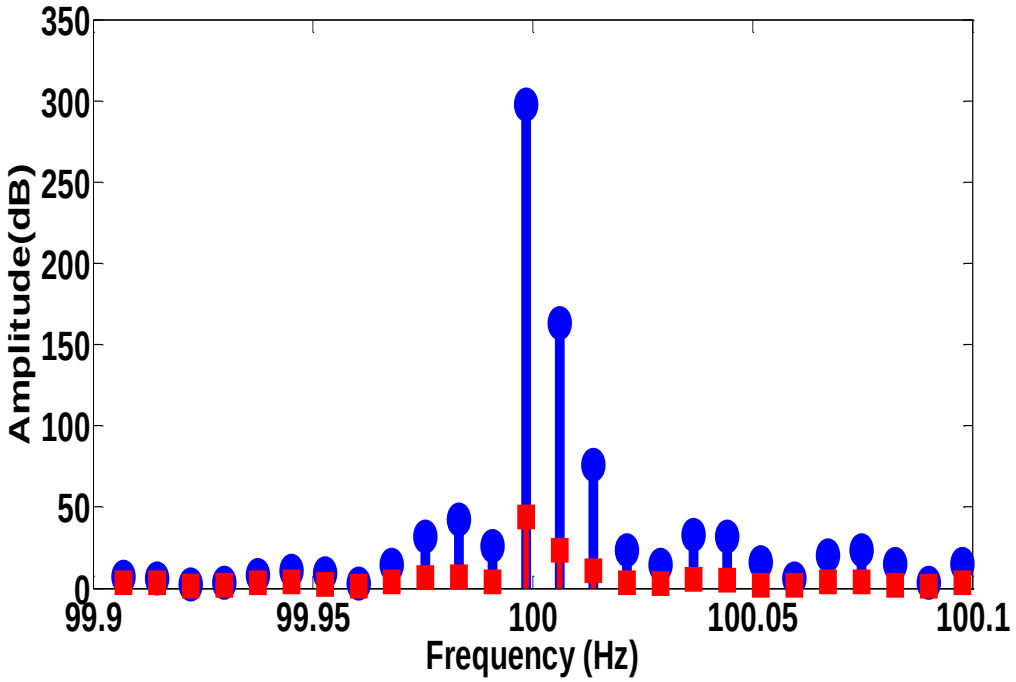

c. No load stator power spectrum

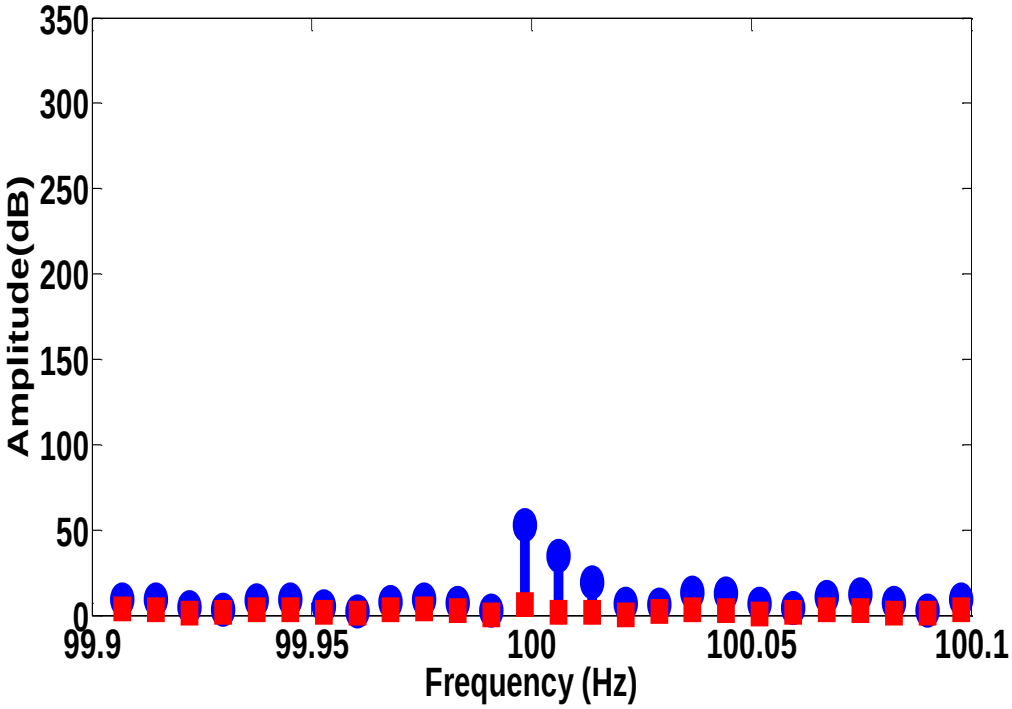

d. Full load stator power spectrum

Figure.59 Rotor and stator spectra for reactive power experiments

4.4.3 Simulation Results of Transformed Power from Mechanical to Electric Form

The simulation results of experiments for the transformed power from the mechanical to electric nature are presented in Fig.60. On can see from Fig.5.a that rotor faults can be easily detected using such method. An evolution of fault amplitude component around 20 dB can be observed. Moreover, Fig.60.b shows, under full load experiments, fault is still detectable with an increase of 40 dB. In the case of stator faults diagnosis one can see that stator fault sideband remains practically load independent, but detectable, with respect to the evolution of the fault from 1SC to 2SC, thus makes transformed power useful for the isolation of load from fault effects.

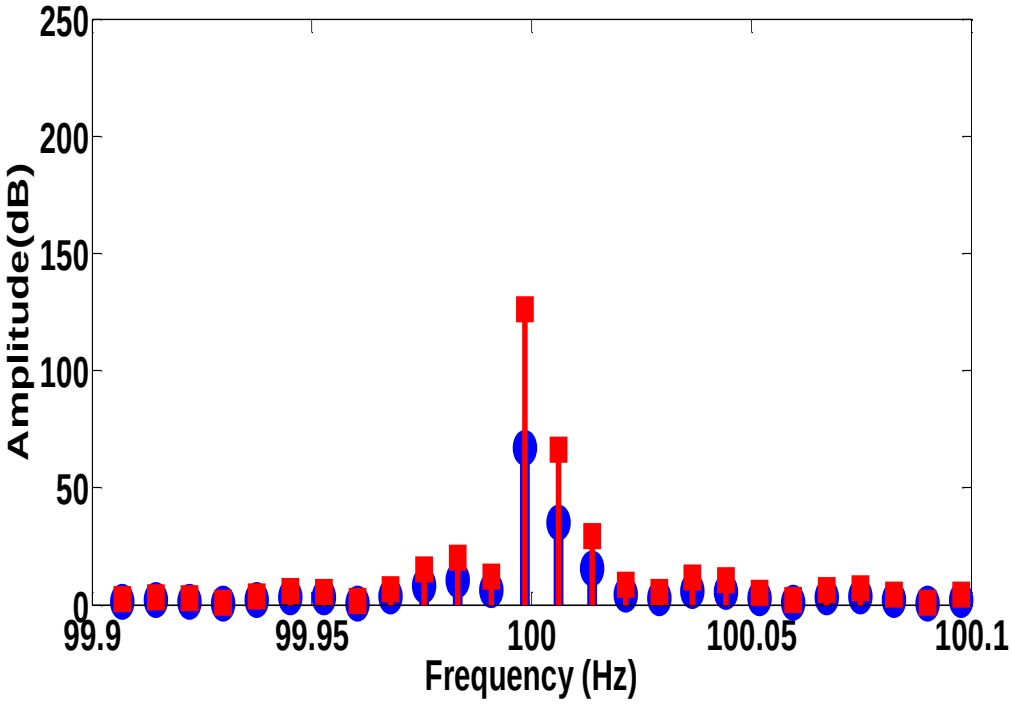

a. No load rotor power spectrum

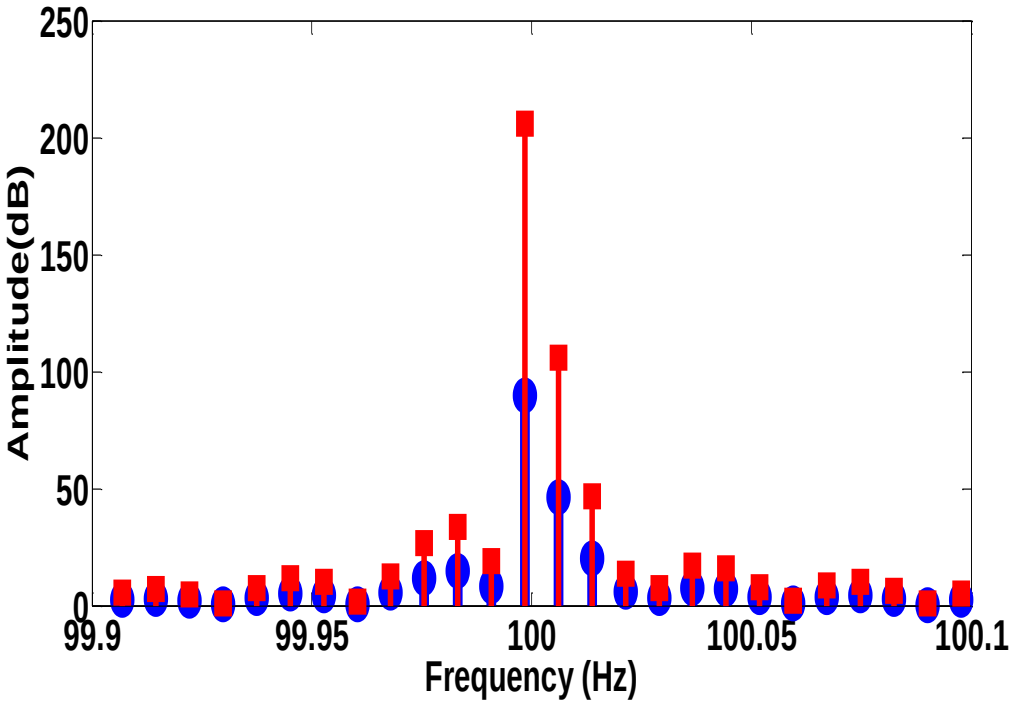

b. Full load rotor power spectrum

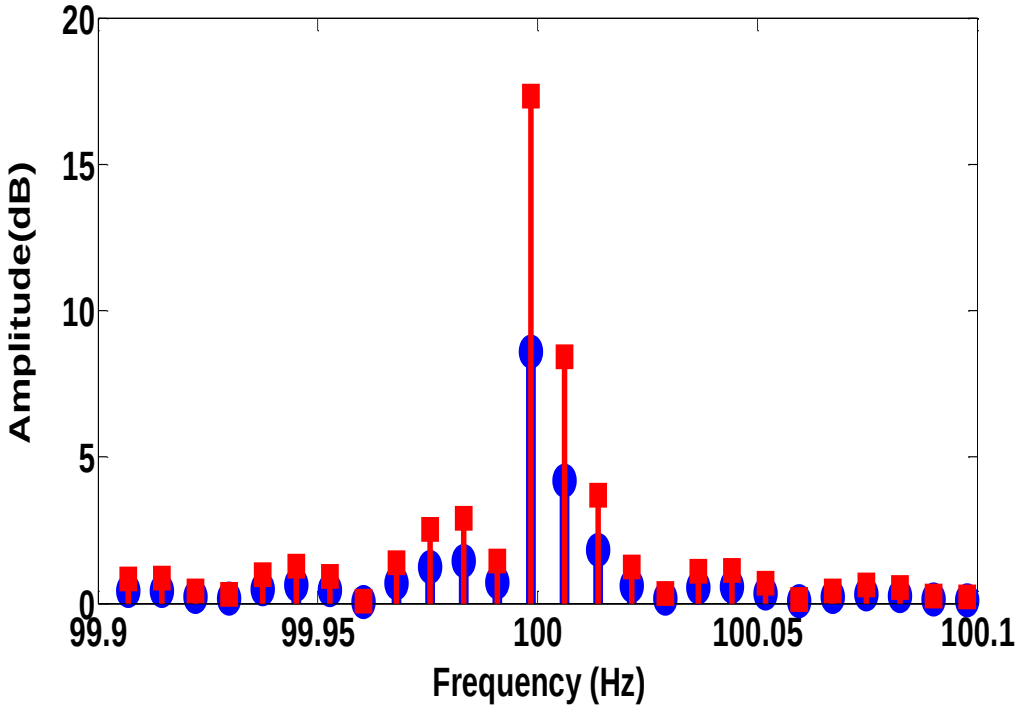

c. No load stator power spectrum

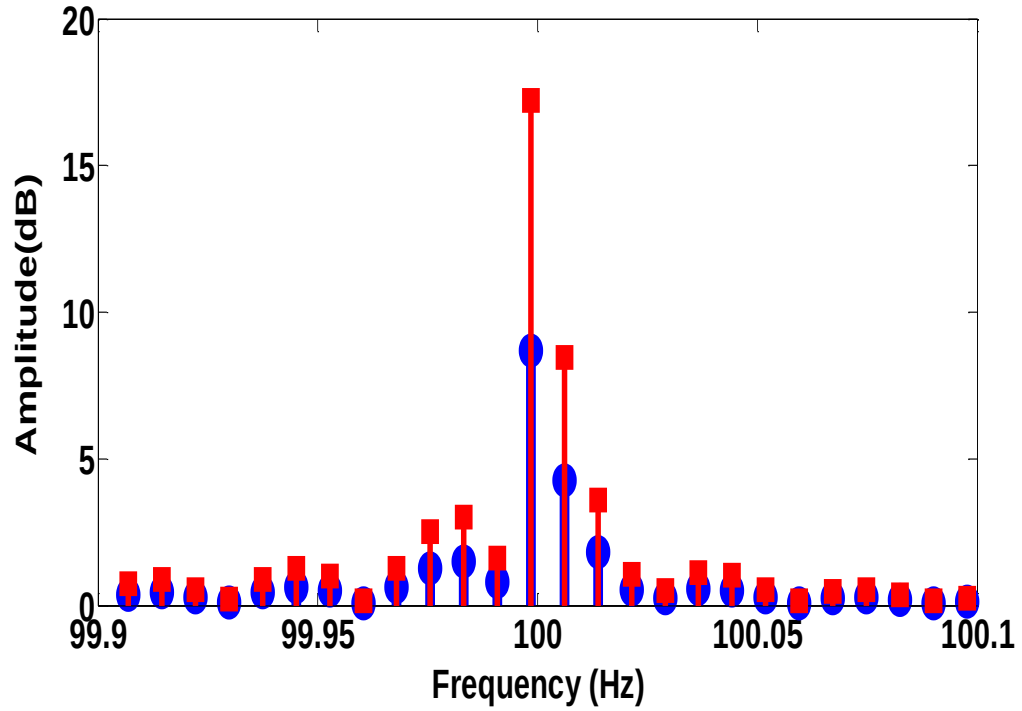

d. Full load stator power spectrum

Figure. 60 Rotor and stator spectra of transformed power from mechanic to electric nature

4.4.4. Simulation Results of Complex Apparent Power

Finally, Fig.61 shows the results of complex apparent power experiments. It can be clearly seen, Fig.61.a, that rotor faulty power main component is largely greater in 2BB (130dB) compared to 1BB (100dB). In the case of load influence, Fig.61.b, the spectrum of faulty apparent power gap separate 1BB from 2BB, this makes the fault detection an easy task. In the case of stator faults, the complex apparent power spectrum shown in Fig.61.c presents clearly only a fundamental component that appears at the frequency of 100 Hz with amplitude of 45 dB for the no load case and 12 dB in the case of full load. As a result stator faults cannot be detected based on complex apparent power. Fig.61.d presents the spectrum of faulty complex apparent power in presence of load, a clear separation of 1CC from 2CC observed makes faults easy to detect.

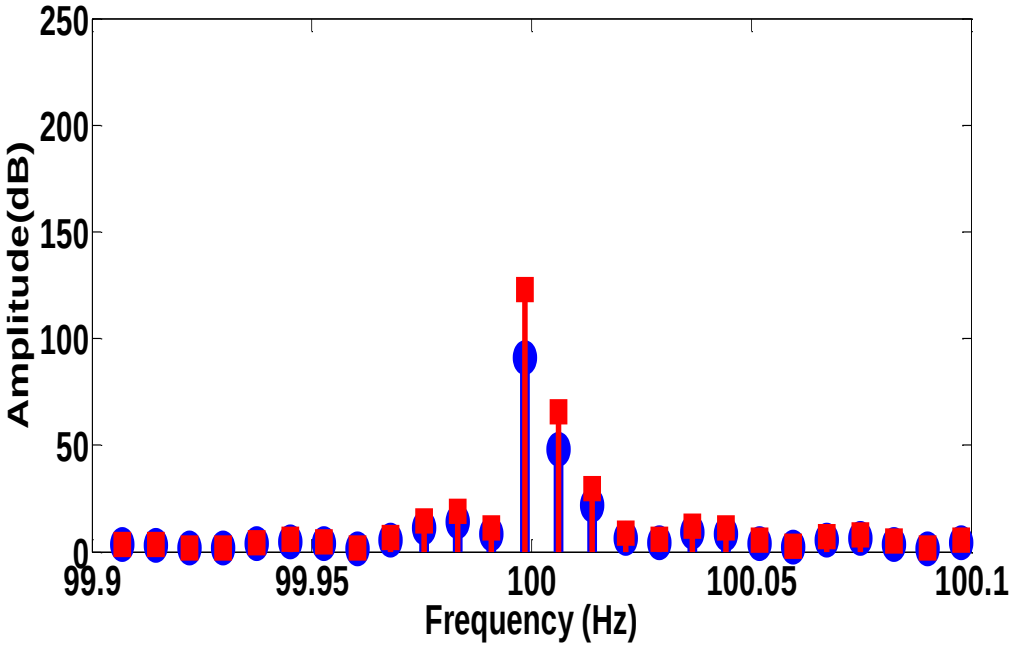

a. No load rotor power spectrum

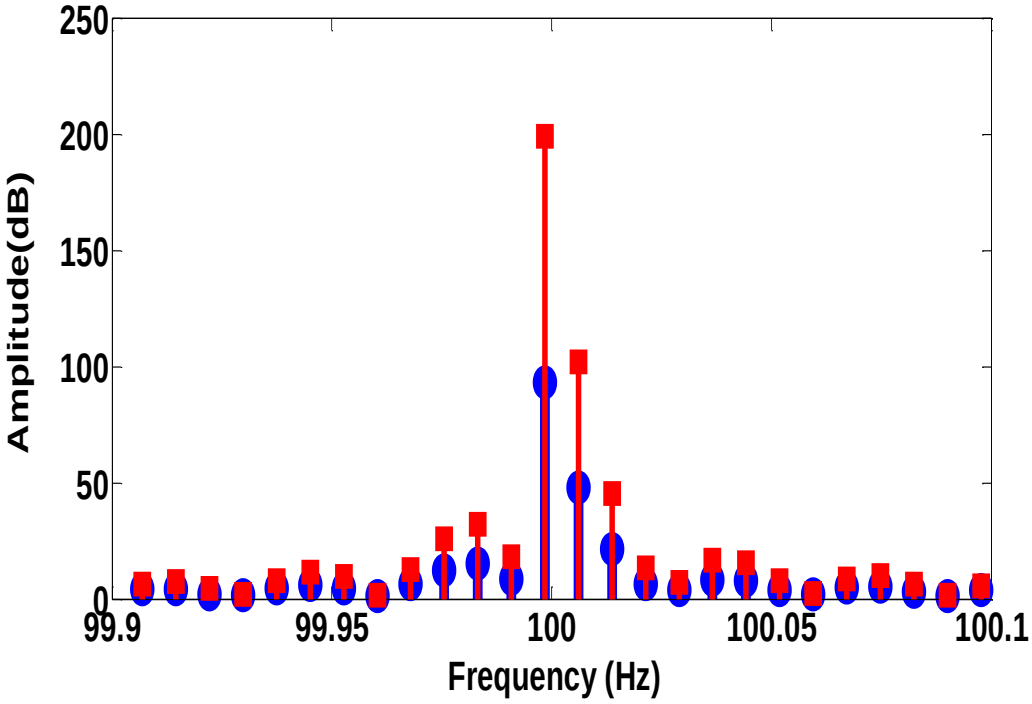

b. Full load rotor power spectrum

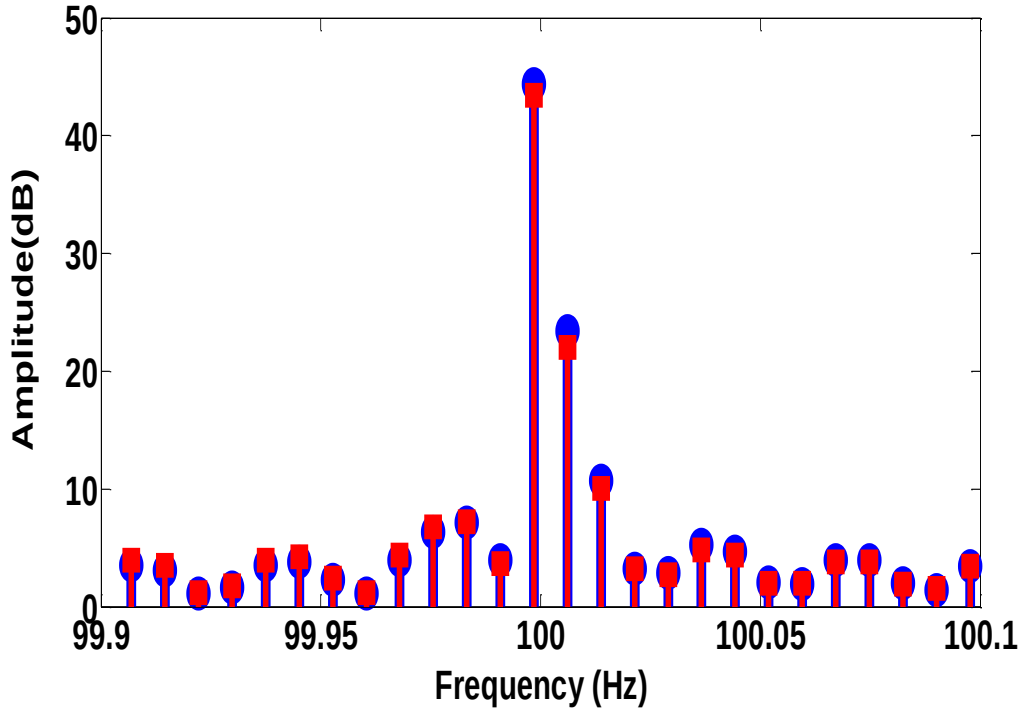

c. No load stator power spectrum

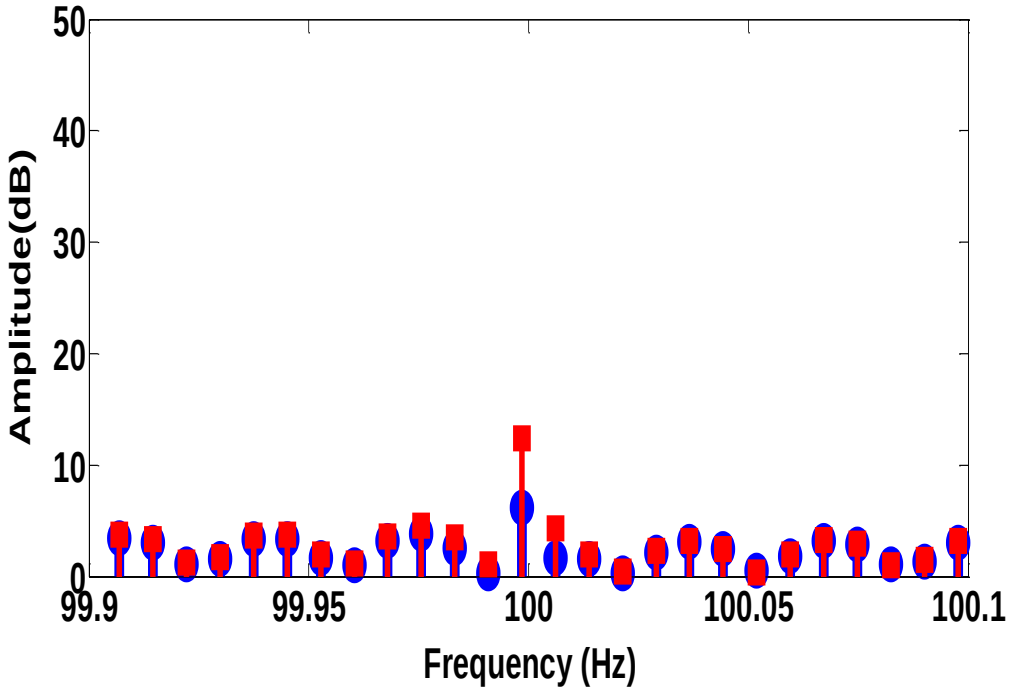

d. Full load stator power spectrum

Figure. 61 Rotor and stator spectra for complex apparent power experiments

4.5 Different Powers Comparative Study

Table 2 presents the results of the comparative study between the different experiments performing the different induction generator analytical power expressions to diagnose the rotor and stator faults. The symbol Y means that the fault is detectable and N means it is not detectable. One can see, on one hand that partial, total power and transformed power can be used to detect rotor and stator faults and the active, the reactive and the complex apparent power can be used to detect either rotor or the stator faults on the other hand. Moreover, it can be noticed, from the obtained simulation experiments that the load has not remarkable effect on the retained power to diagnose induction generator faults.

Table 2 Faults detection results

Symbol	No load		Full load	
power	Rotor fault	Stator fault	Rotor fault	Stator fault
Partial	Y	Y	Y	Y
Total	Y	Y	Y	Y
Active	Y	N	Y	N
Reactive	N	N	N	N
Power Transferred	Y	Y	Y	Y
Complex power	Y	N	Y	Y

In order to detect and to distinguish the rotor faults from the stator ones a severity factor (SF) is proposed and evaluated in this thesis.

Table 3 presents the obtained values of the proposed severity factor, as example for the partial power experiments performed in this thesis. One can see that this severity factor will go down for load or no load conditions in the presence of rotor broken bars. Conversely for the stator shorted turns it goes up. Moreover, it can be effortlessly visible that load has not remarkable impact on the proposed severity factor, which makes power method appropriate for diagnosing induction generator faults.

Table 3 SeverityFactor Results

Load	No load				Full load			
Faults type	Rotor fault		Stator fault		Rotor fault		Stator fault	
Faults quality	1BB	2BB	1CC	2CC	1BB	2BB	1CC	2CC
SF	0.229305	0.215301	0.250858	0.260521	0.230742	0.218717	0.250984	0.260637

Given the state-of-the-art in this field, this thesis proposes a new methodology for the diagnosis of rotor faults, independently of the type of load coupled to the motor. The method relies on a combined analysis of the active and reactive powers of the motor and is able to detect a rotor fault and distinguish it from a load torque variation even when they occur simultaneously.

According to results obtained in the different simulation experiments for different power models, one can states that not all power methods might be used to diagnose rotor and/or stator faults in induction generator systems. Using a power expression as a diagnostic tool, the power spectrum will contain a dc component, invisible in figures to avoid a complicated spectrum, and a fundamental component oscillating at twice the supply frequency. Based on the fact that the value of slip is very small, the rotor fault components will be very close to the supply frequency. Thus, diagnostic will be a complicated task because of the fusion between the two components.

Conclusion

A comparison among induction generator fault detection methods based on power analysis showed that all methods can be used for detection the most common generator's faults. Generally, each previous diagnosis process uses one form of power which will symbolize the curve variations introduced by faults. In reality, every power representation receives part of fault influences and the comparison will guide to the appropriate method. Even if the mathematical presentation of power seems similar, the simulation results show that they are different and must be taken as a form a part. As results, detecting faults is feasible using all methods previously detailed. Nevertheless, sensing evolution of faults orientate diagnosis procedure toward the appropriate power. More research can be addressed to point out the influence of other parameters rather than load influence, and then an experimental application of powers previously treated will be the objective of a new work.

In this thesis several theoretical PQ models are proposed to be used for induction generators faults detection and diagnosis, a combination between rotor and/or stator variables constitute the state space system for PQ models. Each

model can be used separately to embody the generator behaviors in healthy and faulted conditions.

As it is pointed out before, the level of confidence can be up if crossing the methods and select the common zone. Generally, each diagnosis process uses one element of PQ ellipse which will symbolize the curve variations introduced by faults. In reality, every parameter receives part of faults influences and repetition leads to confirm the results, this hypothesis is theoretically validated by the principle of cross probability.

Analyzes of faults evolution results, could lead to two categories of power, in terms of faults evolution detection. Partial power, total power and transformed power can be used to detect evolution of either rotor and or stator faults. Active, reactive and complex apparent power can be used to detect evolution of rotor faults only. Moreover, it can be noticed, from the obtained simulation experiments that the load has not remarkable effect on the retained power to diagnose induction generator faults.

BIBLIOGRAPHY

CONFERENCES AND PUBLICATIONS OF THE AUTHOR

Leksir, A. and Bensaker, B. (2009) ''Asynchronous Generator's Active and Reactive Power Modelling for Faults Diagnosis Purposes in Wind Energy Conversation Systems'' 2nd International Conference On Electronics Systems CISE'09, Oct, 25-26, 2009, Batna, Algeria

Leksir, A. and Bensaker, B. (2009) '' Modeling of Asynchronous Generator Power for Rotor Faults Diagnosis Based on Double PQ Transformation '' 3rd International Conference on Electrical Engineering ICEE2009 Boumerdes 5-7 December 2009

Leksir, A. and Bensaker, B. (2011) '' Induction Generator Rotor Faults Modeling and Diagnosis Based on Double PQ Transformation'', IEEE International Conference on Multimedia Computing and Systems (ICMCS), Morocco7-9 April.

leksir, a. bensaker, b.(2019) ''Simulation of Different Power Methods for Induction generator Faults Detection and Diagnosis.'' international journal of power and energy conversion. vol.10 no.1, pp.89 - 104

REFERENCES

Akagi, H., Kanazawa, Y., Nabae, A., (1984) "Instantaneous Reactive Power Compensators Comprising Switching Devices without Energy Storage Components" IEEE Transactions on Industry Applications, Vol. IA-20, No. 3, pp.625-630.

Amirat, Y., Benbouzid, M., Al-Ahmar, E., Bensaker, B., Turri, S., (2009) "A Brief Status on Condition Monitoring and Fault Diagnosis in Wind Energy Conversion Systems" Renewable & Sustainable Energy Reviews,Vol. 3, No.9, pp.2629-2636.

A. M. Da Silva, R. J. Povinelli and Demerdash N. A. O, MARCH, (2008) "Induction Machine Broken Bar and Stator Short-Circuit Fault Diagnostics Based on Three-Phase Stator Current Envelopes" IEEE Transactions on Industrial Electronics, Vol. 55, No. 3,

A. Prudhom, J. Antonino-Daviu, H. Razik, and V. Climente-Alarcon, (2017)"Time-frequency vibration analysis for the detection of motor damages caused by bearing currents" Mechanical Systems and Signal Processing, Vol. 84, pp. 747–762.

Arkan, M., Kostic-Perovic, D., Unsworth, P.J., (2005) "Modelling and Simulation of Induction Motors with Inter-Turn Faults for Diagnostics" Electric Power Systems Research, Vol. 75, pp.57–66.

A. Zaafouri, F. Farhani1, A. Chaari, (2015) " Robust Observer Design with Pole Placement Constraints for Induction Motor Control " Elektronika Ir Elektrotechnika, VOL. 21, NO. 1, pp. 18-22.

Bensaker, B., Kherfane, H., Metatla A., Wamkeue, R., (2003) "State Space Modeling of Induction Motor For Sensorless Control and Monitoring Proposes" International Journal Electromotion,Vol. 10, No. 4, pp.483-488.

Benbouzid, M. E. H., (2000) "A Review of Induction Motors Signature Analysis as a Medium for Faults Detection" IEEE Transactions on Industrial Electronics, Vol. 47, No. 5.

Bellini, A., Filippetti, F., Franceschini, G., Tassoni, C., Kliman, G.B., (2001) "Quantitative evaluation of induction motor broken bars by means of electrical signature analysis" IEEE Trans. on Ind. Appl., 37(5):1248-1255.

Bitoleanu, A., Popescu, M., Linca, M., (2007) "Instantaneous Complex Apparent Power Theory And Apparent Power Definitions – Case" 6-thInternational Conference on Electrical and Power Systems, Chisinau, Moldova, Vol.31,pp.285-289.

Boudebbouz, O., Boukadoum, A., Leulmi, S. (2014) "Effective Apparent Power Definition Based on Sequence Components for Non-Sinusoidal Electric Power Quantities" Electric Power Systems Research. Vol. 117, pp.210–218.

Bourbia,W., Berrezzek, F., Bensaker, B. (2014) "Circle-criterion Based Nonlinear Observer Design for Sensorless Induction Motor Control" International Journal of Automation and Computing, Vol.11, No 6, pp.598-604.

Calıs, H. and Cakır, A. (2007) "Rotor Bar Fault Diagnosis in Three Phase Induction Motors by Monitoring fluctuations of Motor Current Zero Crossing Instants" Electric Power Systems Research,Vol. 77, pp.385–392.

Chilengue, Z., Dente, J.A., Costa Branco, P.J. (2011) "An Artificial Immune System Approach for Fault Detection in the Stator and RotorCircuits of Induction Machines" Electric Power Systems Research, Vol. 81, pp.158–169.

Cruz S M A, Cardoso A J M, Toliyat H A. (2003) "Diagnosis of stator rotor and airgap eccentricity faults in three-phase induction motors based on the multiple reference frames theory" ConferenceRecord of The 2003 IEEE Industry Applications Society AnnualMeeting. Salt Lake City, 2: 1340−1346

De Angelo, C.H., Bossio, G.R., Garcia, G.O. (2010) "Discriminating Broken Rotor Bar From Oscillating Load Effects Using the Instantaneous Active and Reactive Powers" IET Electric Power Applications, Vol. 4, No. 4, pp.281-290.

Drif, M. and Cardoso, M. A. J. (2009) "The use of the Instantaneous Reactive Power Signature Analysis for Rotor-Cage-Fault Diagnostics in Three-PhaseInduction Motors" IEEE Transactions on Industrial Electronics,Vol. 56, No. 11, pp.4606-4614.

Drif, M.and Cardoso, M. A. J. (2012) "Discriminating the Simultaneous Occurrence of Three-Phase Induction Motor Rotor Faults and Mechanical Load Oscillations by the Instantaneous Active and Reactive

Power Media Signature Analyses" IEEE Transactions on Industrial Electronics, Vol. 59, No. 3, pp.1630-1639.

Didier E. T. G., Caspary O., Razik H., (2006) "Fault detection of broken rotor bars in induction motor using a global fault index" IEEE Transactions Industry Applications, vol. 42, pp. 79-88,

Dmytro M.,(2011) " An Instantaneous Power Spectra Analysis As A Method For Induction Motors Fault Detection" Xiii International Phd Workshop Owd, 407-412.

Dybowski, P., Rams, W., Rusek, J. (2008) "Problems of Practical Diagnostics of InductionMachines in Industry" Electrical Power Quality and Utilisation, Vol. 14, No. 1, pp.79-84.

Elayaraja, T., NatarajanS. (2015) "Diagnosis of stator winding of induction machine using hystresis curves based on maximum partial discharge magnitude" International Journal of Applied Engineering Research Vol. 10 No.9, pp.23367-23377 ·

E. Schaeffer, M.E. Zaım, E. Le Carpentier, (1998) "Unbalanced induction machine simulation dedicated to condition monitoring" Proceedings of the International Conference on Electrical Machines, Istanbul (Turkey),Vol. 1, pp. 414-419.

Fiorucci, E. (2015) "The Measurement of Actual Apparent Power and Actual Reactive Power from the Instantaneous Power Signals in Single-Phase and three-Phase Systems" Electric Power Systems Research, Vol. 121, pp.227–242.

F. Filippetti, G. Franceschini, C. Tassoni, and P. Vas, (1998) "AI techniques in induction machines diagnosis including the speed ripple effect" IEEE Transactions on Industry Applications, Vol. 34, pp. 98-108.

Gidwani, L. and Tiwari, H.P. (2012) "A comparative study on the grid integrated wind energy conversion systems (WECS) using different generator models" Int. J. of Power and Energy Conversion, Vol. 3, No. 1/2, pp.94 -100.

I. Ahmed, M. Ahmed, K. Imran1, M. Shuja. Khan, T. Akram1, M. Jawad, (2010) "Spectral Analysis Of Misalignment In Machines Using Sideband Components Of Broken Rotor Bar, Shorted Turns And Eccentricity" International Journal Of Electrical & Computer Sciences Ijecs-Ijens Vol. 10 N°6, pp. 85-93.

Intesar, A., Manzar, A., Kashif, I., Shuja Khan M., Akram.T., Jawad. M., (2010) "Spectral Analysis of Misalignment in Machines Using Sideband Components of Broken Rotor Bar, Shorted Turns and Eccentricity" International Journal of Electrical & Computer Sciences Ijecs-Ijen,Vol. 10, No. 6, pp.85-93.

I.Bakhti, S. Chaouch, A. Makouf, T. Douadi, Jan (2019) "Robust integral back stepping control with extended Kalman filter of permanent magnet synchronous motor" International Journal of Industrial and Systems Engineering, , Vol. 31, Issue 1, pp. 1-14.

Jin, H., Faliang, N., Jiaqiang, Y. (2007) "Induction motor rotor fault diagnosis method based on doublePQ transformation" Front. Electr. Electron. Eng. China,Vol. 2 No.1, pp., 117–122.

Kucuker, A. and Bayrak, M. (2013) "Detection of Mechanical Imbalances of Induction Motors with Instantaneous Power Signature Analysis" Journal of Electrical Engineering and Technology, Vol.8, No. 5, pp.742-747.

Lebaroud, A. and Medoued, A. (2013) "Online Computational Tools Dedicated to the Detection of Induction Machine Faults" Electrical Power and Energy Systems. Vol. 44, pp.752–757.

Leksir, A. and Bensaker, B. (2011) "Induction Generator Rotor Faults Modeling and Diagnosis Based on Double PQ Transformation" IEEE International Conference on Multimedia Computing and Systems (ICMCS), Morocco7-9 April.

Liang, B., Simon, D. I., Yunshi, Z. (2013) "Application of Power Spectrum, Cepstrum, Higher Order Spectrum and Neural Network Analyses for Induction Motor Fault Diagnosis" Mechanical Systems and Signal Processing, Vol. 39, pp.342–360.

Liu, Z., Zhang, X., Wei, Y. (2007) "Rotor Faults Diagnosis Way for Induction Motors Based on PQ Transformation" IEEE International Conference on Control and Automation Guangzhou, Vol. 8, No 8, pp.1067-1071.

Maouche,Y., Oumaamar, M. E. K., Boucherma, M., Khezzar, A. (2014) "Instantaneous Power Spectrum Analysis for Broken Bar Fault Detection in Inverter-fed Six-phase Squirrel Cage Induction Motor" International Journal Of Electrical Power & Energy Systems,Vol. 62, pp.110–117.

Mehla, N.;Dahiya,R.(2007)"An Approach of Condition Monitoring of Induction Motor Using MCSA"International Journal of Systems Applications, Engineering and Development. Vol. 1, No. 1, pp.13-17.

Mehrjou,M. R., Mariun, N., Marhaban, M. H., Misron, N. (2011) "Rotor Fault Condition Monitoring Techniques for Squirrel-Cage Induction Machine—A Review" Mechanical Systems and Signal Processing, Vol. 25, pp.2827–2848.

Mehrjou M.R., Mariun N., Marhaban M. H., Misron N. (2011) "Rotor fault condition monitoring techniques for squirrel-cage induction machine—A review" Mechanical Systems and Signal Processing 25, 2827–2848

Mohamed E. K. O., Yassine M., Mohamed B., Abdelmalek K. (2017) "Static air-gap eccentricity fault diagnosis using rotor slot harmonics in line neutral voltage of three-phase squirrel cage induction motor"Mechanical Systems and Signal Processing, Volume 84, Part A, Pages 584–597

Mustafa M. I., Habeeb J. N., (2013) "Induction Motor Bearing Fault Detection Under Transient Conditions" International Journal Of Current Engineering And Technology, Vol.3, No.4 ,Pp. 1287 – 1292.

M. Zeraoulia. A. Mamoune, H. Mangel and M. E. H. Benbouzid, (2005) "A Simple Fuzzy Logic Approach for Induction Motors Stator Condition Monitoring" J. Electrical Systems Vol. 1, Issue 1, pp. 15-25

Olivier,O.,Guy, C., Boutleux, E., Eric, B. (2009)"Fault Detection and Diagnosis in a Set Inverter–Induction MachineThrough Multidimensional Membership Function and Pattern Recognition" IEEE Transactions on Energy Conversion, Vol. 24, No. 2, pp.431-441.

Pablo, D., Guillermo B., Cristian D. A., Guillermo G., Marcos D. (2016) "Voltage unbalance and harmonic distortion effects on induction motor power, torque and vibrations" Electric Power Systems Research, Volume 140, Pages 866–873.

Patel, R., Gupta, S.P., Kumar, V. (2014) "Bearing fault severity estimation using time-based descriptors for rotating electric machines" Int. J. of Power and Energy Conversion, Vol. 5, No. 2, pp.197 - 209.

Prakasam, K., Ramesh, S. (2016) "Testing and Analysis of Induction Motor Electrical Faults Using Current Signature Analysis" Circuits and Systems, Vol.7, pp.2651-2662.

Samaga, B.L.R. and Vittal, K.P. (2012) "Comprehensive Study of Mixed Eccentricity Fault Diagnosis in Induction Motors Using Signature Analysis" International Journal of Electrical Power & Energy Systems. Vol. 35, No. 1, 180–185.

Shehata, S. A. M., El-Goharey, H. S., Marei, M. I., Ibrahi, A. K. (2013) "Detection of Induction Motors Rotor/Stator Faults Using Electrical Signatures Analysis" International Conference on Renewable Energies and Power Quality, Bilbao (Spain), Vol. 11, pp.20-22.

Singhal, A. and Khandekar, M. A. (2013) "Bearing Fault Detection in Induction Motor Using Motor Current Signature Analysis" International Journal of Advanced Research In Electrical, Electronics and Instrumentation Engineering,Vol. 2, No. 7, pp.3258-3264.

Singh, G. K. and Saad Ahmed, S. A. (2003) "Induction Machine Drive Condition Monitoring and Diagnostic Esearch-A Survey" Electric Power Systems Research, Vol. 64, pp.145–158.

Thomson, W. and Fenger, M. (2001) "current signature analysis to detect induction motor faults" IEEE Industry Applications Magazine, Vol. 7,no4, pp.26–34.

Trzynadlowski, A. M. (1999) "Detection of Mechanical Abnormalities in Induction Motors by Electric Measurements" International Journal of Rotating Machinery,Vol. 5, No. 1, pp.41-52.

Y. Gritli, L. Zarri, C. Rossi, F. Filippetti, G. A. Capolino, D. Casadei, (2013) "Advanced Diagnosis of Electrical Faults in Wound Rotor Induction Machines" IEEE transactions on industrial electronics, vol. 60, no. 9.

Zagirnyak, M., Mamchur, D., Kalinov, A. and Al-Mashakbeh, A. S. (2013) "Induction Motors Faults Detection Based on Instantaneous Power Spectrum Analysis with Elimination of the Supply Mains Influence" ACEEE Int. J on Electrical and Power Engineering, Vol. 4, N°. 3.

Z.Liu, X.Zhang, Y.Wei,(2007) "Rotor Faults Diagnosis Way For Induction Motors Based On Pq Transformation," IEEE International Conference On Control And Automation Guangzhou, China Pp1067_1071.